# BIODEGRADABILITY ASSESSMENT OF ANILINE UNDER METHANOGENIC AND SALINE CONDITIONS IN BATCH AND ANMBR

A thesis submitted to the Delft University of Technology in partial fulfilment of the requirements for the degree of

Master of Science in Civil Engineering

by

Daniël Huisman

March 2020

Daniël Huisman: *Biodegradability assessment of aniline under methanogenic and saline conditions in batch and AnMBR* (2020)

The work in this thesis was part of:


BioXtreme project
Department of Water Management
Faculty of Civil Engineering & Geosciences
Delft University of Technology

| | |
|---|---|
| Supervisor: | Ir. Victor Servando Garcia Rea |
| Assessment Committee: | Dr. Ir. Henri Spanjers |
| | Prof. Dr. Ir. Jules van Lier |
| | Asst. Prof. Dr. Ir. David Weissbrodt |
| | Ir. Victor Servando Garcia Rea |

# ABSTRACT

Aniline, a toxic aromatic amine present in certain wastewaters from the petroleum-, pharmaceutical- , and textile industry is regarded recalcitrant under strict anaerobic conditions. This study assessed the feasibility of methanogenic aniline biodegradation under saline (8 $gNa^{+} \cdot L^{-1}$) conditions (1) by performing biodegradability batch assays using biomass from three different origins, and (2) by treating aniline-containing synthetic wastewater in a continuous anaerobic membrane bioreactor (AnMBR), seeded with granular sludge coming from an up-flow anaerobic sludge blanket (UASB) reactor treating petrochemical wastewater. In addition, the inhibitory effect of aniline and phenol on the aceticlastic methanogenesis, as well as the toxic effect on the integrity of cell membranes of the anaerobic biomass were assessed. Methanogenic biodegradation of aniline was not observed in the AnMBR, nor in the biodegradability assays. However, the results from the AnMBR operation fed with synthetic wastewater (20-200 $mg$ aniline$\cdot L^{-1}$) demonstrated a 10-20% aniline removal, which was mainly attributed to volatilisation of aniline. Results from specific methanogenic activity (SMA)-inhibition tests demonstrated a half maximal inhibitory concentration ($IC_{50}$) of aniline for the aceticlastic methanogenesis of 2.5 $g$ aniline$\cdot L^{-1}$. The $IC_{50}$ of phenol for the aceticlastic methanogenesis was 1.0 $g$ phenol$\cdot L^{-1}$. The cell membrane integrity (CMI) of the anaerobic biomass was not significantly affected after 72 hours of exposure to 4 $g$ aniline$\cdot L^{-1}$ or 2 $g$ phenol$\cdot L^{-1}$. This research constituted the first report demonstrating the application of an AnMBR with the aim to biodegrade aniline-containing synthetic wastewater under methanogenic saline conditions. The results of this research demonstrated that, after 200 days of AnMBR operation, the methanogenic enrichment culture was not able to biodegrade aniline.

# ACKNOWLEDGEMENTS

First of all, I would like to thank the members of the assessment committee, Jules, Henri, David, and Victor, for allowing me to work on this interesting topic, for all the refreshing discussions, for your critical view on the subject, and for the numerous amount of challenging questions and good suggestions.

Besides, I would like to thank Alberto and Beatriz for their help and patience during my first weeks in the lab. Your demonstrations and suggestions enabled me to master the necessary lab-skills in a short time. Joonyeob, thank you for sharing your knowledge on performing experiments for assessing inhibition of methanogenesis. Daniel, thank you for helping me out in the last few weeks of my lab work, which enabled me to focus on the writing of my thesis. I would like to thank you all for your friendliness and positive attitude, it was a pleasure working with you.

My parents, I am very thankful for all the love and support you have given me. You have always been there for me, I will always be there for you. My friends, thank you for all the distractions in the past months, I needed that. Amarinske, thank you for your love and your patience. Finally we can go live together.

I would like to express my sincere appreciation to Lenie Groenewegen, who allowed me to live at the most beautiful place near the city of Delft. I feel very lucky having lived at this peaceful place, I will always be grateful for that.

A big thanks to the roommates with whom I have lived together at de Tochtige Koe. Having a comfortable place to come home to, and sociable people to share it with has been very important to me. Thanks to Dominic and Moos in particular, with whom I have lived together for almost six years. I will always remember the interesting discussions and personal conversations, the countless games of Catan (especially the competitiveness of Moos and myself), having dinner at the balcony while looking at the sunset, doing the dishes while listening to rock music, swimming in the canal during warm summer nights, and so on.

Finally, I would like to express my gratitude once more to my supervisor during this project, Victor. I have really enjoyed working together, and I sincerely appreciate all the support and advise you have given me. Thank you for not just being a supervisor, but a mentor and a friend at the same time.

# CONTENTS


1 INTRODUCTION 1
1.1 Objective . . . 2
1.1.1 Main research question . . . 3
1.1.2 Sub-questions . . . 3
1.1.3 Experimental plan . . . 3
1.2 Outline of this thesis . . . 4
2 LITERATURE RESEARCH 5
2.1 Aniline . . . 5
2.2 Inhibition & toxicity . . . 7
2.3 Aniline- & phenolic wastewater . . . 9
2.4 Treatment methods for aniline-containing wastewater . . . 10
2.4.1 Aerobic biological degradation of phenol and aniline . . . 11
2.4.2 Anaerobic digestion . . . 13
2.4.3 Alternative removal mechanisms of phenol and aniline . . . 16
2.4.4 Microorganisms associated with aniline degradation . . . 16
2.4.5 Stoichiometry & thermodynamics . . . 17
2.5 Anaerobic membrane bioreactor . . . 21
2.5.1 Operational considerations . . . 22
3 MATERIALS & METHODS 27
3.1 Biomass characterisation . . . 27
3.1.1 Source of the anaerobic biomass for experimental purposes . . . 27
3.1.2 Total- & volatile suspended solids . . . 28
3.1.3 Specific methanogenic activity of the UASB reactor sludge . . . 28
3.2 Experimental setup: Batch tests . . . 30
3.2.1 Biodegradability assay . . . 30
3.2.2 Inhibition & toxicity . . . 31
3.3 Experimental setup: AnMBR . . . 33
3.3.1 Critical flux determination . . . 35
3.3.2 AnMBR feeding medium . . . 35
3.3.3 AnMBR operation & sampling . . . 36
3.3.4 Microbial community dynamics . . . 36
3.3.5 Alternative aniline removal mechanisms in the AnMBR . . . 37
3.4 Additional analytical procedures . . . 37
3.4.1 Gas chromatography . . . 37
3.4.2 Chemical oxygen demand cuvette test kit . . . 38
3.4.3 Particle size distribution analysis . . . 38
4 RESULTS 39
4.1 Batch experiments . . . 39
4.1.1 Specific methanogenic activity determination for reactor start-up 39
4.1.2 Anaerobic aniline biodegradability . . . 39
4.1.3 Inhibition & toxicity . . . 40
4.2 AnMBR operation . . . 41
4.2.1 Removal of aniline . . . 41
4.2.2 Removal of phenol and benzoate . . . 43
4.2.3 VFA- and total COD removal . . . 44
4.2.4 Microbial community dynamics . . . 44
4.2.5 Alternative aniline removal mechanisms in the AnMBR . . . 44
5 DISCUSSION 47
5.1 Batch biodegradability assays . . . 47
5.2 Inhibition & toxicity . . . 48
5.3 AnMBR performance treating aniline containing wastewater . . . 49

5.3.1 Removal of aniline . . . 49
5.3.2 Removal of phenol and benzoate . . . 51
5.3.3 Removal of VFAs and total COD . . . 51
6 CONCLUSION 53
6.1 Conclusion . . . 53
6.2 Recommendations . . . 54
A CHEMICAL OXYGEN DEMAND 69
B THERMODYNAMIC DATA 71
C MATLAB SCRIPT GOMPERTZ MODEL 73
D ANMBR FEED 75
E MACRO- & MICRONUTRIENT SOLUTIONS AND PHOSPHATE BUFFER 77
F PREPARATION OF STAIN SOLUTIONS 79
F.1 10 $mM$ Tris buffer pH 8 (1 $L$) . . . 79
F.2 SG working solution . . . 79
F.3 SGPI working solution . . . 79
G DATA PROCESSING SMA-INHIBITION TEST 81
G.1 Effect of aniline on the SMA . . . 81
G.1.1 Effect of phenol on the SMA . . . 82
H MEMBRANE CRITICAL FLUX 83
I COD BALANCE 85
J BIOGAS PRODUCTION IN THE ANMBR 87
K TEMPERATURE AND PH IN THE ANMBR 89
L SUSPENDED SOLIDS IN THE ANMBR 91
M PARTICLE SIZE DISTRIBUTION 93
N TRANSMEMBRANE PRESSURE 95
O ADDITIONAL OBSERVATIONS 97

# LIST OF FIGURES


Figure 2.1 Electrostatic potential maps . . . 6
Figure 2.2 Resonance structures of aniline . . . 6
Figure 2.3 Enzyme inhibition . . . 7
Figure 2.4 Redox potential range in the environment . . . 11
Figure 2.5 Aerobic upper degradation pathway . . . 12
Figure 2.6 Thermodynamic methanogenic niche . . . 13
Figure 2.7 Anaerobic degradation pathway . . . 15
Figure 2.8 $\Delta G_R^1$ as function of $H_2$ . . . 19
Figure 3.1 Sigmoidal curve described with the modified Gompertz model 29
Figure 3.2 Processing flow cytometry data in FlowJo . . . 33
Figure 3.3 Schematic overview of the AnMBR configuration . . . 34
Figure 4.1 SMA test results . . . 39
Figure 4.2 Biodegradability assays UASB- & bitumen sludge . . . 40
Figure 4.3 Biodegradability assay aniline sludge . . . 40
Figure 4.4 $IC_{50}$ of aniline & phenol for the SMA . . . 41
Figure 4.5 Effect of aniline & phenol on cell viability . . . 41
Figure 4.6 FC: negative controls . . . 42
Figure 4.7 Aniline concentration in the AnMBR . . . 43
Figure 4.8 Phenol concentration in the AnMBR . . . 43
Figure 4.9 Methane production in the AnMBR . . . 44
Figure 4.10 Volatilisation of aniline . . . 45
Figure 4.11 Adsorption of aniline . . . 45
Figure 5.1 Comparison of $IC_{50}$ values . . . 48
Figure G.1 SMA inhibition by aniline - Gompertz model fit . . . 81
Figure G.2 SMA inhibition by phenol - Gompertz model fit . . . 82
Figure H.1 Critical flux determination . . . 83
Figure I.1 COD balance in the AnMBR . . . 85
Figure J.1 Biogas production in the AnMBR . . . 87
Figure K.1 Temperature and pH in the AnMBR . . . 89
Figure L.1 Suspended solids in the AnMBR . . . 91
Figure M.1 PSD evolution in the AnMBR . . . 93
Figure N.1 TMP evolution in the AnMBR . . . 95
Figure O.1 Colour change of the AnMBR feed . . . 97
Figure O.2 Colour difference of the AnMBR feed . . . 97
Figure O.3 Biogas production in the AnMBR . . . 98

# LIST OF TABLES


Table 2.1 Reported $IC_{50}$-values . . . . . 8
Table 2.2 Wastewater characteristics . . . . . 10
Table 3.1 Sources of the biomass . . . . . 27
Table 3.2 TSS and VSS concentrations of the sludge . . . . . 28
Table 3.3 Conditions of the biodegradability assays . . . . . 31
Table 3.4 Membrane characteristics . . . . . 34
Table 3.5 Stages of the AnMBR operation. . . . . 36
Table A.1 COD of the relevant compounds . . . . . 69
Table B.1 Thermodynamic data of the relevant compounds . . . . . 71
Table D.1 AnMBR feed . . . . . 75
Table E.1 Micronutrient solution . . . . . 77
Table E.2 Macronutrient solution . . . . . 77
Table E.3 Phosphate buffer solutions . . . . . 77

# ABBREVIATIONS & ACRONYMS

**AD** anaerobic digestion . . . 8
**AMPTS** automatic methane potential test system . . . 3
**AnMBR** anaerobic membrane bioreactor . . . iii
**APAP** N-acetyl-para-aminophenol . . . 9
**BA** biodegradability assays . . . 3
**CFV** cross-flow velocity . . . 22
**CGWW** coal gasification wastewater . . . 1
**CMI** cell membrane integrity . . . iii
**CoA** coenzyme A . . . 14
**COD** chemical oxygen demand . . . 1
**CT** capillary tube . . . 34
**DMSO** dimethyl sulfoxide . . . 79
**DNA** deoxyribonucleic acid . . . 16
**DPG** diphenylguanidine . . . 9
**EGSB** expanded granular sludge bed . . . 21
**EPS** extracellular polymeric substances . . . 8
**FC** flow cytometry . . . 3
**FID** flame ionization detector . . . 37
**GC** gas chromatography . . . 30
**HPLC** high-performance liquid chromatography . . . 55
**HRT** hydraulic retention time . . . 21
**IC** internal circulation . . . 21
**MBR** membrane bioreactor . . . 21
**NAD** nicotinamide adenine dinucleotide . . . 11
**OLR** organic loading rate . . . 21
**PAC** powdered activated carbon . . . 10
**PBS** phosphate-buffered saline . . . 32
**PCR** polymerase chain reaction . . . 36
**PI** propidium iodide . . . 32
**PSD** particle size distribution . . . 36
**PVDF** polyvinylidene fluoride . . . 34
**SD** standard deviation . . . 28
**SG** SYBR® Green I . . . 32
**SIP** stable isotope probing . . . 16
**SMA** specific methanogenic activity . . . iii
**SRT** sludge retention time . . . 21
**SS** suspended solids . . . 16
**TCD** thermal conductivity detector . . . 38
**TEA** terminal electron acceptor . . . 11

**TMP** transmembrane pressure . . . . . 22
**TSS** total suspended solids . . . . . 3
**UAFP** up-flow anaerobic filter process . . . . . 16
**UASB** up-flow anaerobic sludge blanket . . . . . iii
**UF** ultra-filtration . . . . . 33
**VFA** volatile fatty acids . . . . . 3
**VSS** volatile suspended solids . . . . . 3
**WWTP** wastewater treatment plant . . . . . 9
**ZVI** zerovalent iron . . . . . 55

# SYMBOLS

| | | |
|---|---|---|
| $IC_{50}$ | half maximal inhibitory concentration | iii |
| $LC_{50}$ | median lethal concentration | 3 |
| $LMH$ | $L \cdot m^{-2} \cdot h^{-1}$ | 23 |
| $n$ | sample size | 28 |
| $K_{OC}$ | organic carbon-water partitioning coefficient | 9 |
| $R_{CH_4}$ | methane production rate | 87 |
| $RPM$ | rotations per minute | 29 |
| $TMP_f$ | final transmembrane pressure | 35 |
| $TMP_i$ | initial transmembrane pressure | 35 |

# 1 INTRODUCTION

Industrial wastewater is frequently characterised by its high chemical oxygen demand (COD). In addition, in the petroleum-, chemical- and textile industry, high saline wastewaters are generated that contain toxic organic pollutants such as aromatic compounds, among which, the phenolics are a major group. Considering the presence of aniline in some of these phenolic wastewaters such as (petro-) chemical wastewaters, e.g. coal gasification wastewater (CGWW), and/or wastewater from the textile industry, it is of great interest for these industries to study the potential simultaneous biodegradability of this compound together with phenolics [Neufeld and Spinola, 1978; Singer et al., 1978; Rawlings and Samfield, 1979; Wada et al., 1995; Yuan et al., 2006; Wang et al., 2007; Zhang et al., 2009; Zhao and Liu, 2016; Ji et al., 2016; Rava et al., 2016]. The salt concentration of such industrial wastewater varies depending on the industrial process, with reported values between 20 and 150 $g \cdot L^{-1}$ [Castillo-Carvajal et al., 2014]. In most cases, such high concentrations will inhibit the microorganisms which are suppose to degrade the organic pollutants.

The inhibitory effect of the elevated salt concentration can be resolved by e.g. dilution, or by salt removal using reverse osmosis, ion exchange, or electrodialysis [Afzal et al., 2007]. However, these are expensive methods, and in the case of dilution it results in an increase of the wastewater volume. Fortunately, despite the negative impact of high sodium concentrations on the microbial degradation processes, it has been shown that anaerobic biomass is capable of adapting to conditions with high salinity (up to 20 $gNa^{+} \cdot L^{-1}$), and is still able to degrade toxic, aromatic compounds [Muñoz Sierra et al., 2018a; Gao, 2019]. Therefore, in the BioXtreme project, the goal is to promote the growth of anaerobic microorganisms which withstand extreme conditions, such as high salinity and toxicity, and are able to degrade a variety of organic pollutants, such as phenol and other aromatics. The AnMBR was used to retain the slow-growing anaerobic microorganisms in the system, needed for the degradation of toxic compounds. In this research, the aim was to apply an AnMBR to develop an anaerobic microbial community capable to biodegrade aniline.

Aniline ($C_6H_5NH_2$) has been used for more than 150 years in the chemical industry as an intermediate compound in different fields of application [Kahl et al., 2012]. Since the invention of the first synthetic dyestuff by William Henry Perkin in 1856, aniline based azo dyes were widely used in Western Europe [Travis, 1997]. These azo dyes are characterised by the diazinyl ($R - N = N - R'$) functional group, in which the azo ($N = N$) bond connects substituted aromatic structures [Carliell et al., 1995].

Besides the production of dyes and pigments, N-substituted aromatic compounds such as nitroaromatics and aromatic amines are used in a variety of processes. These processes include the production of rubber, agricultural chemicals, pharmaceuticals, and the synthesis of 4,4'-methylene diphenyl diisocyanate to produce polyurethanes [Kahl et al., 2012]. Wastewater produced in these processes usually contains nitroaromatics and aromatic amines such as aniline, which is regarded toxic to aquatic life and is suspected to be carcinogenic [EPA, 2000]. Considering the aforementioned problems caused by N-substituted aromatic compounds, it is important that these organic pollutants are removed from the wastewater stream completely.

Aromatic amines are generated during anaerobic biological treatment by reduction of N-substituted compounds such as nitroaromatics and azo dyes.

Nitroaromatic- and azo dye compounds have been found more toxic to anaerobic biomass than aromatic amines [Razo Flores, 1997; Knackmuss, 1996]. Because of the electron-withdrawing character of the functional groups, these compounds are resistant to electrophilic attack by oxygenases which makes them poorly degradable under aerobic conditions [Knackmuss, 1996]. Therefore, treatment under anaerobic conditions is usually applied. Because of the recalcitrance of aromatic amines under anaerobic conditions due to the presence of the electron donating functional group, a subsequent aerobic treatment step is required for the degradation of these compounds [Brown and Hamburger, 1987; Dickel et al., 1993; Field et al., 1995].

To reduce costs for the degradation of N-substituted aromatics, the avoidance of an energy-intensive treatment step, such as the aerobic, would be preferred. It has already been shown that unsubstituted aniline can be biologically degraded under anaerobic conditions by sulphate reducing bacteria and in mixed cultures under denitrifying conditions [Schnell and Schink, 1991; de Alexandra et al., 1994; Field, 2002; Pereira et al., 2011]. Nevertheless, it would be preferred that aniline can be biologically degraded under strict anaerobic (i.e. methanogenic) conditions, so that the formation of toxic by-products such as $H_2S$ is avoided and energy can be recovered in the form of biogas.

Only a few studies claim to have observed methanogenic aniline biodegradation [Yumihara et al., 2002; Sun et al., 2015], but there is not much evidence supporting the likelihood of this phenomenon [Battersby and Wilson, 1989; Schink, 1988; de Alexandra et al., 1994; Razo Flores, 1997]. Even though it was already stated by de Alexandra et al. that there is "a paucity of data on the anaerobic metabolism of unsubstituted aniline" back in 1994, not much has changed for the time being. The AnMBR can be an appealing system for the treatment of saline aniline-containing wastewater, as the suspended biomass can be retained and enriched for a certain type of microorganisms.

This study aimed to evaluate the biodegradation of aniline in an AnMBR under methanogenic and saline conditions. Microbial community dynamics in the AnMBR sludge was analysed to get an insight into the microbial populations that were related to the applied conditions and observed events during the reactor operation. Biodegradability batch assays were performed to assess the biodegradation of aniline under methanogenic and saline conditions. In addition, the inhibitive effect of aniline and phenol on the aceticlastic methanogenesis, and the effect of aniline and phenol on the CMI of the anaerobic biomass were be assessed.

This research constitutes the first report demonstrating the application of an AnMBR with the aim to develop a methanogenic enrichment culture able to biodegrade aniline under saline (8 $gNa^+ \cdot L^{-1}$) conditions. Demonstration of methanogenic aniline biodegradation in an AnMBR would provide the (petro-) chemical industry with an attractive sustainable solution for the treatment of aniline-containing wastewater.

## 1.1 OBJECTIVE

The main objective of this research was (1) to assess the feasibility of biodegradation of aniline under methanogenic and saline conditions either in continuous AnMBR operation or batch assays. In addition, the sub-objectives were (2) to assess the inhibitory effect of aniline and phenol on the aceticlastic methanogenesis, (3) to assess the effect of aniline and phenol on the CMI of anaerobic biomass, and (4) to get insight into the microbial community dynamics in the AnMBR during treatment of aniline- and phenol containing wastewater.

### 1.1.1 Main research question

The main research question derived from these objectives is described as follows:

- What is the removal percentage of aniline under methanogenic saline (8 $gNa^{+} \cdot L^{-1}$) conditions when treated in an AnMBR amended with granular sludge coming from an UASB reactor treating petrochemical wastewater and with phenol, acetate, propionate, and butyrate as additional carbon and energy sources?

### 1.1.2 Sub-questions

The sub-questions are as follows:

1. What is the anaerobic biodegradability of aniline in $gCOD_{CH_4} \cdot gCOD^{-1}_{aniline}$ under saline (8 $gNa^{+} \cdot L^{-1}$) conditions, when using:
   a) granular sludge from an UASB reactor of a petrochemical wastewater treatment plant (Shell, Moerdijk, NL)?
   b) bitumen condensate-degrading sludge (BioXtreme)?
   c) AnMBR sludge exposed to aniline for >100 days (BioXtreme)?
2. What is the $IC_{50}$ of aniline for the aceticlastic methanogenesis of petrochemical granular sludge from an UASB reactor?
3. What is the median lethal concentration ($LC_{50}$) of aniline for the biomass of petrochemical granular sludge from an UASB reactor?
4. What is the $IC_{50}$ of phenol for the aceticlastic methanogenesis of petrochemical granular sludge from an UASB reactor?
5. What is the $LC_{50}$ of phenol for the biomass of petrochemical granular sludge from an UASB reactor?
6. What are the changes in the microbial community of the AnMBR sludge during phenol, acetate, propionate, butyrate, and (possible) aniline degradation?
7. What is the effect of aniline (20-200 $mgAn \cdot L^{-1}$) on the specific phenol conversion rate in $mgP \cdot gVSS^{-1} \cdot day^{-1}$ in an AnMBR?

### 1.1.3 Experimental plan

The main research question and sub-questions 6, and 7, were answered by studying the biodegradation of the specified organic compounds in a continuously operated AnMBR. Broth was frequently extracted for analysis of the total suspended solids (TSS)-, volatile suspended solids (VSS) concentration, and the microbial community structure in the reactor. Permeate samples were analysed to determine the volatile fatty acids (VFA) and phenol concentration, and biogas samples were extracted for assessing the methane content.

To answer sub-question 1, biodegradability assays (BA) were performed. For the determination of the $IC_{50}$ of aniline and phenol for the aceticlastic methanogenesis of the sludge listed in sub-question 2 and 4, multiple SMA-inhibition tests were carried out with the use of the automatic methane potential test system (AMPTS). Data required for answering sub-questions 3 and 5 was obtained using flow cytometry (FC), which yielded information about the viability of the cells before and after exposure to toxic conditions.

## 1.2 OUTLINE OF THIS THESIS

Chapter 2 provides literature information regarding (1) physicochemical characteristics and industrial applications of aniline, (2) the origin of aniline-containing wastewater and its main components, (3) mechanisms of inhibition and toxicity, (4) application of AnMBRs, and (5) treatment of phenol- and aniline-containing wastewater. Chapter 3 describes the applied experimental methods during this research. In chapter 4, the results are presented, which will be discussed in chapter 5. The conclusion is presented in chapter 6, which also includes suggestions and recommendations for supplementary research.

# 2 LITERATURE RESEARCH

## 2.1 ANILINE

Aniline ($C_6H_5NH_2$), also known as arylamine or aminobenzene, has been used in the chemical industry as an intermediate compound in many different fields of application for more than 150 years. Already since the invention of the first synthetic dyestuff in 1856, aniline based dyes were widely used in Western Europe [Kahl et al., 2012; Travis, 1997]. Currently, besides the production of dyes and pigments, aniline is used in a variety of industrial production processes. Together with many other non-biological (xenobiotic) aromatic compounds, aniline can be found in the effluents from fuel, chemical, plastic, explosive, ink, and pharmaceutical industries [Ladino-Orjuela et al., 2016]. For instance, aniline is used as a basic ingredient or intermediate in the production process of rubber, agricultural chemicals, pharmaceuticals and the synthesis of 4,4'-methylene diphenyl diisocyanate to produce polyurethanes [Kahl et al., 2012].

Besides the wastewater streams from the aforementioned industries and processes, low concentrations of aniline can be found in wastewater from the petrochemical industry [Neufeld and Spinola, 1978; Singer et al., 1978; Yuan et al., 2006]. As a result of these industrial production processes, traces of aniline end up in the industrial wastewater. Considering its high toxicity to aquatic life and suspected carcinogenicity, it is important that this organic compound is removed from the wastewater stream [EPA, 2000].

Aniline is known to be a recalcitrant compound, mainly due to the presence of the amino ($-NH_2$) group. This electron donating functional group gives the molecule extra stability [Knackmuss, 1996; Field, 2002]. The electrostatic potential map of benzene, aniline and phenol in figure 2.1 can clarify this phenomenon. The aromatic ring for benzene, aniline and phenol is an electron rich zone, carrying a partial negative charge. However, where benzene has polar characteristics (electrons are distributed symmetrically), this is not the case for aniline and phenol. Both the amino ($-NH_2$) group in aniline and the hydroxyl ($-OH$) group in phenol are so called 'activating groups', which donate electrons to the aromatic ring. This makes the aromatic ring more electron-rich, stabilising the carbocation intermediate (usually unstable and highly reactive due to positively charged carbon atom with three bonds instead of four) resulting in a lower activation energy. [McMurry, 2011]

The oxygen atom in the hydroxyl group of the phenol has one extra lone electron pair, resulting the asymmetrical potential distribution, and consequently a lower stability compared to aniline (figure 2.1). In the case of aniline and phenol, the $-NH_2$ and $-OH$ substituents have an electron-withdrawing inductive effect due to the electronegativity of the $-O$ or $-N$ atom, and an electron donating resonance effect because of the lone-pair electrons on those $-O$ or $-N$ atoms. These two effects act in opposite directions. The electron-donating resonance effect is stronger and will therefore dominate. Regarding aniline, the lone electron pair of the nitrogen atom is delocalised by an orbital overlap with the pi electron system of the aromatic ring. This lone pair can be in several positions through the resonance between five structures, resulting in high resonance stabilisation (figure 2.2). Phenol shares the same resonance effect, with similar resonance structures. [McMurry, 2011]

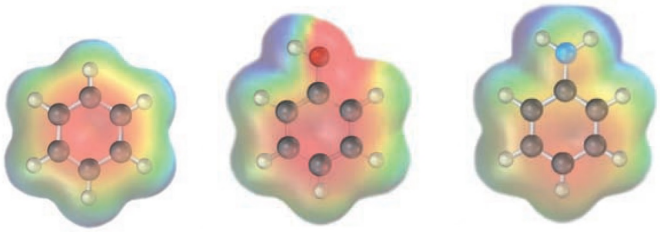

**(a)** Benzene **(b)** Phenol **(c)** Aniline

**Figure 2.1:** Electrostatic potential maps of benzene **(a)**, phenol **(b)** and aniline **(c)**. In this molecular representation, the electron distribution is visualized by colours, ranging from red (electron-rich; $\delta-$) to blue (electron-poor; $\delta+$). In the electrostatic potential map of benzene, the negative potential (red) is evenly distributed between all the carbon bonds due to the absence of a functional group. In phenol, the charge is delocalised towards the aromatic ring, but the other lone electron pair of the oxygen atom gives the phenol an asymmetrical electrostatic potential distribution. In the electrostatic potential map of aniline, it can be seen that the charge of the lone electron pair is delocalised towards the aromatic ring. The electrostatic potential maps are adopted from Mecozzi et al. [1996]

.

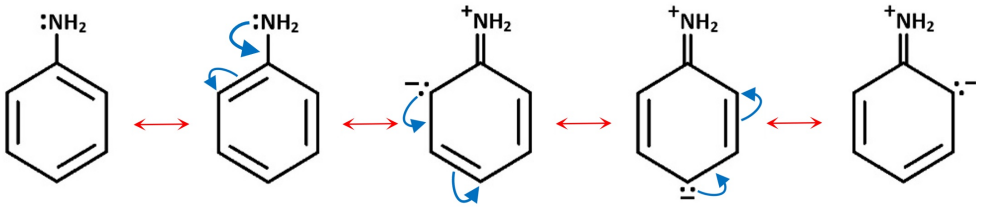


**Figure 2.2:** The lone electron pair of the nitrogen is drawn to the aromatic ring, causing aniline to appear as five different resonance structures of aniline.

.

Because of the lone pair of electrons of either the $N$ (aniline) and $O$ (phenol), the $-NH_2$ and $-OH$ groups, respectively, act as ortho- and para directors. Since ortho and para substitutions result in more resonance forms than the meta substitution intermediate, these intermediates are more stabilised compared to the meta intermediate. [McMurry, 2011]

Where aromatics with electron-withdrawing functional groups (e.g. nitro-, azo- and chloro-groups) are generally not degraded during aerobic wastewater treatment due to their resistance to electrophilic attack by oxygenases, it is expected that for aromatics with electron-donating functional groups (e.g. amino- or hydroxyl groups) such an electrophilic attack of aromatics is facilitated by electron-donating functional groups. Under anaerobic conditions it is the other way around: aromatics with electron-withdrawing functional groups are reduced after nucleophilic attack, where electron-donating functional groups persist such a nucleophilic attack [Razo Flores, 1997].

Therefore, for the treatment of wastewater containing nitroaromatics or azo dyes, it is proposed to perform a sequencing (or simultaneous) anaerobic-aerobic processes, for the reduction of azo dyes and nitroaromatics under anaerobic conditions, followed by mineralisation of the produced aromatic amines under aerobic conditions [Tan et al., 1999]. The application of sequenced anaerobic-aerobic systems for the degradation of several azo dyes have been proven successful by multiple studies [Haug et al., 1991; Fitzgerald and Bishop, 1995; Kudlich et al., 1996; An et al., 1996; Tan, 2001]. However, autoxidation and polymerisation of unstable aromatic amines in this subsequent aerobic stage, can result in humic-like oligomeric and polymeric structures, which might increase methanogenic toxicity [Razo Flores,

1997]. Methanogenic degradation of aniline would phase out the need for this subsequent aerobic treatment step, thereby reducing the costs for the overall treatment of wastewaters containing N-substituted aromatics.

## 2.2 INHIBITION & TOXICITY

For biological treatment of saline industrial wastewaters, it is relevant to assess the inhibitory- and toxic effects of the constituents in these wastewaters, such as sodium and aromatics, or possible intermediates, like ammonia, on the functionality of the biomass. This is the case for wastewater from the (petro-) chemical industry, which often contains aromatic by-products that can be characterised by either their inhibitive effect or high toxicity on microbial processes.

In biological wastewater treatment, the definitions of toxicity and inhibition formulated by Speece [1996], and adopted by the IWA [2005], are generally used:

- **Toxicity**: "an adverse effect (not necessarily lethal) on bacterial metabolism"
- **Inhibition**: "an impairment of bacterial function"

Several mechanisms can result in inhibition of the microbial activity, such as competitive, uncompetitive and non-competitive inhibition of specific enzymatic reactions (figure 2.3), intracellular pH fluctuations, and increasing energy requirement for cell maintenance [Wittmann et al., 1995].

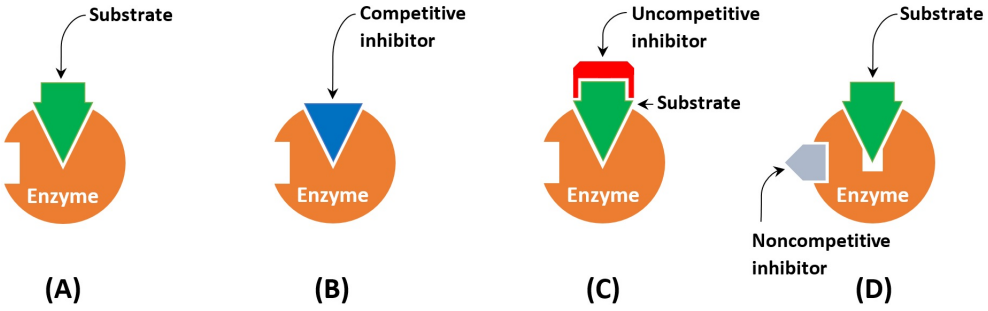


**Figure 2.3:** (A) an enzyme-substrate complex; (B) a competitive inhibitor binds at the active site of the free enzyme: the inhibitor competes with the substrate, preventing the substrate from binding to the active site of the enzyme; (C) an uncompetitive inhibitor binds to the enzyme-substrate complex only; (D) a non-competitive inhibitor changes the shape of the active site. This does not prevent the substrate from binding but hinders the consequent enzymatic chemical reaction [Berg et al., 2012]

.

For cyclic hydrocarbons, interactions with the hydrophobic parts of the cell as a result of the lipophilic (i.e. lipid soluble) character of these compounds, play a major role in the inhibition mechanism [Sikkema et al., 1995]. However, due to the presence of a hydroxyl group and an amino group in phenol and aniline, respectively, these compounds have a more hydrophilic character compared to other cyclic hydrocarbons.[1]

Sikkema et al. [1995] hypothesised that the inhibitory effects of phenolics are exerted at the membrane level. As reported by Sierra-Alvarez and Lettinga [1991] and Donlon et al. [1995], there is a high correlation between hydrophobicity and toxicity of different phenolic compounds on methanogenic granular sludge. Donlon et al. [1995] explain that hydrophobicity is directly related to the "partitioning

1 The aqueous solubility of phenol and aniline are 82.8 $g \cdot L^{-1}$ and 36 $g \cdot L^{-1}$ at 25°C, respectively. This is much higher compared to the aqueous solubility of monocyclic hydrocarbon such as benzene (1.8 $g \cdot L^{-1}$), methylbenzene (0.5 $g \cdot L^{-1}$), and chlorobenzene (0.5 $g \cdot L^{-1}$). (pubchem.com, U.S. National Library of Medicine, National Center for Biotechnology Information)

of the compound into bacterial membranes", expectedly because more hydrophobic compounds accumulate more efficiently in membranes. This accumulation causes disturbance to the membrane structure, resulting in swelling and leaking of the cell membrane, eventually followed by the disintegration of the cell by rupture of the cell wall or membrane (a process called 'lysis'). In addition, it was reported that modifications of the membranes of the facultative anaerobic bacterium *Escherichia coli* occur when grown under aerobic conditions in the presence of phenol. Exposure of *E. coli* to phenol can result in an affected membrane functioning through influenced protein-to-lipid ratios in the cell membrane, an efflux of potassium ions, and increased membrane permeability [Keweloh et al., 1990; Heipieper et al., 1991]. Escher et al. [1996] stated that inhibition could be the result of phenol interference with the transmembrane electrochemical proton gradient and electron transport in the catabolism.

Mohammed et al. [2020] hypothesised that the mechanism of aniline toxicity is based on the interaction of aniline with proteins of the cell membrane. Mujahid et al. [2015] reported that *rubrivivax benzoatilyticus* JA2, an anoxygenic photosynthetic purple bacterium, is able to survive under high concentrations of aniline (2.3 $g \cdot L^{-1}$). The tolerance of this bacterium to aniline is associated with its envelope stress response to toxic compound stress or membrane damage as a result of aniline exposure. This stress response results in the production of extracellular polymeric substances (EPS) and increased saturated fatty acid ratios in the membranes [Mujahid et al., 2015; Mohammed et al., 2020].

In anaerobic digestion (AD), inhibition due to exposure to a chemical can occur in each of the stages of the AD process (hydrolysis, acidogenesis, acetogenesis and methanogenesis). To determine this inhibitory effect of a compound on bacterial function, one can perform experiments in which the reduction of microbial activity caused by exposure to a range of concentrations of the specified compound is assessed. For the degradation of soluble organic material, the methanogenesis has been recognised as the rate-limiting step [Speece, 1996], and it has been shown that "the aceticlastic methanogens are most sensitive to toxic chemicals" [Yumihara et al., 2002]. Therefore, for AD, an inhibition assessment is usually conducted by looking at the effect of the inhibitive compound on the SMA ($gCOD_{CH_4} \cdot gVSS^{-1} \cdot day^{-1}$) of the anaerobic biomass.

In this project, the $IC_{50}$ of the specified compound for the SMA will be determined, yielding a reference inhibition coefficient that can be compared to reported $IC_{50}$ values. It should be noted that this $IC_{50}$ is not fixed or constant: it is depending on the microbial community composition [Chen et al., 2008]. The determination of the $IC_{50}$ can be used as an indication of the inhibitive effect of the specified compound on biomass, but should be determined for each biomass individually. Additionally, it was stated by Chen et al. [2008] that the variety in the reported inhibition coefficients for a certain compound is also related to the type of substrate, environmental conditions, experimental techniques and acclimatisation period.

It has been shown that nitroaromatic compounds, like nitrobenzene, (di)nitrophenols and nitrobenzoates, are inhibitory and toxic to anaerobic biomass. Depending on the compound, concentrations between 0.01-100 $mg \cdot L^{-1}$ result in moderate inhibition to complete reduction of microbial activity [Donlon et al., 1995].

Aromatic amines seem to be less inhibitory to anaerobic biomass compared to nitroaromatics. Donlon et al. [1995] reported that the "nitroaromatic compounds were, on average, 500-fold more toxic than their corresponding amine analogues". Furthermore, it was reported that after the reduction of nitroaromatics to aromatic amines, the inhibition of methanogenesis caused by exposure to the more toxic nitroaromatics ceased [Boyd et al., 1983; Battersby and Wilson, 1989]. In this sense, Fedorak et al. [1990] observed no inhibition on the phenol degradation in the presence of 97 $mg \cdot L^{-1}$ aniline. However, at higher aniline concentrations, inhibition of the SMA has been observed in various studies (table 2.1).

Table 2.1: Reported $IC_{50}$-values of aniline and phenol for the SMA.

| Reference | **Aniline** $[mg \cdot L^{-1}]$ | **Phenol** $[mg \cdot L^{-1}]$ | Inoculum |
|---|---|---|---|
| **Donlon et al. [1995]** | 900 | 1,300 | Granular sludge from an UASB treating chemical industry wastewater, not acclimated to N-substituted aromatics. |
| **Olguin-Lora et al. [2003]** | | 470 | Non-acclimated granular sludge from an UASB treating brewery wastewater |
| | | 1,400 | Acclimated granular sludge from a laboratory UASB degrading phenol as sole carbon & energy source during 8 months |
| **Kayembe et al. [2012]** | 1,400 | 1,250 | Digested pig manure, not acclimated to aromatic compounds. |
| **Poirier et al. [2016]** | | 1,250 | Sludge from a digester treating primary and excess sludge on a municipal wastewater treatment plant (WWTP), acclimated to mashed biowaste. |

In this research, the effect of exposure to aniline and phenol on the CMI of the anaerobic biomass will be used as a measure for toxicity. The $LC_{50}$, which is defined as the concentration of a toxicant that results in 50% reduction of viable cells, will be related to the effect of the toxicant on the CMI. This reference parameter can be compared to reported $LC_{50}$ values. However and similarly to the $IC_{50}$ values, the $LC_{50}$ should be determined for each biomass individually. To the best of the author's knowledge, values for the $LC_{50}$ of aniline and phenol on anaerobic biomass have not been reported yet.

## 2.3 ANILINE- & PHENOLIC WASTEWATER

Aniline containing wastewater is produced by various industrial processes. Examples of this wastewater with the corresponding characteristics can be found in table 2.2. In pharmaceutical wastewater, aniline can originate from the production of N-acetyl-para-aminophenol (APAP) (also known as paracetamol). In wastewater from the rubber production, aniline can come from the synthesis of diphenylguanidine (DPG), an accelerator in the vulcanisation of rubber [Dvořák et al., 2014].

Additionally, considering the presence of aniline in some saline phenolic wastewaters, such as (petro-) chemical wastewaters [Neufeld and Spinola, 1978; Singer et al., 1978; Wang et al., 2007; Zhao and Liu, 2016; Ji et al., 2016; Rava et al., 2016], wastewater from the textile industry [Rawlings and Samfield, 1979], and various other industries, it is important to study the potential simultaneous biodegradability of this aminobenzene together with phenolics [Wada et al., 1995; Yuan et al., 2006; Zhang et al., 2009]. Examples of such combined wastewaters are listed in table 2.2. Besides aniline and phenol, these wastewaters often contain aromatic compounds, such as quinoline, naphthalene and pyridine.

Many of these aromatic compounds are characterised by their hydrophobic character, resulting in the tendency to adsorb to river sediments [Karickhoff et al., 1979], thereby decreasing the bioavailability of these aromatics. The organic carbon-water partitioning coefficient ($K_{OC}$), defined by the ratio between the adsorbed amount of the contaminant (normalised to organic carbon content) and the concentration of the contaminant in water, can be used to estimate the bioavailability of contaminants [Wilczyńska-Piliszek et al., 2012]. Karickhoff et al. [1979] reported that $K_{OC}$ values are the highest for the fine fraction of the river sediment ($<50\ \mu m$), and are largely depending on the organic carbon content of these silt and clay particles. $K_{OC}$ values for aniline, phenol, and benzene are 0.96, 1.24 and 1.82 $logL \cdot kg^{-1}$, respectively, indicating a higher mobility and thus a higher bioavailability of aniline compared to phenol and benzene [Ladino-Orjuela et al., 2016].

Table 2.2: Reported aniline- and phenol concentrations and total COD in aniline wastewaters and phenol/aniline containing wastewaters. The phenol- and aniline concentration in the CGWW from the Synthane process was reported by Neufeld and Spinola [1978] including ortho-cresol and naphthalene, respectively

| | **Industry** | **Pharmaceutical** | **Rubber** | **Chemical** |
|---|---|---|---|---|
| | Source | E.g. APAP production | DPG production | Aniline production |
| **Aniline** | $mgAn \cdot L^{-1}$ | 1,370–2,980 | 8–4,970 | 650–2,110 |
| | $mgCOD \cdot L^{-1}$ | 3,300–7,180 | 20–11,970 | 1,570–5,070 |
| **COD** | $mgCOD \cdot L^{-1}$ | 19,400–58,200 | 40–11,970 | 4,550–8,350 |
| | **Reference** | **Li and Jin [2009]** | **Dvořák et al. [2014]** | **Patil and Shinde [1988]** |

**(a)** Aniline wastewater

| | **Industry** | **Petrochemical** | **Petrochemical** | **Chemical** |
|---|---|---|---|---|
| | Source | CGWW (Synthane process) | CGWW (Lurgi process) | Dye production |
| **Phenol** | $mgPh \cdot L^{-1}$ | 2,209 (incl. o-cresol) | 1,250 | 23 |
| | $mgCOD \cdot L^{-1}$ | $\leq$5,260 | 2,980 | 55 |
| **Aniline** | $mgAn \cdot L^{-1}$ | 21 (incl. naphtalene) | 12 | 13 |
| | $mgCOD \cdot L^{-1}$ | $\leq$51 | 29 | 31 |
| **COD** | $mgCOD \cdot L^{-1}$ | 15,000-43,000 | 12,500-30,000 | 1,350 |
| | **Reference** | **Neufeld and Spinola [1978], Singer et al. [1978]** | **Singer et al. [1978], Ji et al. [2016]** | **Yuan et al. [2006]** |

**(b)** Phenol/aniline wastewater

## 2.4 TREATMENT METHODS FOR ANILINE-CONTAINING WASTEWATER

Various techniques have been used for the treatment of aniline wastewater, among which anodic oxidation, ozonation, photodecomposition, electrolysis, adsorption, and biological treatment are traditionally applied [Kirk et al., 1985; Gheewala and Annachhatre, 1997; Orshansky and Narkis, 1997; Sarasa et al., 1998; Qi et al., 2002]. However, for the removal of low concentrations of aniline ($< 1\ g \cdot L^{-1}$), biodegradation is considered the preferred method mainly because of its costs-effectiveness [Jin et al., 2012; Liu et al., 2015; Li et al., 2017]. Though, because of the toxicity and inhibitory effect of wastewater with higher aniline concentration ($> 1\ g \cdot L^{-1}$) on the biomass [Donlon et al., 1995], biological treatment is not applied to all industrial effluents [Li et al., 2017].

Research is continuously being performed on the development of novel treatment techniques, based on: (1) chemical oxidation, by e.g. supercritical water oxidation [Qi et al., 2002] or advanced oxidation processes such as (photo-) Fenton oxidation [Brillas and Casado, 2002; Liu et al., 2012] where the produced $HO\cdot$ radicals have a good capability of aromatic degradation. (2) Membrane technology, by e.g. reverse osmosis [Gómez et al., 2009], micellar-enhanced ultrafiltration, based on the binding to surfactants [Fu et al., 2017], or hollow fibre renewal liquid membrane [Ren et al., 2014]. (3) Adsorption, by e.g. powdered activated carbon (PAC) [Orshansky and Narkis, 1997], multi-walled carbon nanotubes [Yang et al., 2008], or resins [An et al., 2009]. All these methods seem to be applicable options, but in most cases, complete aniline removal is not achieved.

Aniline wastewater can contain many other aromatic compounds and is usually characterised by a high COD (table 2.2). Because of the high concentration of toxic (e.g. aromatic) compounds, biological treatment of highly toxic wastewater used to be considered inappropriate. However, the application of combined systems such as the AnMBR, enabling enrichment of slow-growing, specialised microorgan-

isms with high tolerance to toxicity and/or inhibition, could be a feasible treatment method for this wastewater [van Lier et al., 2008].

In general, for the biodegradation of organic material, a terminal electron acceptor (TEA) is required. This TEA "determines the energy balance and the metabolic reaction used by microorganisms" [Ladino-Orjuela et al., 2016]. In case of multiple available electron acceptors, the microorganisms will first consume the electron acceptor with the highest redox potential. The redox potential of a chemical species is defined as the measure of the intensity of its oxidising or reducing power, or in other words, its ability to acquire electrons or lose electrons: the higher the redox potential, the stronger the tendency for the compound to gain electrons. Usually, the strongest available oxidising agent found in environmental systems is oxygen. Therefore, oxygen will be used as the first TEA by the microorganisms to degrade organic material. In figure 2.4, the redox conditions, microbial metabolic processes (aerobic respiration, anaerobic fermentation, or anaerobic respiration with electron acceptors other than $O_2$) and the TEA for the environmental redox potential range at neutral pH are visualised. The corresponding redox potential and the availability of a TEA will determine the favourability of a given microbial conversion. [DeLaune and Reddy, 2005]

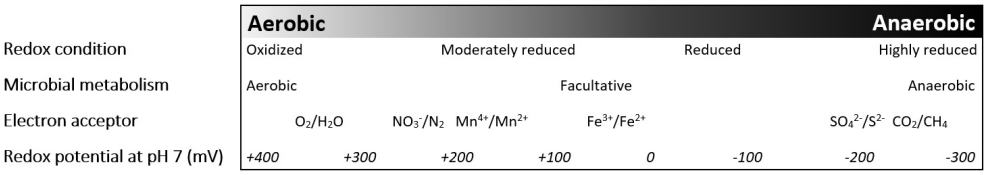


**Figure 2.4:** The redox condition, electron acceptors and metabolic processes for the environmental redox potential range [DeLaune and Reddy, 2005]

.

Because of their hydrophobic character and chemical stability of the aromatic ring, the biological activity of aromatic compounds is low, which is the major challenge in the biodegradation of these contaminants [Heider and Fuchs, 1997]. Nevertheless, studies have shown that biodegradation of aromatics such as aniline and phenol is feasible under either aerobic [Coe, 1952; McKinney et al., 1956; Gheewala and Annachhatre, 1997; O'Neill et al., 2000] or anaerobic conditions [Healy Jr. and Young, 1978; Tschech and Fuchs, 1987; Schnell and Schink, 1991; de Alexandra et al., 1994].

Under both conditions, the metabolic pathway of aromatic hydrocarbon biodegradation can be subdivided into upper pathways, where the original aromatic compound is converted into central intermediates, and lower pathways, where dearomatisation (ring cleavage) of the intermediates takes place [Ladino-Orjuela et al., 2016]. In sections 2.4.1 and 2.4.2, the upper pathways for the biodegradation of aniline and phenol will be discussed.

### 2.4.1 Aerobic biological degradation of phenol and aniline

To fully degrade aromatic compounds under aerobic conditions, the aromatic ring has to be destabilised via addition of oxygen ring by mono- and dioxygenases [Ladino-Orjuela et al., 2016]. For phenol, molecular oxygen is used to hydroxylate the ring by the enzyme phenol hydroxylase which requires the reduced form of the nicotinamide adenine dinucleotide (NAD) cofactor ($NADH$), resulting in formation of catechol (figure 2.5), one of the central intermediates on the aerobic biodegradation of aromatic compounds [van Schie and Young, 2000; Al-Kahlid and El-Naas, 2012; Ladino-Orjuela et al., 2016].

For the aerobic metabolism of aniline, a multistep reaction is required. First, $\gamma$-glutamylanilide is formed from L-glutamate and aniline, an oxidation reaction catalyzed by a glutamine synthetase-like enzyme. Secondly, the aromatic ring is oxidised by dioxygenases, after which the oxidised $\gamma$-glutamylanilide is hydrolysed into L-glutamate (recycled towards the first oxidation reaction) and an unstable intermediate (figure 2.5), which is spontaneously oxidatively deaminated to form catechol (the same central intermediate as for phenol) and ammonia [Lyons et al., 1984; de Alexandra et al., 1994; Takeo et al., 2013]. Catechol, the central intermediate, can subsequently be degraded via ortho or meta-oxidation, where ring fission occurs between (ortho) or adjacent to (meta) the hydroxyl groups, forming compounds which are metabolised to intermediates of the Krebs cycle, ultimately releasing the aniline carbon as carbon dioxide [Lyons et al., 1984; van Schie and Young, 2000; Al-Kahlid and El-Naas, 2012].

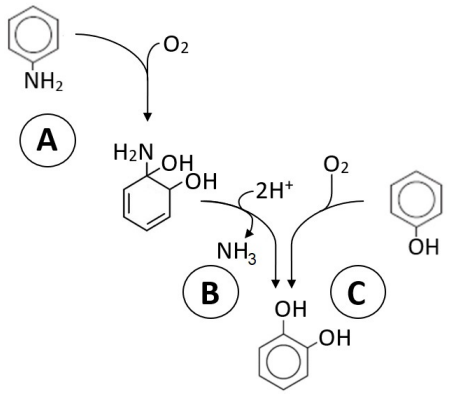


**Figure 2.5:** The aerobic upper degradation pathway of aniline and phenol to the same central intermediate: catechol. (A) Formation of $\gamma$-glutamylanilide, dioxygenase & hydrolysis; (B) Oxidative deamination; (C) Hydroxylase [Lyons et al., 1984; de Alexandra et al., 1994; van Schie and Young, 2000; Al-Kahlid and El-Naas, 2012; Arora, 2015]

.

Even though it has been shown that aerobic treatment of (petro-) chemical wastewater is able to remove phenolics and/or aniline, there are some major drawbacks. First of all, the net operating cost for aerobic treatment is significantly higher compared to anaerobic treatment due to electrical power usage for aeration, and the production of substantial amounts of biomass, which requires additional treatment and disposal [Speece, 1983]. Generally, for (petro-) chemical wastewaters that contain aromatic compounds which are biodegradable under anaerobic conditions, the presence of aromatic amines (such as aniline) requires an additional aerobic treatment step after the anaerobic treatment, thereby increasing the total costs for the treatment of such wastewaters significantly.

Additionally, Gheewala and Annachhatre [1997] found that under aerobic conditions, nitrification is severely inhibited by high aniline concentrations (100 $mg \cdot L^{-1}$). In their study, they found that nitrification was restored as soon as the aniline concentration dropped from 100 $mg \cdot L^{-1}$ to 4 $mg \cdot L^{-1}$, but the nitrifiers did not recover after exposure to aniline concentrations higher than 250 $mg \cdot L^{-1}$. Similar findings were stated by J.W. Mulder, manager Process & Technology at Evides Industriewater [email communication, December 2019]. In case of too high aniline concentration in the influent, the wastewater has to be buffered and distributed towards the treatment system at a later stage, or PAC has to be dosed to absorb the excess aniline.

### 2.4.2 Anaerobic digestion

In the past decades, AD has evolved into a competitive technology for the treatment of industrial wastewater because of its advantages with respect to aerobic treatment. For example, reduced costs for excess sludge treatment/disposal, lower operational costs, and recovery of biogas [Speece, 1983]. Because of its proven effectiveness, AD has become a technology of interest for the treatment of complex wastewaters, such as those produced in the (petro-) chemical industry.

In the AD process, a mix of microbial populations cooperate in a multi-stage process to degrade organic compounds and produce biogas. As oxygen is not available under anaerobic conditions, compounds such as $NO_3^-$, $Mn$(IV), $Fe$(III), $SO_4^{2-}$ and $CO_2$ can act as electron acceptors (figure 2.4). During the first stage (hydrolysis), the large undissolved organic polymers (e.g. lipids, polysaccharides and proteins) are broken down by enzymes into smaller dissolved molecules (e.g. long chain fatty acids, simple saccharides and amino acids). In the second stage (acidogenesis), acidogenic (fermentative) bacteria convert these dissolved compounds into VFAs, alcohols, lactic acid ($C_3H_6O_3$), carbon dioxide ($CO_2$), hydrogen gas ($H_2$), and ammonia ($NH_3$). During the third stage (acetogenesis), acetogenic bacteria produce acetate ($CH_3COO^-$), $H_2$ and $CO_2$ from VFAs. Besides, other intermediary products like alcohols, lactate, and $H_2$ + $CO_2$ are converted into acetate by these acetogenic bacteria. In the final stage (methanogenesis), aceticlastic- and hydrogenotrophic methanogens produce biogas ($CH_4$ + $CO_2$) from acetate or $H_2$ + $CO_2$ respectively.

The symbiotic relationship between these acetogens and acetate- and hydrogen scavenging methanogens is emphasised in figure 2.6: the hydrogenotrophic methanogens must maintain the partial pressure of hydrogen in the system at a very low level to maintain thermodynamic favourability and thus prevent accumulation of VFAs, thereby avoiding acidification of the fermentation broth and subsequent inhibition of the methanogens. [Speece, 1983; van Lier et al., 2008; Ziels et al., 2019]

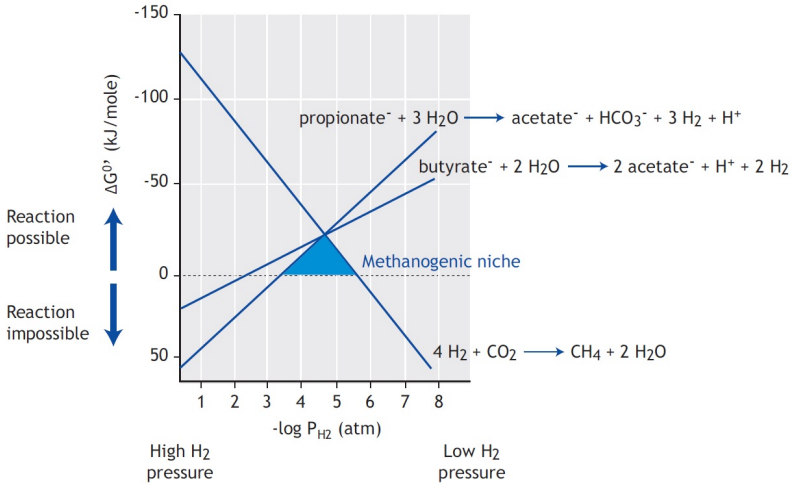


**Figure 2.6:** Thermodynamic methanogenic niche in AD, represented by the blue area in the graph. The hydrogen uptake of the hydrogenotrophic methanogens must be in balance with the hydrogen production by the acetogenic microorganisms for a stable AD process. Adopted from van Lier et al. [2008]

.

For thermodynamically unfavourable bio-transformations in the AD of organic compounds, microorganisms require a syntrophic partner (e.g. acetate- and hydrogen-scavenging methanogenic partners) which allows them to decrease the Gibbs free energy change of the reaction ($\Delta G_R$), making this bio-transformation thermodynamically favourable [Field, 2002; Ziels et al., 2019].

As aromatics are more reduced than their products, microorganisms have to get rid of the produced reducing equivalents to degrade these compounds under

anaerobic conditions. Only the microorganisms that are capable of interspecies hydrogen-transfer, such as anaerobic respiratory bacteria, anaerobic photosynthetic bacteria and fermenting bacteria, are suitable for this purpose Heider and Fuchs [1997].

Because of this syntrophic relationship and vulnerability of the methanogens in AD, it is essential to ensure sufficient mixing of the inoculum: the methanogenic bacteria must be exposed to the hydrogen produced by the acetogenic bacteria to continue the anaerobic conversion process [Speece, 1983; Liao et al., 2006]. However, shear stress should not exceed certain limits to avoid lower biomass activity due to cell disruption.

Depending on the constituents of the wastewater to be treated, one of the four main processes in AD will be rate-limiting. In many cases, especially for (semi-) solid substrates and raw cellulosic material, the rate-limiting process is hydrolysis. This is because of the inadequate free accessible particle surface area, the overall structure of the particulates, or because of the recalcitrance of lignin to AD [Speece, 1983; van Lier et al., 2008]. However, in this project, due to the absence of large organic particles and the presence of highly stable aromatics, the acetogenic process can be identified as the rate-limiting process.

#### *Anaerobic biological degradation of phenol and aniline*

Only few microorganisms are able to completely degrade aromatics under anaerobic conditions, using the aromatic substrate as carbon and energy source. Most microorganisms catalyse biotransformation (poly-) substituted aromatic compounds to the upper pathway to central intermediates, of which 3-methyl-benzoyl-CoA, 3-hydroxybenzoyl-CoA and 2-amino-benzoyl-CoA are the most common ones [Merkel et al., 1989; Koch and Fuchs, 1992; Boll and Fuchs, 1995; Heider and Fuchs, 1997; Laempe et al., 1999; Philipp and Schink, 2012]. Generally, this conversion of aromatics under anaerobic conditions to a central intermediate is initiated by either insertion of a phosphate group (i.e. "phosphorylation"), insertion of fumarate, hydroxylation ($O_2$ independent), carboxylation, or methylation [Ladino-Orjuela et al., 2016]. After these central intermediates have been formed, dearomatisation will take place in the lower pathway, where after ring cleavage the final products: carboxylic acids, $CH_4$ and $CO_2$ are formed [Heider and Fuchs, 1997; Ladino-Orjuela et al., 2016].

Tschech and Fuchs [1987; 1989] identified para-carboxylation of phenol to 4-hydroxybenzoate as the initial oxidation reaction under denitrifying conditions (figure 2.7), which is initiated by the conversion of phenol to phenylphosphate [Schülhe and Fuchs, 2004]. The phenol carboxylase appeared to be very susceptible to inactivation by oxygen, requiring strict anoxic conditions to maintain its activity [Tschech and Fuchs, 1989]. The degradation process after 4-hydroxybenzoate formation proceeds by activation with coenzyme A (CoA), required to "obtain an active site for the benzoyl-CoA reductase enzyme and to allocate the $\pi$-electrons in the aromatic ring" [Kleerebezem, 1999], followed by dehydroxylation to the central intermediate benzoyl-CoA [Tschech and Fuchs, 1987; Boll and Fuchs, 1995]. This intermediate is further degraded through the benzoyl-CoA degradation pathway, where benzoyl-CoA reductases catalyses the reduction of the ring, ultimately resulting in three molecules of acetyl-CoA [Schnell and Schink, 1991; Fuchs et al., 2011].

The benzoyl-CoA pathway is reported as the fundamental pathway for the degradation of a variety of aromatic compounds, such as hydroxybenzoates, phenylacetate, cresols, toluene, phenol, and aniline [Schink et al., 2000]. Schnell and Schink and Schink found in 1991 that *Desulfobacterium anilini* is able to degrade aniline under sulphate-reducing conditions. This microorganism degrades the aniline "via carboxylation to 4-aminobenzoate, which is activated to 4-aminobenzoyl-CoA and further metabolised by reductive deamination to benzoyl-CoA", a pathway analogous to the degradation of phenol [Schnell and Schink, 1991; Philipp

and Schink, 2012]. The equivalence of these pathways is visualised in figure ref-fig:anaerobicpathway.

Schink et al. [2000] stated that it is still unknown what mechanism provides the necessary energy for the yet unstudied carboxylation reaction, and speculated that "a primary phosphorylation as in the case of nitrate-dependent phenol degradation appears unlikely". However, from yet unpublished research performed by B. Schink, it was found that the pathway does include "phenylphosphoramidate as a transitional energy-rich intermediate" [email communication, April 2019].

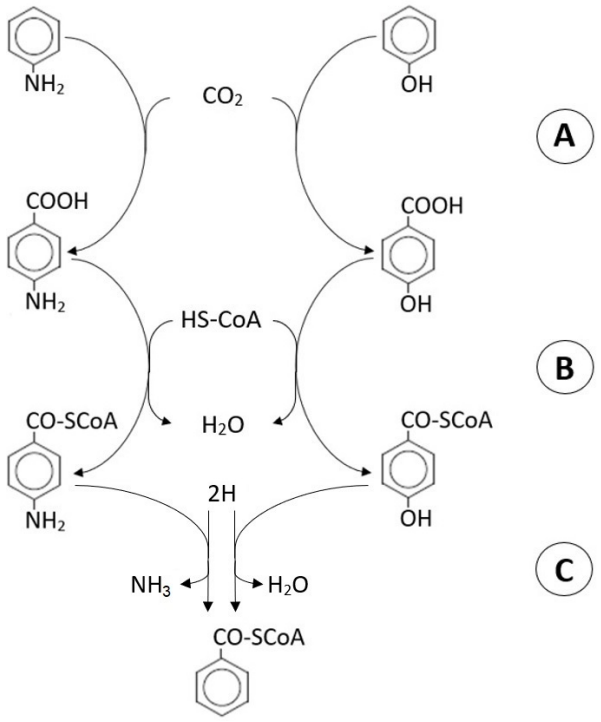


**Figure 2.7:** The analogous anaerobic degradation pathways of aniline (left) and phenol (right): (A) Carboxylation to 4-aminobenzoic acid / 4-hydroxybenzoic acid; (B) Activation to 4-aminobenzoyl-CoA / 4-hydroxybenzoyl-CoA; (C) Reductive deamination / reductive dehydroxylation where reduced ferredoxin is used as a electron donor [Tschech and Fuchs, 1987, 1989; Schnell and Schink, 1991; de Alexandra et al., 1994; Schink et al., 2000; Schülhe and Fuchs, 2004; Philipp and Schink, 2012]

.

de Alexandra et al. [1994] detected 4-hydroxybenzoate in the active aniline metabolising, bicarbonate-rich, denitrifying cultures, which was not detected in cultures without aniline mineralisation or in background controls. Based on the observation of this alternative intermediate, another hypothetical pathway was proposed where after the carboxylation and reductive deamination, hydroxylation takes place, resulting in the formation of 4-hydroxybenzoic acid [de Alexandra et al., 1994].

Schnell and Schink [1991] observed that the metabolism of both aniline and phenol under sulphate-reducing conditions was enhanced by the presence of bicarbonate, whereas the degradation of 4-aminobenzoate was not affected by the presence of $CO_2/HCO_3$. Correspondingly, results obtained by de Alexandra et al. [1994] indicated that bicarbonate enhances the anaerobic mineralisation of aniline under denitrifying conditions, hypothesising that in the absence of bicarbonate, the rate-limiting carboxylation of aniline is hampered.

The major drawback of aniline treatment under sulphate-reducing conditions is the production of hydrogen sulphide ($H_2S$), which can result in operational issues such as a reduced COD-removal, toxicity, corrosion, malodour and decreased biogas quantity and quality [Hulshoff Pol et al., 1998; van Lier et al., 2001]. Considering

the fact that reduction of sulphate to sulphide is thermodynamically favoured over the production of methane by acetogenic- and hydrogenotrophic methanogenesis, one should take measures to reduce undesirable situations during the anaerobic treatment of industrial wastewater that contains high concentrations of oxidised sulphuric compounds [Speece, 1983]. These issues can be avoided by applying a two-stage AD process, or by decreasing the unionised sulphide concentration by e.g. sulphide precipitation or pH/temperature elevations [Hulshoff Pol et al., 1998].

#### *Methanogenic aniline degradation*

Over the past decades, it was repeatedly reported that aniline degradation under methanogenic conditions has not been observed [Schink, 1988; de Alexandra et al., 1994; Razo Flores et al., 1996]. However, Yumihara et al. [2002] reported an aniline degradation efficiency of 40% after 172 days of methanogenic treatment in a up-flow anaerobic filter process (UAFP) bioreactor processing synthetic wastewater containing 500 $mg \cdot L^{-1}$ aniline as the sole carbon source. Besides, 2014 reported that aniline (10 $mg \cdot L^{-1}$ and 140 $mg \cdot L^{-1}$) degradation was observed in microcosms under both nitrate-amended and methanogenic conditions; however, methanogenic degradation was observed after a lag phase of >100 days [Sun et al., 2015].

Four different inocula obtained from a contaminated industrial site (former dye manufacturing area with aniline concentrations ranging from 6 $\mu g \cdot L^{-1}$ to 61 $mg \cdot L^{-1}$) were used: (1) sediment from a highly contaminated aquifer (HCGW), (2) sediment from a lightly contaminated aquifer (LCGW), (3) sediment from a highly contaminated canal (HCFW) and (4) sediment from a lightly contaminated canal (LCFW). Their experiments were performed in triplicate and were divided into two stages: (1) Initial aniline concentration of 10 $mg \cdot L^{-1}$ and (2) increase to 140 $mg \cdot L^{-1}$. Ten out of twelve samples showed degradation of aniline during stage 1, of which six demonstrated complete depletion after >200 days. During stage 2, degradation of aniline was found in six of the twelve samples. In addition, in recent research supervised by S. Gavazza, professor at the Federal University of Pernambuco, complete aniline degradation under methanogenic conditions was repeatedly observed within 60 days, in batch tests with aniline concentrations around 4 $mg \cdot L^{-1}$ [personal communication, December 2019].

### 2.4.3 Alternative removal mechanisms of phenol and aniline

In addition to biodegradation, it must be stressed that alternative mechanisms could result in the removal of aniline. For instance, Lyons et al. [1984] observed aniline removal as a result of evaporation and autoxidation (1% per day), and binding to humic components of sewage sludge (4%). On the other hand, Yumihara et al. [2002] found that the adsorption of aniline to suspended solids (SS) is negligibly small: 0.064 $mg \cdot gSS^{-1}$ after 172 days of continuous treatment in an UAFP bioreactor.

### 2.4.4 Microorganisms associated with aniline degradation

Analysis of the microbial community during biodegradability assays enables researchers to relate certain observations, such as degradation of specific compounds, to the relative abundance of specific microorganisms. By performing deoxyribonucleic acid (DNA)-stable isotope probing (SIP) using $^{13}C$-labelled aniline in experiments performed under methanogenic conditions, [Sun et al., 2015] aimed to identify methanogenic aniline-degrading bacteria. It was reported that, among multiple other bacterial phylotypes, "a phylotype with 92.7% sequence similarity to *Ignavibacterium album*", "a bacterial phylotype within the family *Anaerolineaceae*, but without a match to any known genus", and some phylotypes of *Acidovorax* (facultative bacteria [Huang et al., 2012]) showed accumulation of $^{13}C$, and can therefore be associated with methanogenic aniline degradation. *Anaerolineaceae*, which are also

frequently found in environments contaminated with hydrocarbons [Gray et al., 2010] and have been associated with anaerobic biodegradation of (aromatic) hydrocarbons [Yamada et al., 2006; Sherry et al., 2013]. More specifically, Rosenkranz et al. [2013] identified phylotypes of *Anaerolineaceae* as putative anaerobic phenol degraders. Besides, the fermentative genus *Ornatilinea* (classified within the family *Anaerolineaceae*) was also observed by S. Gavazza, as the expected genus responsible for methanogenic aniline degradation [personal communication, December 2019]. Furthermore, in a microaerated UASB reactor treating textile wastewater, Carvalho et al. [2020] identified *Ornatilinea* sp. with a relative abundance of 13.5% in the microbial community that was attached to the microaerator, where a relative abundance of 1–2.5% was determined in the community from the sludge bed. Regarding phenol degradation under saline conditions, *Clostridia* [Wang et al., 2017b; Muñoz Sierra et al., 2018a] and members from the *Anaerolineaceae* family [Rosenkranz et al., 2013; Wang et al., 2017a] were identified as the major putative phenol degraders, where the *C. hydroxybenzoicum* phylotype showed the ability to convert phenol to 4-hydroxybenzoate [Zhang and Wiegel, 1994]. Additionally, under methanogenic conditions the *Deltaproteobacteria* and *Clostridia* were identified as "the key syntrophic populations of phenol-degrading consortia" [Wang et al., 2017a].

The activity of microorganisms responsible for anaerobic degradation of monocyclic aromatic compounds can be affected by the presence of their intermediates. This has been reported by Kleerebezem [1999], who conducted a study regarding the methanogenic degradation of terephthalate, a monocyclic aromatic which shares the same central intermediate (benzoyl-CoA) as phenol and aniline. Kleerebezem [1999] reported that the presence of acetate and benzoate hampers the degradation of terephthalate, probably attributed to substrate inhibition. Besides, Kleerebezem [1999] found that "the terephthalate-degrading culture almost completely lost its capacity to degrade terephthalate during short periods of starvation". Short periods of starvation did not seem to affect the conversion of terephthalate and benzoate when a terephthalate-benzoate mixture was used.

### 2.4.5 Stoichiometry & thermodynamics

The standard Gibbs free energy change of the reactions ($\Delta G_R^0$) (equation 2.1) for the methanogenic aniline degradation can be assessed after derivation of the stoichiometry of the theoretical catabolic reactions. Since the carboxylation (for both phenol and aniline) seems to be the rate-limiting conversion, this is the reaction of interest. The standard Gibbs free energy of formation ($\Delta G_f^0$) and the standard enthalpy of formation ($\Delta H_f^0$) of the products of these carboxylation reactions (4-hydroxybenzoate and 4-aminobenzoate, respectively) is not available. Therefore, it was decided to focus on the conversion from aniline and phenol to benzoate.

$$\Delta G_R^0 = \sum_{i=1}^{n} Y_i^R \cdot G_{f_i}^0 \tag{2.1}$$

where:

- $\Delta G_R^0$ = standard Gibbs free energy change of reaction $R$;
- $G_{f_i}^0$ = standard Gibbs free energy of formation of compound $i$;
- $Y_i^R$ = stoichiometric coefficient for the production/consumption of compound $i$ in reaction $R$.

With the use of the elemental- and electro-neutrality balances, the catabolic reactions are derived (reactions 2.2 and 2.3). $\Delta G_R^0$ is derived from the stoichiometric coefficients ($Y_i^R$) and $G_f^0$ of the individual compounds involved in the reaction (appendix B) [Kleerebezem and van Loosdrecht, 2010].[2]

$$\begin{aligned} &- C_6H_5OH - CO_2 - H_2 + C_6H_5COO^- + H_2O + H^+ \\ &\bullet\ \Delta G_R^0 = -31.68\ kJ \cdot mol^{-1} \end{aligned} \tag{2.2}$$

$$\begin{aligned} &- C_6H_5NH_2 - CO_2 - H_2 + C_6H_5COO^- + NH_3 + H^+ \\ &\bullet\ \Delta G_R^0 = 0\ kJ \cdot mol^{-1} \end{aligned} \tag{2.3}$$

After applying equation 2.1 to reactions 2.2 and refeq:aniline, it was found that the Gibbs energy change of the catabolic conversion from phenol to benzoate under standard conditions is negative (-31.68 $kJ \cdot mol^{-1}$) and therefore thermodynamically favourable, which is not the case for the catabolic conversion from aniline to benzoate (0 $kJ \cdot mol^{-1}$). However, after applying a correction for physiological pH conditions (pH = 7) using equation 2.4[3], the Gibbs energy change for reaction 2.2 was estimated to be -71.61 $kJ \cdot mol^{-1}$, and for reaction 2.3 to be -39.93 $kJ \cdot mol^{-1}$ [Kleerebezem and van Loosdrecht, 2010].

$$\Delta G_R^{01} = \Delta G_R^0 + R \cdot T \cdot Y_{H^+}^R \cdot ln(1 \cdot 10^{-7}) \tag{2.4}$$

where:

- $\Delta G_R^{01}$ = Standard Gibbs free energy change corrected for pH 7.0;
- $R$ = ideal gas constant (=8.31446 $J \cdot K^{-1} \cdot mol^{-1}$);
- $T$ = temperature in Kelvin;
- $Y_{H^+}^R$ = stoichiometric coefficient for the protons involved in reaction $R$.

Accordingly, the actual Gibbs free energy change of the reaction ($\Delta G_R^1$) can be calculated by applying equation 2.5, thereby including the activities of all the involved reactants and products. A 0.6 $atm$ partial pressure of methane was used, and an activity corresponding to 1 $mmol \cdot L^{-1}$ was applied to all soluble compounds.

$$\Delta G_R^1 = \Delta G_R^0 + R \cdot T \cdot \sum_{i=1}^{n} Y_i^R \cdot ln(a_i) \tag{2.5}$$

where:

- $a_i$ = activity of compound $i$ involved in reaction $R$.

The catabolic reactions from aniline to benzoate and phenol to benzoate depend on the availability of hydrogen. Knowing that in a properly functioning methane-producing installation the partial pressure of hydrogen ($P_{H_2}$) is generally between $10^{-4}$ and $10^{-6}$ $atm$ [van Lier et al., 2008], the $\Delta G_R^1$ of methanogenic aniline catabolism can be plotted versus the hydrogen partial pressure (figure 2.8) and compared to the $\Delta G_R^1$ dependency of the acetogenic- and hydrogenotrophic methanogenic reactions as depicted in figure 2.6. As the $\Delta G_R^1$ of aniline and phenol metabolism is a function of the hydrogen partial pressure, a $P_{H_2}$ of $10^{-5}$ $atm$ was used for further evaluation.

2 At standard conditions, the temperature = 298.15 $K$, and the activity of all species in the reaction = 1
3 At pH 7.0, the proton activity = $1 \cdot 10^{-7}$

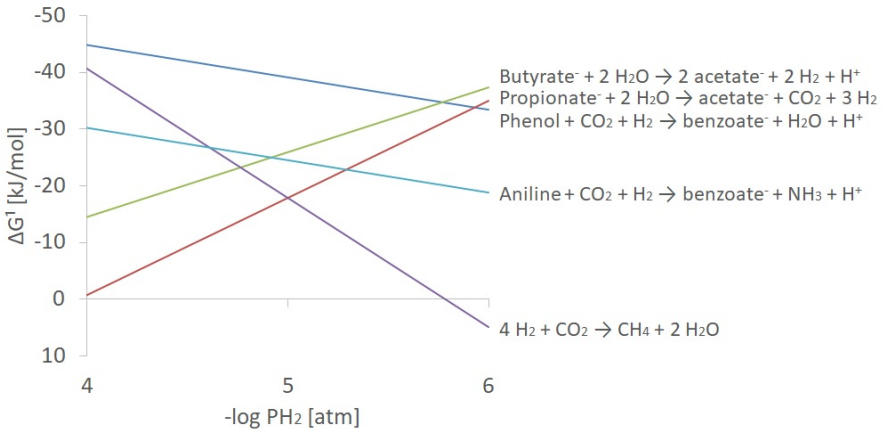


**Figure 2.8:** Actual Gibbs free energy change of methanogenic aniline- and phenol catabolism as a function of hydrogen partial pressure (T = 298.15 $K$). For comparison, the $\Delta G^1_R$ of the acetogenic- and hydrogenotrophic reactions from figure 2.6 are included. Negative $\Delta G^1_R$ values indicate that the reaction is thermodynamically favourable.

.

A temperature correction for mesophilic conditions could not be performed due to the unavailability of $\Delta H^0_f$ data for benzoate. However, for comparable conversions, the reaction generally becomes thermodynamically more favourable under mesophilic conditions (compared to standard conditions).

For estimation of the biomass yield and growth rate of possible methanogenic aniline degrading microorganisms, the following anabolic reaction was determined. Based on this $P_{H_2}$, reaction 2.6 was proposed for stoichiometry of the anabolism.

$$\begin{aligned} &-0.4 \cdot C_6H_5NH_2 - 0.23 \cdot CO_2 - 0.5 \cdot H_2O \\ &\quad + CH_{1.8}O_{0.5}N_{0.2} + 0.23 \cdot C_6H_5COO^- + 0.20 \cdot NH_3 + 0.23 \cdot H^+ \end{aligned} \tag{2.6}$$

- $\Delta G^1_R = 18.65\ kJ \cdot mol^{-1}$

By applying the Gibbs energy dissipation method [Heijnen et al., 1992; Kleerebezem and van Loosdrecht, 2010], the amount of Gibbs free energy dissipated per C-mol biomass formed ($\Delta G_{Dis}$) was estimated to be 218.1 $kJ \cdot C\text{-}mol^{-1}$ (equation 2.7). This method is based on the assumption that "microbial growth can be characterised in terms of the Gibbs energy dissipated per C-mol biomass formed" [Kleerebezem and van Loosdrecht, 2010].

$$\Delta G_{Dis} = 200 + 18(6 - NoC)^{1.8} + exp[\{(-0.2 - \gamma)^2\}^{0.16} \cdot (3.6 + 0.4 \cdot NoC)] \tag{2.7}$$

where:

- $\Delta G_{Dis}$ = Gibbs free energy dissipated per C-mol biomass formed ($kJ \cdot C\text{-}mol^{-1}$);
- $NoC$ = Carbon chain length of the carbon source (= 6 for aniline);
- $\gamma$ = oxidation state of the carbon source per C-mol (= 5.17 $e\text{-}mol \cdot C\text{-}mol^{-1}$ for aniline).

Assuming that all Gibbs free energy generated in the catabolic reaction is conserved for biomass synthesis in the metabolic reaction, equation 2.8 can be used to determine the number of times that the catabolic reaction needs to run to generate the Gibbs free energy required to form one C-mol biomass in the anabolic reaction ($\lambda_{Cat}$). For this case, $\lambda_{Cat}$ was found to be 9.65 (T = 298.15 $K$).

$$\lambda_{Cat} = \frac{\Delta G_{An} + \Delta G_{Dis}}{-\Delta G_{Cat}} \tag{2.8}$$

where:

- $\lambda_{Cat}$ = nr. of catabolic reactions per anabolic reaction;
- $\Delta G_{An}$ = Gibbs free energy change of the anabolic reaction ($kJ \cdot C\text{-}mol^{-1}$);
- $\Delta G_{Cat}$ = Gibbs free energy change of the catabolic reaction ($kJ \cdot C\text{-}mol^{-1}$).

Knowing $\lambda_{Cat}$ and the stoichiometric coefficients for the substrate (aniline) involved in the catabolic reaction ($Y_S^{Cat}$) and anabolic reaction ($Y_S^{An}$), the stoichiometry of the metabolic reaction was determined (reaction 2.9).[4]

$$\begin{aligned} &-10.05 \cdot C_6H_5NH_2 - 9.88 \cdot CO_2 - 9.65 \cdot H_2 - 0.5 \cdot H_2O \\ &\quad + CH_{1.8}O_{0.5}N_{0.2} + 9.88 \cdot C_6H_5COO^- + 9.85 \cdot NH_3 + 9.88 \cdot H^+ \\ &\bullet\ \Delta G_R^1 = -218.1\ kJ \cdot mol^{-1} \end{aligned} \tag{2.9}$$

Subsequently, the biomass yield of the metabolic reaction per mol of substrate ($Y_{X/S}^{Met}$) was estimated with the use of equation 2.10. This resulted in an estimated $Y_{X/S}^{Met}$ of 0.10 $mol$ X$\cdot mol$ S$^{-1}$ for aniline. After applying the same analysis for phenol metabolism, an estimated $Y_{X/S}^{Met}$ of 0.16 $mol$ X$\cdot mol$ S$^{-1}$ was found (T = 298.15 $K$).

$$Y_{X/S}^{Met} = [Y_S^{An} + \lambda_{Cat} \cdot Y_S^{Cat}]^{-1} \tag{2.10}$$

where:

- $Y_{X/S}^{Met}$ = biomass yield of the metabolic reaction per mol of substrate ($mol$ X$\cdot mol$ S$^{-1}$);
- $Y_S^{An}$ = stoichiometric coefficient for the substrate involved in the anabolic reaction;
- $Y_S^{Cat}$ = stoichiometric coefficient for the substrate involved in the catabolic reaction.

Finally, by applying equation 2.11 as reported by Heijnen and Kleerebezem [2010], the $\mu^{max}$ was estimated. From the catabolic reaction (2.3), it was found that the number of electrons transferred in the catabolism per mole of electron donor ($\gamma_D^*$) equals 2. For a hydrogen partial pressure of $10^{-5}$ $atm$, $\Delta G_{Dis}$ equals -218.1 $kJ \cdot C\text{-}mol^{-1}$ (equation 2.7) and $\Delta G_R^1$ equals -24.54 $kJ \cdot mol^{-1}$ (figure 2.8). Subsequently, the following assumption were made required for estimating the maximum specific growth rate ($\mu^{max}$) for the proposed metabolic reaction: (1) the maximum biomass specific rate of electron transfer ($q_e^{max}$) in the microbial electron transport chain is restricted by a maximum value of 3 $e\text{-}mol \cdot mol$ X$^{-1} \cdot h^{-1}$ at 298 $K$, (2) the biomass specific Gibbs energy production rate for maintenance purposes ($m_G$) equals 4.5 $kJ \cdot C\text{-}mol^{-1} \cdot h^{-1}$ at 298 $K$,. [Heijnen and Kleerebezem, 2010]. Based on this, the $\mu^{max}$ for aniline degrading microorganisms was estimated to be 0.19 $h^{-1}$. For phenol degrading microorganisms, the $\mu^{max}$ was estimated to be 0.29 $h^{-1}$.

$$\mu^{max} = \frac{-q_e^{max} \cdot \frac{\Delta G_{Cat}^1}{\gamma_D^*} - m_G}{\Delta G_{Dis}} \cdot exp\left\{\frac{-69 \cdot 10^3}{R}\left(\frac{1}{T} - \frac{1}{298}\right)\right\} \tag{2.11}$$

where:

- $\mu^{max}$ = maximum specific growth rate ($h^{-1}$);
- $q_e^{max}$ = maximum biomass specific electron transfer rate in the microbial electron transport chain ( $e\text{-}mol \cdot mol$ X$^{-1} \cdot h^{-1}$);
- $\gamma_D^*$ = number of electrons transferred in the catabolism per mole of electron donor;
- $m_G$ = biomass specific Gibbs energy production rate for maintenance purposes ($kJ \cdot C\text{-}mol^{-1} \cdot h^{-1}$).

4 Per definition, $\lambda_{An}$ = 1

It has to be stressed that that the approximations of $Y_{X/S}^{Met}$ and $\mu^{max}$ for the specified growth systems are overestimations of the actual $Y_{X/S}^{Met}$ and $\mu^{max}$. The estimations of $Y_{X/S}^{Met}$ and $\mu^{max}$ for the specified growth systems are strictly theoretical, and are based on simplified anaerobic degradation pathways for aniline and phenol. Additionally, these estimations highly rely on the assumption that the mechanism of electron transport is not affected.

## 2.5 ANAEROBIC MEMBRANE BIOREACTOR

In an AnMBR, the AD process is combined with membrane technology, which ensures complete retention of biomass by applying micro- or ultra- or nanofiltration modules. In general, a membrane bioreactor (MBR) offers advantages such as the production of solid-free effluents and a high operational stability [Le Clech et al., 2003; Dvořák et al., 2015]. Because of the complete retention of biomass due to uncoupling of the sludge retention time (SRT) from the hydraulic retention time (HRT), a faster start-up of an AnMBR can be achieved compared to conventional AD systems. Additionally, adaptation/acclimation of microorganisms to extreme conditions is enhanced, a higher tolerance to large organic loading rate (OLR) fluctuations is obtained, and smaller reactors are required [Liao et al., 2006; Ozgun et al., 2013; Dvořák et al., 2015].

Despite the higher capital and operational costs compared to conventional AD systems, AnMBRs provide the industry with a solution for the treatment of high strength wastewater under extreme operational conditions, such as high SS content, high salinity , high temperature and/or toxicity [Jeison and van Lier, 2008; Dereli et al., 2012; Dvořák et al., 2015]. High-rate anaerobic reactor systems such as the UASB, expanded granular sludge bed (EGSB), and internal circulation (IC), which rely on biomass granulation to achieve high performance, are able to adequately treat a wide variety of industrial wastewaters at a high OLR, but can fail when treating extreme high-strength wastewaters. The treatment of industrial wastewater under conditions that impede granule formation is associated with a reduction of the biomass retention and consequently a poor reactor performance [van Lier, 2008; Jeison and van Lier, 2008; Muñoz Sierra et al., 2018a,b]. With the application of AnMBRs, the risk of biomass 'wash-out' is eliminated, offering the possibility to retain slow-growing microorganism which are able to biodegrade recalcitrant and/or toxic constituents [Kleerebezem, 1999; Hwu et al., 1998; Liao et al., 2006; Jeison and van Lier, 2008; Galinha et al., 2018].

So far, AnMBRs have been primarily applied for the treatment of municipal and high strength industrial wastewaters, such as those produced in the food processing and pulp and paper industry [Liao et al., 2006; Dereli et al., 2012]. In recent times, research is being performed for the treatment of high-strength wastewaters under extreme conditions with the application of AnMBR technology. When treating saline, phenol-containing wastewater in an AnMBR under mesophilic conditions, Muñoz Sierra et al. [2018a] achieved COD-removal efficiencies of >99% and phenol removal efficiencies up to 99.9% at specific conversion rates of 5.1 $mgPh \cdot gVSS^{-1} \cdot day^{-1}$, and at sodium concentrations of 15 $gNa^{+} \cdot L^{-1}$. Additionally, in yet unpublished research, Victor Servando Garcia Rea, MSc. and Beatriz Egerland Bueno, MSc. have achieved complete removal of other phenolic compounds present in petrochemical wastewater, such as p-cresol and resorcinol, under saline and mesophilic conditions [personal communication, December 2019].

### 2.5.1 Operational considerations

To apply AnMBR technology for the treatment of saline industrial wastewater containing toxic compounds, such as phenolics and aromatic amines, conditions should be selected so that a high performance, regarding the removal of organic pollutants, is obtained. AnMBR configuration, membrane fouling, operational temperature and salinity in the reactor are factors that significantly influence the performance of an AnMBR.

#### *MBR configuration*

For the application of MBRs, external loop (i.e. side-stream) and submerged configurations are available. In the latter configuration, the membrane (e.g. flat-sheet or hollow fibre) is directly immersed in the reactor broth. With a continuous feed and under a constant reactor volume operation, permeate is removed continuously under a very gentle transmembrane pressure (TMP), generally 0.2-1 *bar* [Judd and Judd, 2011]. Because of the possibility to apply a low TMP to obtain a controlled and constant permeate flow, a sustainable flux can be obtained, resulting in less fouling and consequently requiring less frequent membrane cleaning [Galinha et al., 2018]. The side-stream configuration consists of a reactor that is connected to an external membrane unit. The reactor broth is pumped through the crossflow membrane in the external loop, where solid free permeate is produced and retentate is recycled to the reactor. Typically, cross-flow velocity (CFV) of 1-5 $m \cdot s^{-1}$ and a TMP of 2-7 *bar* are applied to obtain sustainable fluxes [Judd and Judd, 2011]. This configuration gives the operators the opportunity to apply different conditions in the reactor and external loop, and facilitates simple accessibility to the membrane module for maintenance. However, compared to the submerged configuration, this external loop requires additional energy input because of the continuous recirculation of the broth through the membrane module [Galinha et al., 2018].

Commercial applications regarding the paper and pulping industry rely mainly on submerged configurations [Dereli et al., 2012], where both configurations are applied in the food processing industry [Dereli et al., 2012; Dvořák et al., 2015]. The surface shear caused by the crossflow of the broth through the membrane module reduces fouling, but could affect the activity of the microorganisms because of the exposure to high stress [Liao et al., 2006; Jeison and van Lier, 2008]. On the other hand, these shear forces result in disintegration of sludge agglomerates [Dvořák et al., 2015]. From examination of reported data, Judd and Judd [2011] noted that in side-stream AnMBRs the average particle size was much smaller (3-16 $\mu m$) compared to submerged AnMBRs (65-90 $\mu m$), which is associated with a reduced membrane permeability.

#### *Membrane fouling*

A major drawback in the operation of MBRs is fouling of the membrane. This is caused by mechanisms such as pore plugging, macromolecule adsorption, and build-up of a cake layer [Le Clech et al., 2003]. Jeison and van Lier [2008] reported that the latter was the main mechanism accountable for the reduced flux due to increased filtration resistance. Besides biomass, the presence of nutrients such as ammonia ($NH_3$), magnesium ($Mg$), calcium ($Ca$), phosphorus ($P$), and potassium ($K$) in the wastewater can result in the precipitation of inorganic compounds such as (potassium-) struvite ($KMgPO_4 \cdot 6H_2O$ / $NH_4MgPO_4 \cdot 6H_2O$) and calcium carbonate ($CaCO_3$), which contribute to the build-up of such a cake layer [Dvořák et al., 2015].

Eventually, when the degree of fouling reaches a critical level, the filtration capacity of the membrane is reduced, requiring frequent physical and/or chemical cleaning processes. These include (1) applying a reversed flow to remove foulants (i.e. 'backwash' or 'backflush'), (2) ceasing the permeation (i.e. 'relaxation'), and (3)

chemical cleaning with mineral or organic acids, caustic soda, or sodium hypochlorite [Judd and Judd, 2011]. Eventually, when physical and chemical cleaning processes do not suffice because of irrecoverable fouling or damages, replacement of the membrane module is required [Judd and Judd, 2011]. Regardless of the AnMBR configuration (submerged or sidestream), substrate (VFA, VFA + glucose, or ethanol + starch + gelatine), and temperature (mesophilic or thermophilic), Jeison and van Lier [2008] observed low levels of irreversible fouling after >150 days of operation.

Vyrides and Stuckey [2011] reported that in submerged AnMBRs treating high saline wastewater, the bacteria attached to the cake layer of the membrane were able to perform biodegradation at higher rates compared to the bacteria in suspension. So, even though the cake layer in AnMBRs (especially in the submerged configuration) decreases the applicable flux, it was noted that it can improve the quality of the effluent.

#### *Temperature: mesophilic vs. thermophilic*

AD can be performed in a wide range of temperatures. Where most high-rate anaerobic wastewater treatment systems are operated at temperatures between 30 and 40°$C$, in some cases the AD process can be enhanced by applying higher temperatures [van Lier et al., 2001]. Even though it has been reported that under thermophilic conditions (generally 55 °$C$) significantly higher OLR can be achieved because of the high hydrolytic activity, there are some major drawbacks compared to mesophilic conditions (generally 35 °$C$) [van Lier et al., 1997, 2001; Goberna et al., 2010].

First of all, under thermophilic conditions the biological process is vulnerable to acidification due to accumulation of VFAs, especially if fed with concentrated wastewater [van Lier et al., 1997]. This accumulation of VFAs can inhibit microbial activity and consequently affect the reactor performance [Dvořák et al., 2015]. Additionally, as stated by Jeison and van Lier [2008], after 60 days of operation the critical flux of a submerged AnMBR under thermophilic conditions is significantly lower (6-7 $L \cdot m^{-2} \cdot h^{-1}$ ($LMH$)) compared to mesophilic conditions (15 $LMH$). This is in correspondence with the findings of Lin et al. [2009], who reported a 5-10 times higher filtration resistance in submerged AnMBRs under thermophilic conditions compared to mesophilic conditions. The lower critical flux under thermophilic conditions is mainly because of a smaller sludge particle size due to a higher biomass decay rate, higher concentrations of soluble microbial products, biopolymer clusters and fine flocs (<15 $\mu m$) [Lin et al., 2009]. Besides, it was reported that at thermophilic conditions, the degree of fouling caused by struvite increased compared to mesophilic conditions, due to increased concentrations of nitrogen in the form of ammonia [Meabe et al., 2013].

Regarding the effect of temperature on the degradation of stable aromatic compounds, Muñoz Sierra et al. [2018b] found that, after performing a stepwise temperature increases by 5°$C$, the phenol conversion rates of the AnMBR decreased from 3.16 at 35°$C$ to 2.10 $mgPh \cdot gVSS^{-1} \cdot d^{-1}$ at 45°$C$, and further decreased to 1.63 $mgPh \cdot gVSS^{-1} \cdot d^{-1}$ at 50°$C$. At the same time, the COD removal efficiency dropped from 99.8% at 35°$C$ to 38% at 55°$C$. Additionally, Muñoz Sierra et al. [2018b] observed that the degradation process of phenol was less affected by the increasing temperature than the methanogenic process.

#### *Growth under saline conditions*

Nonextremophilic microorganisms, widely applied in conventional wastewater treatment systems, are not able to degrade organic matter under extreme saline conditions [Le Borgne et al., 2008]. However, some microorganisms are metabolically different, which enables them to thrive at high salt concentrations. These microorganisms can be categorised as halophilic [Le Borgne et al., 2008]. Where halophiles require salt for growth, halotolerant microorganisms are characterised

by their ability to grow in both saline and non-saline environments. It has been shown that both halophilic and halotolerant inocula can be applied for anaerobic treatment of saline wastewaters [Lefebvre et al., 2007].

Two main mechanisms for growth under saline conditions have been recognised. (1) Halophilic archaea are able to accumulate intracellular potassium and chloride in order to maintain the osmotic balance of the cytoplasm, requiring adaptation of the intracellular enzymes to function under saline conditions [Margesin and Schinner, 2001; Le Borgne et al., 2008]. Several studies support this theory: Gagliano et al. [2017] found that in a UASB reactor, the inhibitive effect of 20 $gNa^+ \cdot L^{-1}$ is reduced after addition of 0.7 $gK^+ \cdot L^{-1}$, and Muñoz Sierra et al. [2018a] showed that under saline conditions, higher COD removal and methane production rates were achieved at higher $K^+ : Na^+$ ratios. And (2), since the intracellular enzymes of halophilic and halotolerant bacteria have no special salt tolerance, the osmotic balance of the cytoplasm has to be maintained by the biosynthesis of various uncharged and highly water-soluble osmoprotectants. Production and accumulation of these (organic) osmotic solutes neutralises the difference between internal- and external osmotic pressure [Margesin and Schinner, 2001].

Despite their salt tolerance, there are salt concentrations in which halophilic and halotolerant microorganisms cannot grow anymore. Reported values for the inhibition of the methanogenic activity of the biomass by sodium depend on the microbial acclimatisation to saline conditions. Feijoo et al. [1995] reported an overview of $IC_{50}$ values of sodium for the SMA of non-adapted biomass, ranging between 4.4 and 17.7 $gNa^+ \cdot L^{-1}$. For anaerobic biomass obtained from a full-scale UASB reactor treating saline industrial wastewater, an $IC_{50}$ of 23 $gNa^+ \cdot L^{-1}$ for the SMA was reported by Muñoz Sierra et al. [2017].

Salinity fluctuations in the growth medium of microorganisms exposes the cell to changing osmotic pressures. External osmotic pressure decrease induces a water influx, followed by swelling or even lysis, while an osmotic pressure increase induces a water efflux, resulting in cell dehydration [Wood, 2015]. These water fluxes influence properties of the cell, which have major consequences for many biological wastewater treatment processes. For instance, it could result in decreased biodegradation or decreasing VSS concentrations [Abou-Elela et al., 2010; Yogalakshmi and Joseph, 2010; Muñoz Sierra et al., 2018a; Gao, 2019]. Besides, results from Yogalakshmi and Joseph [2010] and Muñoz Sierra et al. [2018a] indicate that high sodium chloride concentrations and $NaCl$ shock loads induce disintegration of biomass granules and flocs, resulting in a more suspended biomass with poor settling characteristics. For granular sludge based anaerobic high-rate reactors, like the UASB and EGSB reactors, which require optimal settling characteristics to minimise biomass washout, a decreasing sludge volume index caused by high salinity is a significant issue [van Lier, 2008; Ismail et al., 2008].

Lefebvre et al. [2007] found that the impact of an increase in sodium chloride concentration on the activity of the biomass depends on the complexity of the substrate. In this study, the same sludge inoculated in two different reactors was exposed to either a complex substrate (distillery vinasse) or a simple substrate (ethanol) followed by increasing saline stress. Inhibition and decrease in microbial diversity caused by saline stress were more severe with a complex substrate (distillery vinasse) than with a simple substrate (ethanol). It was hypothesised that complex substrates might require a larger variety of microorganisms for its degradation, resulting in a higher vulnerability and sensitivity of the biomass to saline stress compared to inocula degrading a simple substrate such as ethanol.

The difference in the sensitivity to sudden salinity changes in aerobic- and anaerobic biomass was discussed by Vyrides and Stuckey [2009]. Besides the observation that the removal efficiency of aerobic biomass was more susceptible to a salinity decrease than a salinity increase, it was found that by comparing the activity of aerobic and anaerobic biomass, a better performance of the anaerobic biomass was observed after a sudden change from saline to non-saline conditions [Kinncannon

and Gaudy, 1966; Burnett, 1974]. Experiments conducted by Vyrides and Stuckey [2009] are in correspondence with the aforementioned findings: only temporary deactivation of the anaerobic bacteria caused by high salinity (40–50 $gNaCl \cdot L^{-1}$) was observed.

# 3 MATERIALS & METHODS

## 3.1 BIOMASS CHARACTERISATION

### 3.1.1 Source of the anaerobic biomass for experimental purposes

#### *Biomass for the anaerobic membrane bioreactor*

Mesophilic anaerobic granular sludge, with a VSS concentration of $34.9 \pm 0.5\ g \cdot L^{-1}$, extracted from a full-scale UASB reactor treating petrochemical wastewater (Shell, Moerdijk, NL), was used as seed sludge for the AnMBR (table 3.1). The granular biomass was tested for its ability to degrade aniline and phenol in synthetic wastewater in the continuous experiment in the AnMBR. The inoculum was adapted to saline wastewater ($\approx 8\ gNa^{+} \cdot L^{-1}$). Previous studies showed that, after acclimation, this sludge is able to degrade phenol under saline conditions [Muñoz Sierra et al., 2018a; Gao, 2019]. During AnMBR operation, 500 $mL$ of inoculum ($32.0 \pm 1.0\ gVSS \cdot L^{-1}$) from an IC reactor treating azo dye-containing textile wastewater (Ten Cate, Nijverdal, NL) was added to the AnMBR.

#### *Biomass for the biodegradability assays*

Sludge from three different sources (table 3.1) was used for performing BAs. (1) Mesophilic anaerobic granular biomass, extracted from a full-scale UASB reactor treating petrochemical wastewater (Shell, Moerdijk, NL). (2) Inoculum from an AnMBR (operated by the BioXtreme research group) treating bitumen condensate. (3) Inoculum from an AnMBR (operated during this research) treating synthetic aniline wastewater.

**Table 3.1:** Definitions of the used biomass, its source, and its application in this research.

| Biomass | Source | Application |
|---|---|---|
| UASB reactor sludge | Granular biomass originating from an UASB reactor treating petrochemical wastewater (Shell, Moerdijk, NL). | BAs, SMA test & SMA-inhibition tests, adsorption tests, AnMBR |
| Bitumen sludge | Biomass developed during the BioXtreme project, with the aim to degrade bitumen condensate under mesophilic conditions in an AnMBR. | BAs |
| Aniline sludge | Biomass developed during this project, with the aim to degrade aniline under mesophilic conditions in an AnMBR. | BAs |
| Thermophilic sludge | Biomass originating from a thermophilic reactor (Wabico B.V., Waalwijk), treating residues and wastewater from egg processing plants and slaughter houses | adsorption tests |
| IC reactor sludge | Biomass originating from an IC reactor (Ten Cate, Nijverdal) treating textile wastewater which contain azo dye | AnMBR |

#### *Biomass for adsorption experiments*

Sludge from two different sources was used for assessing the adsorption of aniline to biomass and other constituents in the broth under mesophilic conditions (table 3.1). (1) Sludge from a thermophilic reactor treating wastewater and residues from slaughterhouses and egg processing plants (Wabico B.V., Waalwijk, NL), and (2) mesophilic UASB reactor granular sludge treating industrial wastewater (Shell, Moerdijk, NL).

### 3.1.2 Total- & volatile suspended solids

The VSS concentration of the sludge ($gVSS \cdot L^{-1}$) is usually used as a measure of the amount of biomass in the solution. However, it should be noticed that the amount of VSS is an approximation of the amount of biomass, since not all VSS consists of active biomass [Spanjers and Vanrolleghem, 2016]. For the determination of the biomass concentration during the experiments, measured in $gVSS \cdot L^{-1}$, the standard method was used, as elucidated by Rice et al. [2012] (equation 3.1). The TSS concentration ($gTSS \cdot L^{-1}$) is determined correspondingly (equation 3.2). The initial TSS and VSS values for the used inocula are listed in table 3.2.

$$VSS = \frac{W_2 - W_3}{V} \tag{3.1}$$

$$TSS = \frac{W_2 - W_1}{V} \tag{3.2}$$

where:

- $W_1$ = weight ($g$) of the metal tray + 0.7 $\mu m$ glass-fibre filter (Merck Millipore Ltd.) after being ignited in the muffle oven (P330 Nabertherm, DE) at 550°$C$ for >2.5 $h$;
- $W_2$ = weight ($g$) of the tray + filter + filtered sample after heating in a constant climate chamber (HPP110 Memmert, DE) at 105°$C$ for >12 $h$;
- $W_3$ = weight ($g$) of the tray + filter + filtered sample after being ignited in the muffle oven at 550°$C$ for >2.5 $h$;
- $V$ = volume ($L$) of the extracted biomass sample.

**Table 3.2:** Initial TSS and VSS concentrations of the sludge, required for performing the SMA tests and BAs. The ± symbol indicates the standard deviation (SD), with sample size ($n$)=3.

| **Biomass** | **Total suspended solids** | **Volatile suspended solids** |
|---|---|---|
| | $[gTSS \cdot L^{-1}]$ | $[gVSS \cdot L^{-1}]$ |
| UASB reactor sludge | 50.3 ±0.8 | 34.9 ±0.5 |
| Bitumen sludge | 9.3 ±0.03 | 5.4 ±0.05 |
| Aniline sludge | 42.4 ±0.3 | 16.0 ±0.4 |
| Thermophilic sludge | 35.4 ±0.01 | 24.9 ±0.01 |
| IC reactor sludge | 41.2 ±1.3 | 32.0 ±1.0 |

### 3.1.3 Specific methanogenic activity of the UASB reactor sludge

The specific methanogenic activity of the UASB reactor biomass was assessed by performing an SMA test ($n$=3). Macro- and micronutrient solutions were supplied based on the feed COD-content (1.53 $mL$ of macronutrient solution per $g$COD, and 0.76 $mL$ of micronutrient solution per $g$COD). Phosphate buffer solutions were added to maintain a neutral pH and a $K^+ : Na^+$ mass ratio of 0.05 $gK \cdot gNa^{-1}$ [Muñoz Sierra

et al., 2018a]. The sodium concentration was maintained at 8.0 $g \cdot L^{-1}$ by the addition of $Na^{+}$ as $NaCl$. The inoculum (34.9 $\pm$ 0.5 $gVSS \cdot L^{-1}$) and medium solution ($NaCl$, micronutrient solution, macronutrient solution, phosphate buffer solutions, and acetate) were supplied to a 500 $mL$ Schott-Duran bottle, with a final liquid volume of 180 $mL$. Acetate at a concentration of 0.5 $gCOD \cdot L^{-1}$ was included to activate the biomass before the start of the SMA test.

The bottles were incubated in a temperature-controlled shaker (Innova®40, Eppendorf/New Brunswick Scientific) at 35°C and 130 rotations per minute (*RPM*), and were connected to the AMPTS (Bioprocess Control, SE). To ensure anaerobic conditions, the reactors were flushed for 2 minutes with a $N_2/CO_2$ (80%/20%) gas mixture. Methane production, as accumulated volume, was measured online using the AMPTS following the specifications of the manufacturer. After the depletion of the acetate for the biomass activation, the SMA test was started by dosing 20 $mL$ of substrate solution (acetate + demiwater + $NaCl$), to achieve a final volume of 200 $mL$ and an acetate COD of 2.0 $g \cdot L^{-1}$.

The modified Gompertz three-parameter model (figure 3.1 and equation 3.3) is an acknowledged model generally used to describe growth in biological systems. Zwietering et al. [1990] reported that the Gompertz model can be regarded as a suitable model to describe growth data, considering its performance and simplicity. Therefore, this sigmoidal model was applied to describe the cumulative methane production in the SMA test. After applying the Gompertz model, the maximum methane production rate was calculated.

$$y = A \cdot exp\left\{ -exp\left[ \frac{\mu_m \cdot e}{A} \cdot (\lambda - t) + 1 \right] \right\} \tag{3.3}$$

where:

- $t$ = time (hour);
- $y$ = cumulative methane production ($NmL_{CH_4}$);
- $\lambda$ = lag period (hour);
- $\mu_m$ = maximum methane production rate ($NmL_{CH_4} \cdot hour^{-1}$);
- $A$ = asymptote as t $\rightarrow \infty$ (i.e. the ultimate methane yield in $NmL_{CH_4}$);
- $e$ = Euler's number (= 2.718281).

Parameter estimation was performed with MATLAB R2018B (The MathWorks, Inc., USA), using a modification of the script for the four parameters logistic regression model, developed by Cardillo [2012] (appendix C). After the estimation of $\mu_m$ for each condition, the maximum SMA in $mgCOD_{CH_4} \cdot gVSS^{-1} \cdot day^{-1}$ was determined by dividing $\mu_m$ by the total amount of biomass in the flask (gVSS) and the theoretical volumetric methane production (= 350 $mL \cdot gCOD^{-1}_{CH_4}$ under normal conditions; $T$ = 0 °C & $P$ = 1.013 $bar$).

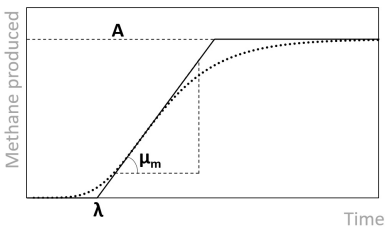


**Figure 3.1:** Sigmoidal curve with lag period '$\lambda$', maximum production rate '$\mu_m$' and asymptote '$A$'.

## 3.2 EXPERIMENTAL SETUP: BATCH TESTS

### 3.2.1 Biodegradability assay

The biodegradation of aniline under methanogenic conditions was assessed with the use of BAs. The BAs were performed following the biochemical methane potential protocol proposed by Angelidaki et al. [2009], for three different inocula: (1) UASB reactor sludge, (2) bitumen sludge, and (3) aniline sludge (table 3.1).

To decrease the residual COD, the sludge from the UASB reactor was pre-digested in a temperature-controlled shaker (Innova®44, Eppendorf/New Brunswick Scientific) at 35 ± 1°C and 130 *RPM* for 4 days before usage. After 4 days of preincubation, the soluble COD was 0.3 $gCOD \cdot L^{-1}$. For the bitumen sludge nearly complete COD removal was achieved by the AnMBR. The biomass of the aniline sludge was washed before usage, to ensure the removal of residual aniline from the biomass. Washing was performed by centrifuging (Heraeus™ Labofuge™ 400, Thermo Fisher Scientific) the biomass at 2,383·$g$ for 10 minutes at 22°C. After centrifugation, the supernatant was disposed, and the biomass pellet was diluted with a saline solution (8 $gNa^{+} \cdot L^{-1}$), followed by another cycle of centrifuging, disposal of the supernatant and dilution.

For the preparation of the BAs with UASB reactor- and bitumen sludge as inoculum, 160 $mL$ glass assay bottles were filled to obtain a liquid volume of 130 $mL$ (0.5 $gVSS \cdot L^{-1}$). Aniline concentration in these assays were 100 $mg \cdot L^{-1}$ (266 $mgCOD \cdot L^{-1}$). Inoculum/substrate ratio in the test bottles was 2 $gVSS \cdot gCOD^{-1}$ Spanjers and Vanrolleghem [2016]. For the BAs with aniline sludge as inoculum, 160 $mL$ glass assay bottles were filled to obtain a liquid volume of 150 $mL$ (2.0 $gVSS \cdot L^{-1}$). Aniline concentrations of 10 and 20 $mg \cdot L^{-1}$ (26.6 and 53.2 $mgCOD \cdot L^{-1}$) were applied, resulting in an inoculum/substrate ratio of 37.5 and 75 $gVSS \cdot gCOD^{-1}$. As control, an equivalent amount of glucose (26.6 $mgCOD \cdot L^{-1}$) was added as carbon and energy source. Sodium chloride, nutrient media and phosphate buffer solutions were added in agreement with the requirements as described in section 3.1.3. Samples (1 $mL$) were extracted and analysed by gas chromatography (GC) to determine the initial conditions, regarding the aniline concentration. The protocol for analysis by GC is discussed in section 3.4.1.

The serum bottles were closed with rubber stoppers, sealed with an aluminium crimp, flushed for 2 minutes with $N_2/CO_2$ (80%/20%) gas mixture, and incubated at 35°C in the dark in a constant climate chamber (HPP110 Memmert, DE). The solutions were manually shaken three times a week. Gas production was measured with a digital manometer. A 0.5 $mL$ gas sample was extracted from the headspace in case a pressure increase was measured, and analysed by GC. Subsequently, the volume of methane produced was derived using the ideal gas law (equation 3.4). After extraction of the gas sample, the pressure in the bottles was measured as reference for the next measurements. An overview of the conditions in the BAs is provided in table 3.3.

$$P \cdot V = n \cdot R \cdot T \tag{3.4}$$

where:

- $T$ = temperature ($K$);
- $R$ = gas constant (= 8.3145·$10^{-2} L \cdot bar \cdot K^{-1} \cdot mol^{-1}$);
- $n$ = number of moles ($mol_{gas}$);
- $P$ = pressure ($bar$);
- $V$ = volume ($L$).

Table 3.3: Overview of the conditions applied in the BAs.

| Parameter | Unit | Biomass | | | | | | |
|---|---|---|---|---|---|---|---|---|
| | | UASB | Bitumen | Aniline | | | | |
| | | | | 1 | 2 | 3 | 4 | 5 |
| Aniline | $mgCOD \cdot L^{-1}$ | 266 | 266 | 53.2 | 26.6 | 26.6 | | 53.2 |
| 4-aminobenzoic acid | $mgCOD \cdot L^{-1}$ | | | | | 26.6 | 53.2 | |
| Bicarbonate | $mM$ | | | | | | | 30 |
| Inoculum/Substrate | $gVSS \cdot gCOD^{-1}$ | 2 | 2 | 37.5 | 75 | 37.5 | 37.5 | 37.5 |
| Headspace volume | $mL$ | ±30 | ±30 | ±10 | ±10 | ±10 | ±10 | ±10 |

### 3.2.2 Inhibition & toxicity

#### *Inhibition of methanogenic activity by exposure to aniline and phenol*

The inhibitory effect of aniline and phenol on the aceticlastic methanogenesis of UASB reactor sludge was assessed by performing a series of SMA tests, as described in subsection 3.1.3. An inoculum to substrate ratio of 2.0 $gVSS \cdot gCOD^{-1}$ was used, corresponding to a concentration of 2 $g \cdot L^{-1}$ for the acetate and 4 $gVSS \cdot L^{-1}$ for the biomass. Sodium chloride, nutrient media and phosphate buffer solutions were added in agreement with the requirements as described in section 3.1.3. The inoculum and medium solution ($NaCl$, micronutrient solution, macronutrient solution, phosphate buffer solutions, and acetate) were supplied to a 500 $mL$ Schott-Duran bottle, with a final liquid volume of 180 $mL$. For the blank, the same solution was prepared without the addition of acetate.

For the determination of the $IC_{50}$ of aniline for the aceticlastic methanogenesis, aniline concentrations ranging from 0 $mg \cdot L^{-1}$ to 4,000 $mg \cdot L^{-1}$ were used. For phenol, concentrations ranging from 0 $mg \cdot L^{-1}$ to 2,000 $mg \cdot L^{-1}$ were used. The SMA-inhibition tests for aniline and phenol were divided over three and two batches, respectively. Triplicates were used for both the blanks and the conditions. The bottles were flushed, incubated, and connected to the AMPTS as described in section 3.1.3. After the depletion of the acetate for the biomass activation, the SMA-inhibition tests were started by injecting 20 $mL$ of solution (acetate + $NaCl$ + specified amount of aniline or phenol) to achieve a final volume of 200 $mL$ and an acetate COD of 2.0 $g \cdot L^{-1}$.

After performing the SMA-inhibition tests, the maximum SMAs were determined as described in subsection 3.1.3. Subsequently, a four-parameter logistic regression model (equation 3.5) was applied to estimate the $IC_{50}$ of these compounds for the aceticlastic methanogenic population.

$$SMA = A_{min} + \frac{A_{max} - A_{min}}{\left(1 + (\frac{x}{IC_{50}})^{H}\right)} \tag{3.5}$$

where:

- $x$ = concentration of inhibitor ($g \cdot L^{-1}$);
- $A_{min}$ = minimum asymptote (i.e. the SMA in $mgCOD_{CH_4} \cdot gVSS^{-1} \cdot day^{-1}$ as $x \to \infty$);
- $A_{max}$ = maximum asymptote (i.e. the SMA in $mgCOD_{CH_4} \cdot gVSS^{-1} \cdot day^{-1}$ at $x$ = 0);
- $H$ = Hill slope (-);
- $IC_{50}$ = half maximal inhibitory concentration ($g \cdot L^{-1}$).

The Hill slope represents the steepness of the dose-response curve. The estimated $IC_{50}$ from the regression model is obtained from the inflection point of the graph, defined as the point in the graph where the sign or direction of the curvature changes (i.e. $x$ where SMA = $(A_{max} - A_{min})/2$). The regression was performed with MATLAB R2018B (The MathWorks, Inc., USA), using the script for the four parameters logistic regression model, developed by Cardillo [2012].

### *Toxicity of aniline and phenol to the anaerobic biomass*

The effect of aniline and phenol on the CMI of the microbial cells was used as a measure of toxicity of the compounds. The cell viability of the anaerobic granular biomass was assessed at the start and the end of the SMA-inhibition tests; thus, after exposure to either aniline (0-4,000 $mg \cdot L^{-1}$) or phenol (0-2,000 $mg \cdot L^{-1}$). Samples were taken by extracting 100 $\mu L$ of medium from the test bottles. The biomass was prepared according to the protocol described by Falcioni et al. [2006]: (1) The samples were diluted 1:500 (v/v) with 0.22 $\mu m$ filtered phosphate-buffered saline (PBS) solution (137 $mM$ $NaCl$, 2.7 $mM$ $KCl$, 10 $mM$ $Na_2HPO_4$, 2 $mM$ $KH_2PO_4$, in ultrapure water). (2) Sonication with a digital sonifier (Branson, U.S.) in 3 cycles of 45 seconds at 100$W$. (3) Dilution 1:500 (v/v) with 0.22 $\mu m$ filtered PBS solution.

For the staining of the cells, SYBR® Green I (SG) nucleic acid gel stain (Invitrogen/ Molecular Probes S7563) and propidium iodide (PI) (Invitrogen/Molecular Probes P1304MP) were used to prepare the SG and SGPI working solutions (see appendix F) [Grégori et al., 2001]. Because SG stains all cells and PI will only stain cells with damaged membrane, a combination of these stains can be used to assess the CMI of the samples [Barbesti et al., 2000]. For the staining protocol, 495 $\mu L$ of each sonicated sample was mixed with 5 $\mu L$ of SG working solution, and another 495 $\mu L$ was mixed with 5 $\mu L$ of SGPI working solution. The stained mixtures were homogenized using a vortex for 3 seconds, and incubated at 37°$C$ for 10 minutes.

The measurements were performed using a BD Accuri® C6 flow cytometer (BD Accuri® cytometers, Belgium), equipped with a 50-$mW$ laser which emits a fixed wavelength of 488 $nm$. The green fluorescence intensity was collected at 533±30 $nm$, and the red fluorescence intensity at >670 $nm$. Sideward and forward scattered light intensities ("SSC" and "FSC") were collected as well. The flow cytometer was equipped with volumetric counting hardware, calibrated to measure the number of particles in 50 $\mu L$ of a 500 $\mu L$ sample [Prest et al., 2013]. The samples (50 $\mu L$) were measured at a flow rate of 66 $\mu L \cdot min^{-1}$. SG fluorescence was detected on the green fluorescence channel (FL1-H), and PI fluorescence was detected on the red fluorescence channel (FL3-H). To exclude cell debris, a threshold value of 800 was applied to FL1-H, and to identify background response, blanks (PBS+SG and PBS+SGPI) were analysed. The obtained data was processed using FlowJo (v10.6.1) software (Becton Dickinson, U.S.). After comparison of the output from the blanks (background identification) with the output from the stained cell suspensions, a polygon (gate) can be defined which includes the events corresponding to all the cells stained with SG or cells stained with SGPI (C and D in figure 3.2, respectively). The number of stained cells (SG vs. SGPI) within the drawn polygon were counted and compared with each other, from which the viability of the cell suspension was determined using equation 3.6. The decrease in the CMI with respect to the average output of the positive control group of the corresponding session (not exposed to aniline/phenol) was determined by comparing the number of cells with non-damaged membranes in the sample obtained at the beginning of the SMA-inhibition test with the number of cells with non-damaged membranes at the end of the experiment, i.e. after exposure to aniline or phenol (equation 3.7). To obtain negative controls, three different methods were applied: granular biomass was either (1) sterilized for 30 minutes at 121°$C$ and 15 $psi$ in an autoclave, (2) exposed to 70% ethanol for 30 minutes, or (3) exposed to 0.5% formaldehyde for 72 hours. Finally, the CMI of the exposed cell suspension with respect to the average viability of the positive control group ($V_{res}$) was plotted versus the concentration of toxicant, from which the $LC_{50}$ can be estimated by applying the four-parameter logistic regression model (equation 3.5).

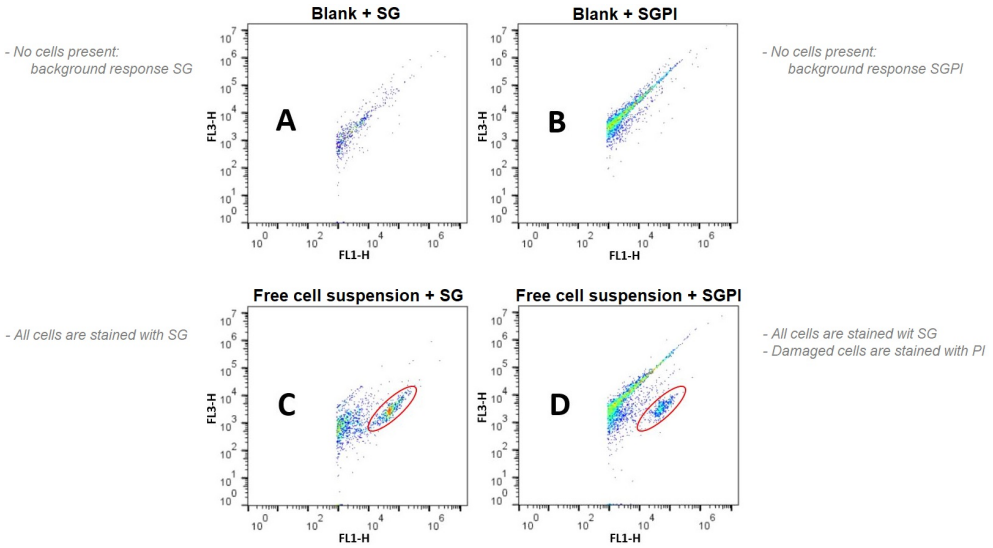


**Figure 3.2:** Processing of the FC data in FlowJo. The horizontal axis corresponds with the green fluorescence channel (FL1-H), and the vertical axis corresponds with the red fluorescence channel (FL3-H). The upper two graphs correspond to the blanks, either with SG (A) or SGPI (B). Graphs (C) and (D) depict the samples stained with SG and SGPI, respectively. A gate was drawn to compare the number of stained cells (SG (C) vs. SGPI (D)) within the drawn polygon with each other, from which the viability of the cell suspension was determined.

$$V[\%] = \frac{n_{SGPI}}{n_{SG}} \cdot 100\% \tag{3.6}$$

$$V_{res}[\%] = \left(\frac{V_{final}}{V_{initial}}\right)\left(\frac{V_{final,(control)}}{V_{initial(control)}}\right)^{-1}_{average} \cdot 100\% \tag{3.7}$$

where:

- $n$ = number of cells in the gate (-);
- $V$ = percentage of viable cells (%);
- $V_{res}$ = viability of the exposed cell suspension with respect to the average viability of the positive control group (%).

## 3.3 EXPERIMENTAL SETUP: ANMBR

A schematic diagram of the AnMBR used in the continuous experiments is provided in figure 3.3. The AnMBR consisted of a reactor with a volume of 7.0 $L$ and working volume of 6.5 $L$, connected to an external ultra-filtration (UF) polymeric membrane module with 30 $nm$ mean pore size (Pentair, U.S.). The characteristics of this membrane are summarized in table 3.4. The temperature in the AnMBR was maintained at 35 $\pm$ 1°C using a thermostatic water bath (Tamson TC16, NL). A recirculation pump (Watson-Marlow 540Du, UK) was used to pump the bulk biomass into the external polymeric membrane module. The membrane worked with a flux of 6.0 $LMH$ corresponding to a flow of 1.5 $L \cdot day^{-1}$. The AnMBR feed solution was dosed to the reactor with a pump (Watson-Marlow 120U, UK). The permeate was obtained using a pump (Watson-Marlow 120U, UK), while the retentate was recirculated into the AnMBR. The applied CFV through the membrane module was 1 $m \cdot s^{-1}$. Three

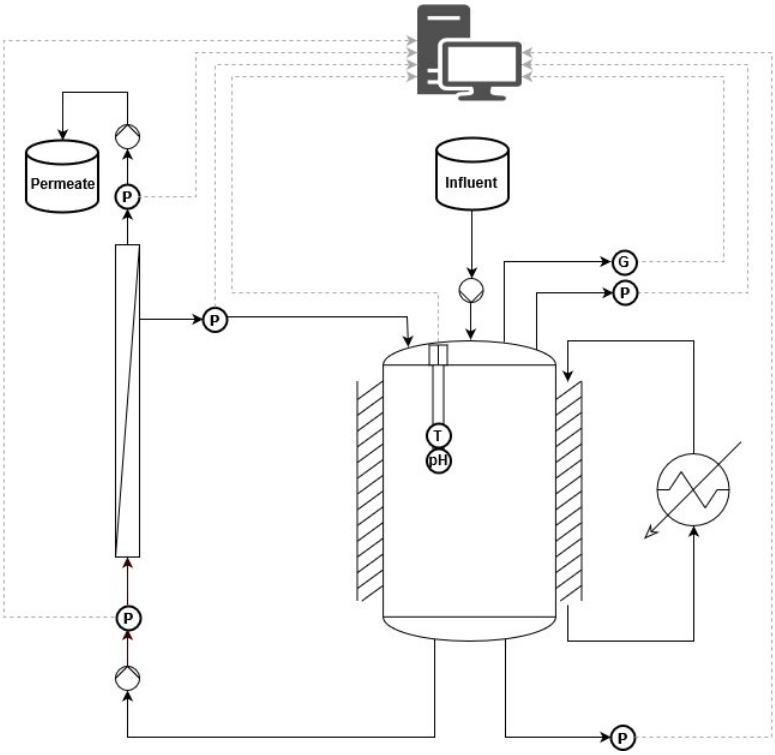


**Figure 3.3:** Schematic overview of the AnMBR used in the continuous experiments. The pressure sensors, gas meter, temperature- & pH sensor are indicated in the figure by P, G, T and pH, respectively. The specifications of the membrane are listed in table 3.4.

pressure sensors (AE Sensors ATM [-800-600 *mbar*], NL) were used to measure the pressures at the membrane module inlet, -outlet and -permeate exit. The TMP was calculated based on the pressure at the membrane module inlet, -outlet and -permeate exit, automatically carried out by the LabVIEW software. The produced biogas was measured with a gas meter (Ritter MGC-10 PMMA R, DE). The AnMBR filtration cycle was as follows: (1) 500 *s* of filtration, (2) 10 *s* of backwash.

Chemical cleaning was performed when a TMP of >250 *mbar* was reached, by immersing the membrane in a 300 *ppm* sodium hypochlorite (*NaOCl*, active chlorine) solution for 3 hours to remove organic matter, after which the membrane module was immersed in a 5 $g \cdot L^{-1}$ citric acid ($C_6H_8O_7$) solution for 3 hours to remove inorganic matter.

**Table 3.4:** Characteristics of the polymeric UF membrane used in the AnMBR configuration [Pentair, 2015].

| **Pentair X-Flow Compact 33 Ultrafiltration Membrane** | |
|---|---|
| Material | polyvinylidene fluoride (PVDF) |
| Configuration | capillary tube (CT) |
| Hydraulic membrane diameter | 5.2 *mm* |
| Membrane length | 0.64 *m* |
| Mean pore size | 30 *nm* |
| Membrane surface area | 0.0105 $m^2$ |

The AnMBR was fully automated and controlled. LabVIEW software (version 15.0.1f1, National Instruments, USA) developed by Carya (Carya, NL) was used to register and monitor all the data obtained from the sensors online and in real time. For volume control in the reactor, the gas pressure in the AnMBR was measured with a pressure sensor (AE Sensors ATM [0-20 *mbar*], NL) in the headspace, and the total pressure (hydrostatic + gas) was measured with a pressure sensor (AE Sensors ATM [0-70 *mbar*], NL) at the bottom of the AnMBR. The broth volume was determined in the LabVIEW software using the differences between the gas and total pressures, and regulated by controlling the flow rate of the permeate pump. pH and temperature were measured by a combined pH-temperature sensor (Endress & Hauser, Memosens, CH).

### 3.3.1 Critical flux determination

Before its first use, the new membrane was de-coated by immersing it in a 300 *ppm* citric acid solution for one day, and cleaned subsequently with demineralised water. To assess appropriate operating conditions before application, the critical flux of the membrane was determined. This determination was based on the flux-step method as demonstrated by Le Clech et al. [2003]. Starting with an initial flux of 2.55 *LMH* (=1 *RPM*), the flux was increased by 3.82 *LMH* (=1.5 *RPM*) every 15 minutes. The initial transmembrane pressure ($TMP_i$), defined as the TMP obtained directly after the increase in filtration resistance caused by each flux-step; and final transmembrane pressure ($TMP_f$), defined as the TMP obtained at the end of the flux-step, were reported for each flux used. The critical flux was determined based on the point where a discontinuity in the trend was observed. In other words, a sudden increase in difference between $TMP_f^n$ and $TMP_i^n$ compared to previous applied fluxes will indicate that the critical flux of the membrane has been reached [Le Clech et al., 2003]. The results of this critical flux determination can be found in appendix H.

### 3.3.2 AnMBR feeding medium

Besides aniline, additional carbon- and energy sources such as (1) phenol, (2) acetate, (3) propionate, and (4) butyrate, were supplied to the AnMBR. Phenol was added because of its presence (1-2.5 $g \cdot L^{-1}$) in CGWW (table 2.3b), and to aim for microorganisms with the ability to degrade a compound, such as aniline, with an anaerobic degradation pathway analogous to that of phenol. The mixture of VFA was dosed to obtain the desired OLR, and to increase the diversity of acetogens. An acetate:butyrate:propionate COD-ratio of 2.5:2:1 was applied, as it was shown in previous results of the BioXtreme project that the acetate/butyrate mixture can promote a higher specific phenol conversion rate. The substrate uptake rate ($k_m$ in $gS \cdot gVSS^{-1} \cdot day^{-1}$) and growth rate ($\mu$ in $hour^{-1}$) of propionate degraders are generally low compared to butyrate- and acetate degraders [IWA, 2005; van Lier et al., 2008]. Consequently, a lower propionate concentration was dosed. Acetate supplementation should ensure a strong aceticlastic methanogenic population that can act as an electron sink. Yeast extract was dosed based on the organic content of the synthetic wastewater, being 5% of the total COD in the feed. Macro- and micronutrient solutions were supplied based on the feed COD-content (1.53 $mL$ of macronutrient solution per gCOD, and 0.76 $mL$ of micronutrient solution per gCOD). Phosphate buffer solutions were added to maintain a neutral pH and a $K^+ : Na^+$ mass ratio of 0.05 $gK \cdot gNa^{-1}$ [Muñoz Sierra et al., 2018a]. A detailed overview of the AnMBR feed composition, and the composition of the nutrient- and phosphate buffer solutions A and B can be found in appendices D and E, respectively. The sodium concentration was maintained at 8.0 $g \cdot L^{-1}$ by the addition of $Na^+$ as $NaCl$.

### 3.3.3 AnMBR operation & sampling

At the start of the AnMBR operation, the reactor was seeded with UASB sludge with a VSS concentration of 35 $g \cdot L^{-1}$. The OLR applied to the AnMBR was based on the SMA value of the UASB sludge, as determined in subsection 3.1.3. 250 $mgCOD_{CH_4} \cdot gVSS^{-1} \cdot day^{-1}$, one-third (approx.) of the SMA, was applied to the AnMBR as the initial OLR [J.B. van Lier, personal communication, August 2019]. The corresponding volumetric loading rate to achieve this OLR was 1.5 $L \cdot day^{-1}$ (HRT = 4.3 days).

Biogas samples (10 $mL$), and samples of the feed and permeate (2 $mL$) were extracted and analysed by COD cuvette test kits (section 3.4.2) and GC (section 3.4.1) three times a week. Broth samples were extracted for a variety of purposes. (1) 2 $mL$ were extracted once a month for analysis of the particle size distribution (PSD) in the Microtrac Bluewave Particle Size Analyzer (Microtrac Inc, U.S.) as described in section 3.4.3. (2) 8 $mL$ were extracted once a week for determination of the TSS and VSS concentration. (3) 9 $mL$ were extracted for analysis of the microbial community structure before adjustments of the feed composition and when a change was observed in the permeate composition during the AnMBR operation.

The operation of the reactor was divided into six different stages in which different conditions regarding the COD- and aniline concentration in the feed were applied (appendix D). These six stages are defined in table 3.5.

Table 3.5: Defined stages of the AnMBR operation.

| Stage | Time frame | Condition (adjustments) |
|---|---|---|
| **I** | Day 1-13 | $[An]_{feed}$ = 100 $mgAn \cdot L^{-1}$<br>$[COD]_{feed}$ = 30 $gCOD \cdot L^{-1}$ |
| **II** | Day 13-67 | $[COD]_{feed}$ decreased to 10 $gCOD \cdot L^{-1}$ |
| **III** | Day 67-101 | $[An]_{feed}$ increased to 200 $mgAn \cdot L^{-1}$ |
| **IV** | Day 101-119 | $[An]_{feed}$ decreased to 50 $mgAn \cdot L^{-1}$ |
| **V** | Day 119-169 | $[An]_{feed}$ decreased to 20 $mgAn \cdot L^{-1}$ |
| **VI** | Day 169-end | Anaerobic (degassed) AnMBR feed<br>Introduction of 500 $mL$ IC reactor sludge in the AnMBR |

### 3.3.4 Microbial community dynamics

The microbial community dynamics in the biomass of the AnMBR were assessed to get an insight into the microbial populations that could be related to the applied conditions and observed events during the reactor operation.

For sampling, 1.5 $mL$ of broth ($n$=3) was extracted from the reactor, and centrifuged for 5 minutes in a high-speed mini-centrifuge at 12,400·$g$ (Microspin 12, Biosan). The supernatant was disposed of, and the biomass pellets were stored in an ultra-low temperature freezer at -80°C (Innova®U101, Eppendorf/New Brunswick Scientific). DNeasy® UltraClean® Microbial Kit (Qiagen, Germany) was used for extraction of the DNA from the biomass according to the specifications provided by the manufacturer. After extraction, the DNA concentration of the samples was assessed with the Qubit dsDNA HS Assay Kit with the Qubit Fluorometer (Thermo Fisher Scientific, U.S.).

For the sequencing, the samples were packed in dry ice and shipped to the Novogene UK Sample Collection Group (Novogene UK Company LTD). Here, the V3-V4 region of the 16S rRNA gene was amplified using the polymerase chain reaction (PCR) with the primer pair 341F/806R. 30-35 PCR cycles were carried out with Phusion® High-Fidelity PCR Master Mix (New England Biolabs, U.S.). The sequencing was performed with NovaSeq™ 6000 Sequencing System (Illumina®, U.S.), after which the results were compared with the reference genomic sequence database ("Gold" database, UCHIME).

### 3.3.5 Alternative aniline removal mechanisms in the AnMBR

#### *Volatilisation of aniline*

To assess volatilisation of aniline, 100 $mL$ Schott Duran glasses were filled with 50 $mL$ of a 200 $mgAn \cdot L^{-1}$ stock solution. The bottles were closed with a connection cap system, which was not sealed to enable gas exchange between the headspace of the bottle and the room. The bottles were placed in the temperature-controlled shaker (Innova®40, Eppendorf/New Brunswick Scientific) at 35°$C$ and 130 *RPM*. Samples were taken regularly over a period of 17 days to determine the aniline concentration using GC. A decrease of the aniline concentration could indicate volatilisation of aniline. The 200 $mgAn \cdot L^{-1}$ stock solution was stored with a sealed cap in the fridge (4°C) and used as a control group.

#### *Adsorption of aniline*

Thermophilic biomass was used to assess whether aniline adsorbs to a mixture of biomass and residual lipid components. Additionally, UASB reactor sludge was used to assess whether aniline adsorbs to mesophilic granular biomass. This mesophilic biomass was pre-digested at 35°$C$ for 5 days to minimise the presence of organic matter. In both batch experiments (thermophilic- and UASB reactor sludge), 250 $mL$ Schott Duran glasses were filled with sludge and aniline solution (saline for UASB reactor sludge) to a final liquid volume of 200 $mL$, such that a VSS concentration of 10 $gVSS \cdot L^{-1}$ ($n$=3) and 20 $gVSS \cdot L^{-1}$ ($n$=3), and an aniline concentration of $mg \cdot L^{-1}$ was achieved. The bottles were placed in the temperature-controlled shaker (Innova®40, Eppendorf/New Brunswick Scientific) at 35°$C$ and 130 *RPM*. Samples were extracted regularly over a period of 17 days to determine the aniline concentration using GC. A decrease of the aniline concentration could indicate adsorption of aniline onto the biomass and/or residual lipid components.

To assess possible adsorption of aniline to glassware, 100 $mL$ Schott Duran glasses were rinsed with demineralised water and filled with 50 $mL$ of a 200 $mgAn \cdot L^{-1}$ stock solution. All bottles were closed with connection caps that were sealed to prevent any removal of aniline from the bottle through volatilisation. The bottles were placed in the temperature-controlled shaker (Innova®40, Eppendorf/New Brunswick Scientific) at 35°$C$ and 130 *RPM*. Samples were extracted regularly over a period of 11 days to determine the aniline concentration using GC. A decrease of the aniline concentration could indicate adsorption of aniline to the glassware. The 200 m$gAn \cdot L^{-1}$ stock solution was stored with a sealed cap in the fridge (4°$C$) and used as a control group.

## 3.4 ADDITIONAL ANALYTICAL PROCEDURES

### 3.4.1 Gas chromatography

The VFA-, aniline- and phenol concentrations in the inocula, the AnMBR permeate and AnMBR broth, as well as the biogas from the AnMBR were analysed by GC with a flame ionization detector (FID). For the analysis of the inocula and AnMBR broth, supernatant was extracted by centrifuging the broth sample (2 $mL$) for 5 minutes in a high-speed mini centrifuge at 12,400·$g$ (Microspin 12, Biosan). For the preparation of the sample, 1.5 $mL$ of supernatant or permeate were filtered through a 0.45 $\mu m$ polyethersulphone membrane filter (Chromafil Xtra PES-45/25, IRL), and 750 $\mu L$ of the filtered sample were transferred to a 1.5 $mL$ vial. 750 $\mu L$ of pentanol (30%) were added for dilution, and acted as an internal standard. 10 $\mu L$ of formic acid (98%) were added for acidification. The prepared samples were analysed by a gas chromatograph (Agilenttech 7890A, U.S.) with a capillary HP-FFAP column size of 25 $m$ x 0.32 $mm$ x 0.50 $\mu m$ (Agilent 19091F-112, U.S.). The GC temperatures were

maintained at 225°C for the detector and at 240°C for the injector. The FID was used with helium as carrier gas (pressure = 11 *psi*, flow rate = 2.45 $mL \cdot min^{-1}$).

For biogas analysis, GC (Agilenttech 7890A, U.S.) with a thermal conductivity detector (TCD) was used, with helium as carrier gas (pressure = 14.8 *psi*, flow rate = 23 $mL \cdot min^{-1}$). The GC had a HP-PLOT Molesieve GC column (Agilent 19095P-MS6, U.S.) of 60 *m* x 0.53 *mm* x 200 $\mu m$, and was maintained at an operational temperature of 200°C for both the injector and detector.

### 3.4.2 Chemical oxygen demand cuvette test kit

The COD in the AnMBR feed and permeate, and the initial and final COD concentrations in the solutions of batch tests were measured using a COD cuvette test kit (Lange Hach COD Cuvette Test LCK 314, 114 and 514), according to the manufacturer specifications with proper dilution ratios to avoid interference with chloride (max. 1,500 $mg \cdot L^{-1}$). The COD vials were digested (Lange Hach, LT200) during two hours at 148°C. Finally, a spectrophotometer (Lange Hach, DR3900) was used to obtain the COD concentration of the diluted samples.

### 3.4.3 Particle size distribution analysis

For analysis of the PSD of the AnMBR sludge, the Microtrac Bluewave Particle Size Analyzer (Microtrac Inc, U.S.) and Microtrac FLEX 11.1.0.2 software (Microtrac Inc, U.S.) was used. Before analysis of each sludge sample, the sample system was rinsed (4 runs) with demineralised water. A set-zero was performed (30 sec., 3 runs) to collect a background level measurement. Sludge samples ($n$=3) were loaded according to the loading indicator and analysed with demineralised water as dilution medium. The following settings were used: (1) 25% flow rate, (2) 3 deaeration cycles, (3) 30 sec. measurement time, (4) 3 runs.

# 4 RESULTS

## 4.1 BATCH EXPERIMENTS

### 4.1.1 Specific methanogenic activity determination for reactor start-up

After processing the data obtained from the AMPTS, the maximum methane production rate ($\mu_m$) was measured to be 10.4 $\pm$ 0.2 $NmL_{CH4} \cdot h^{-1}$ (figure 4.1). With a liquid volume of 200 $mL$ and a VSS concentration of 4 $gVSS \cdot L^{-1}$, a SMA value of 891 $\pm$ 15 $mgCOD_{CH4} \cdot gVSS^{-1} \cdot day^{-1}$ was calculated.

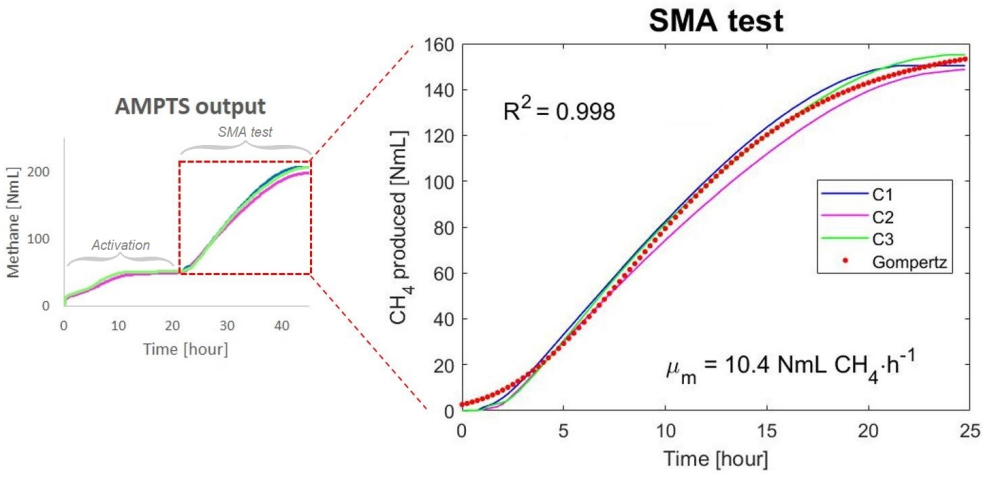


**Figure 4.1:** Results from the SMA test using the UASB reactor mesophilic granular biomass (Shell, Moerdijk, NL). In the left graph, the output data from the AMPTS is depicted, including the activation step. In the right graph, the AMPTS-data regarding the actual SMA test (lines) is depicted, where the markers represent the fitted Gompertz three parameter model (equation 3.3, appendix C). The model fit the data satisfactorily, with $R^2$ = 0.998.

### 4.1.2 Anaerobic aniline biodegradability

The anaerobic biodegradability of aniline under varying conditions was evaluated using three types of inocula (table 3.1). Figures 4.2a and 4.2b show the cumulative methane production for the 100 $mgAn \cdot L^{-1}$, blank- and control groups from the UASB reactor sludge and the bitumen sludge. After 177 days (UASB reactor sludge) and 168 days (bitumen sludge), biomethane production from aniline was not observed. Figures 4.3a and 4.3b show the cumulative methane production for the batches with lower concentrations of aniline (10 $mg \cdot L^{-1}$ and 20 $mg \cdot L^{-1}$) and amended with either the intermediate 4-aminobenzoic acid (16 $mg \cdot L^{-1}$) or bicarbonate (30 $mM$), using aniline sludge as inoculum. From these graphs, it can be concluded that aniline was not mineralised into methane after an incubation period of 85 days. After 67 days, methane production from 4-aminobenzoic acid was observed.

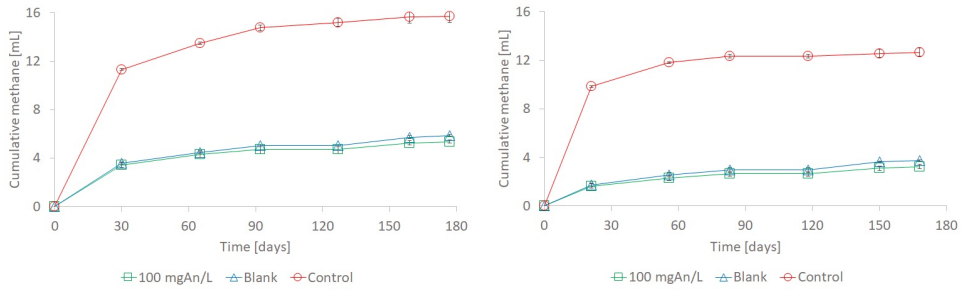


**(a)** UASB reactor sludge.

**(b)** bitumen sludge.

**Figure 4.2:** Cumulative methane production for the BAs of aniline under anaerobic conditions, with the use of UASB reactor sludge **(a)** and bitumen sludge **(b)**. The blank- (△) and control group (◯), and conditions with 100 $mgAn \cdot L^{-1}$ (□) are depicted. The error bars indicate the SD with $n$=3.

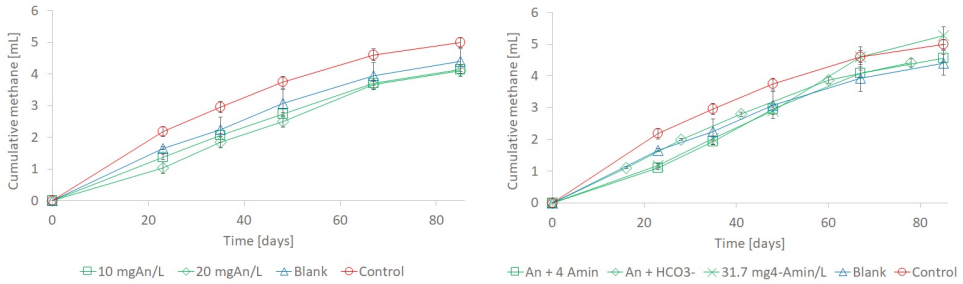


**(a)** Aniline.

**(b)** Aniline + additive.

**Figure 4.3:** Cumulative methane production for the BAs of aniline under anaerobic conditions, with the use of aniline sludge. **(a)** The blank- (△) and control group (◯), and conditions with 20 $mgAn \cdot L^{-1}$ (◊) and 10 $mgAn \cdot L^{-1}$ (□) are depicted. **(b)** The blank- (△) and control group (◯), and conditions with 10 $mgAn \cdot L^{-1}$ + 30 $mM\ HCO_3^-$ (◊), 10 $mgAn \cdot L^{-1}$ + 15.9 $mg$ 4-aminobenzoic acid·$L^{-1}$ (□) and 31.7 $mg$ 4-aminobenzoic acid·$L^{-1}$ (×) are depicted. The error bars indicate the SD with $n$=3.

### 4.1.3 Inhibition & toxicity

In addition to the biodegradability assessments, the inhibitory effect of aniline and phenol on the activity of the aceticlastic methanogens, and the toxic effect of these compounds on the anaerobic biomass of the UASB sludge were evaluated. It was found that aniline and phenol had an $IC_{50}$ for the SMA of 2.5 $gAn \cdot L^{-1}$ and 1.0 $gPh \cdot L^{-1}$, respectively (figures 4.4a and 4.4b). For the toxicity, after 72 hours (approx.) exposure of the anaerobic biomass to aniline concentrations up to 4 $g \cdot L^{-1}$ and phenol concentrations up to 1 $g \cdot L^{-1}$, a cell viability decrease of 24 ± 4% and 20 ± 4%, respectively, was observed (figures 4.5a and 4.5b). Consequently, the $LC_{50}$ for these compounds on the anaerobic biomass could not be determined. From figure 4.6 it can be seen that all cell membranes of the anaerobic biomass were damaged ($V_{res}$ = 100%) after autoclave sterilisation or after exposure to ethanol (70%, 30 minutes). Exposure to formaldehyde (0.5%, 72 hours) resulted in $V_{res}$ of 26%.

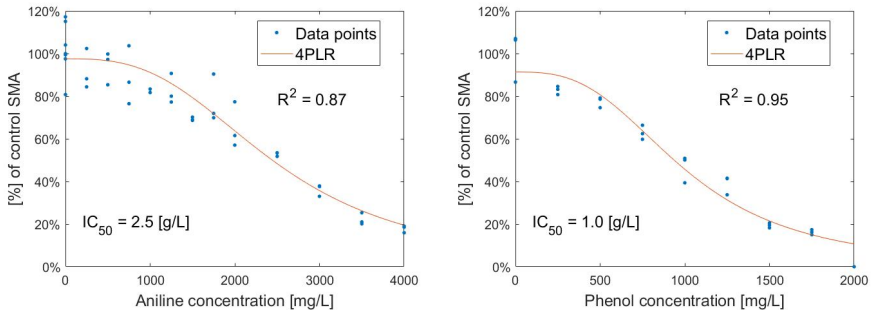


**(a)** $IC_{50}$ of aniline for the SMA. **(b)** $IC_{50}$ of phenol for the SMA.

**Figure 4.4:** Determination of the $IC_{50}$ of aniline and phenol for the SMA of UASB reactor sludge. The percentage of SMA with respect to the control group is plotted versus the concentration ($mg \cdot L^{-1}$) of the aniline **(a)** and phenol **(b)**. The continuous line represents the four parameters logistic regression (equation 3.5), from which the $IC_{50}$ was estimated. 4PLR = Four parameter regression model.

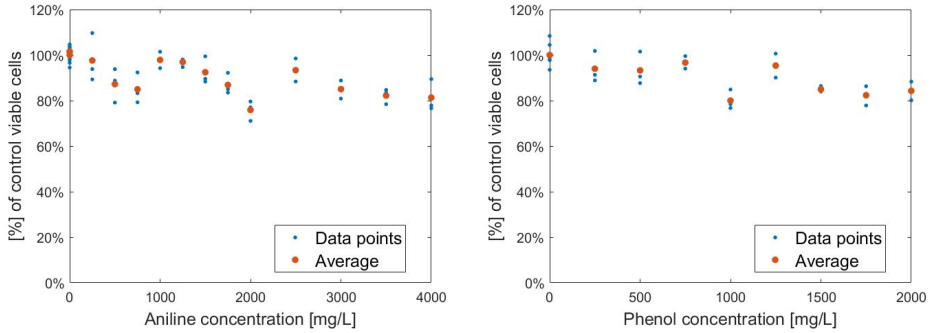


**(a)** Effect of aniline on cell viability. **(b)** Effect of phenol on cell viability.

**Figure 4.5:** Effect of aniline and phenol on the CMI of UASB reactor sludge. The graphs display the percentage of cell viability of the anaerobic biomass after exposure to aniline **(a)** and phenol **(b)** for 72 hours (approx.), with respect to the positive control group, versus the concentration ($mg \cdot L^{-1}$) of aniline or phenol.

## 4.2 ANMBR OPERATION

The AnMBR was operated under mesophilic (35°C) and saline (8 $gNa^{+} \cdot L^{-1}$) conditions with the aim to develop a microbial community capable of degrading synthetic wastewater, containing aniline, phenol, acetate, propionate, and butyrate, under strict anaerobic (methanogenic) conditions. The performance of the AnMBR was assessed in terms of the removal of aniline, phenol, and VFAs from the synthetic wastewater.

### 4.2.1 Removal of aniline

The aniline removal and the effect of aniline on the anaerobic degradation of phenol and the VFA mixture was assessed by applying different concentrations of aniline in the synthetic wastewater, ranging from 20-200 $mgAn \cdot L^{-1}$. When a steady state was reached, after the start-up of the AnMBR and after adjustment of the AnMBR composition, the aniline concentration in the permeate was found to be consistently lower compared to the influent concentration (figure 4.7). After reaching a steady state in stage II and III, a 11% reduction of aniline concentration was observed in the effluent. In stage V, the observed removal of aniline increased from 13% (day 133) to 32% (day 172). After reaching a steady state in stage VI, a 15% reduction of aniline concentration was observed in the effluent.

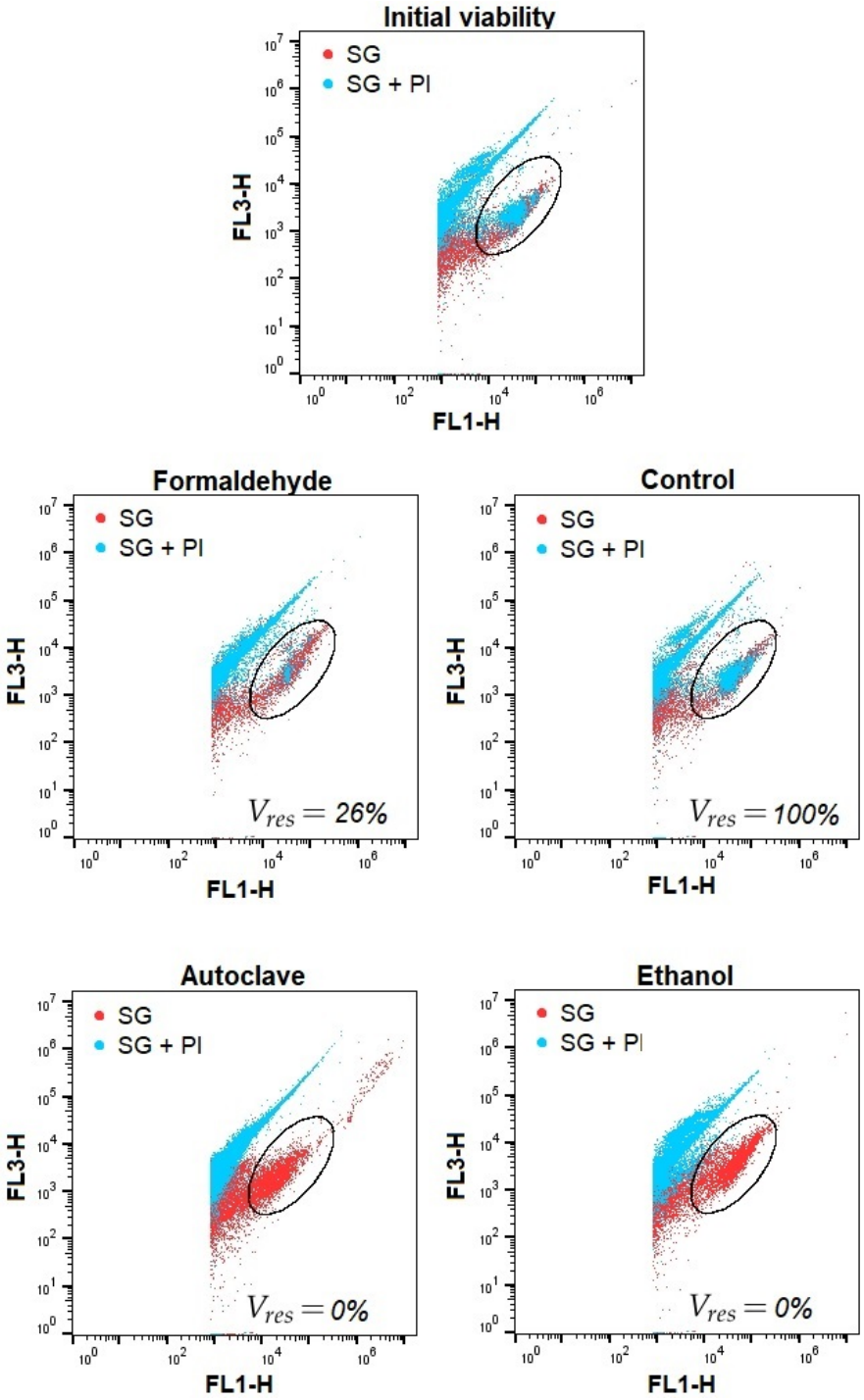


**Figure 4.6:** Cell viability of the cell suspensions with respect to the average viability of the control group. The horizontal axis corresponds with the green fluorescence channel (FL1-H), and the vertical axis corresponds with the red fluorescence channel (FL3-H). The upper graph visualises the cell viability of the biomass before autoclave sterilisation or exposure to either formaldehyde (0.5%, 72 hours) or ethanol (70%, 30 minutes).

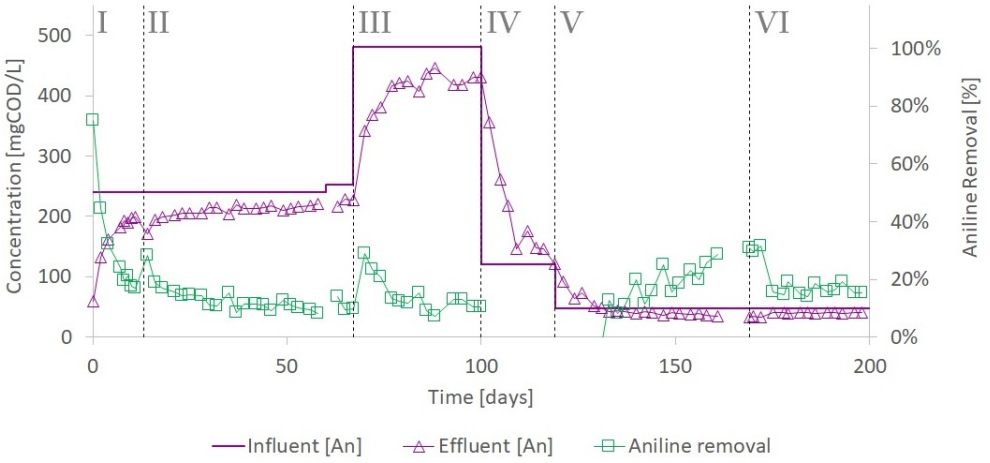


**Figure 4.7:** Aniline concentration in the influent and effluent (permeate), and the aniline removal percentage in the AnMBR over time. From the primary vertical axis, the aniline concentrations (—: influent, and △: effluent) can be read, and from the secondary vertical axis the aniline removal percentage (□) can be read. The numerals indicate stages as defined in table 3.5.

### 4.2.2 Removal of phenol and benzoate

During the whole operation, the reactor was fed with synthetic wastewater with a constant phenol concentration of 500 $mgPh \cdot L^{-1}$ (1,190 $mgCOD_{Ph} \cdot L^{-1}$). After day 20, the AnMBR removed >90% of the phenol (figure 4.8). From day 50 onwards, the phenol removal was >98%. Regarding benzoate (one of the central intermediates of the anaerobic phenol degradation), COD concentrations that corresponded with the COD of the degraded phenol were found between days 20 and 50. After day 50, >90% removal of the COD of this intermediate was observed. After increasing the aniline concentration to 200 $mgAn \cdot L^{-1}$ in stage III, the phenol- and benzoate concentration in the effluent increased to 20 $mgCOD_{Ph} \cdot L^{-1}$ and 100 $mgCOD_{Benz} \cdot L^{-1}$, after which near complete phenol- and benzoate removal (>99%) was achieved again from stage IV onwards.

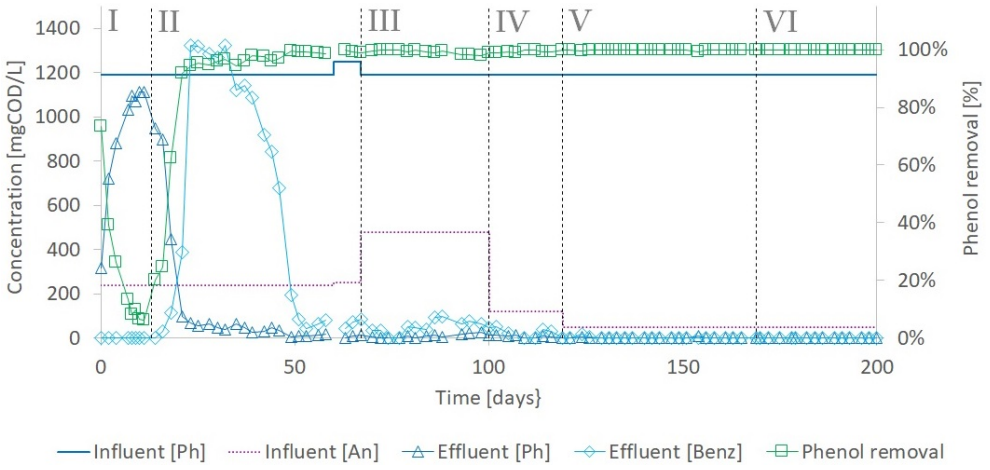


**Figure 4.8:** Phenol and benzoate concentrations in the AnMBR effluent (permeate), and phenol removal percentage in the AnMBR over time. From the primary vertical axis, the phenol- (—: influent, and △: effluent), aniline- (···) and benzoate (◊) concentration can be read, and from the secondary vertical axis the phenol removal percentage (□) can be read. The numerals indicate stages as defined in table 3.5.

### 4.2.3 VFA- and total COD removal

After 30 days of operation, the removal of VFAs was >95% (acetate), 100% (butyrate), and >90% (propionate). During the first half of stage V and in stage VI, the removal of VFAs was highest with >98% (acetate), 100% (butyrate), and >97% (propionate). After 50 days of operation, a total COD-removal of >90% was obtained (figure 4.9), and varied between 92-97% until stage V (plus a lag time of a week). In stage IV, V and VI, from day 109 onwards, the COD removal was usually 99%, except for the end of stage V where the COD removal decreased to 96%. The biogas production (i.e. the converted COD) and its composition during the AnMBR operation can be found in appendix J. An overview of the COD balance (influent COD, effluent COD, methane COD and residual COD) can be found in appendix I.

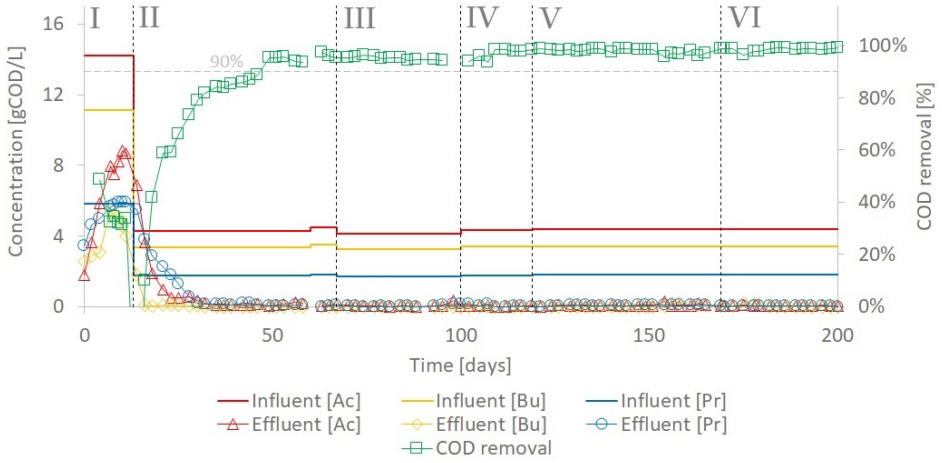


**Figure 4.9:** Concentration of the VFA mixture and removal of the total COD in the AnMBR over time. From the primary vertical axis the VFA concentrations can be read, where the red colour represents acetate (—: influent, and △: effluent), yellow butyrate (—: influent, and ◊: effluent), and blue propionate (—: influent, and ◯: effluent). From the secondary vertical axis, the COD removal percentage (□) can be read. The numerals indicate stages as defined in table 3.5.

### 4.2.4 Microbial community dynamics

All the DNA samples from the biomass were gathered with the DNeasy® Ultra-Clean® Microbial Kit (Qiagen, Germany) and were shipped to the Novogene UK Sample Collection Group (Novogene UK Company LTD) for the sequencing. Due to measures to reduce the spread of SARS-CoV-2, the sequencing data could not be processed on time.

### 4.2.5 Alternative aniline removal mechanisms in the AnMBR

#### *Volatilisation of aniline*

A decrease of the aniline concentration was observed in the bottles with an unsealed connection cap system, which was not observed in the control group (figure 4.10). A simple linear regression was applied to estimate the rate of volatilisation, which was found to be 2 $mgAn \cdot L^{-1} \cdot day^{-1}$.

#### *Adsorption of aniline*

From the assessment of aniline adsorption to glassware, a difference in the aniline concentration between the control group and the test group was not observed (figure 4.10).

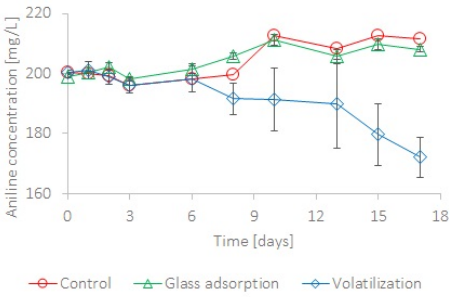


**Figure 4.10:** The average aniline concentrations during the volatilisation and glass adsorption tests. The change in aniline concentration for the volatilisation test (◊) and glass adsorption test (□) are compared to the control (◯). The error bars indicate the SD, where $n$=3 for the volatilisation test and $n$=2 for the glass adsorption test.

Regarding adsorption of aniline to thermophilic biomass and residual lipid constituents, a rapid reduction of the aniline concentration was observed. At t = 0 days (measured 30 minutes after dosing aniline to ensure complete solubilisation), the measured aniline concentrations were 20% (10 $gVSS \cdot L^{-1}$) and 50% (20 $gVSS \cdot L^{-1}$) below the theoretical concentration of 200 $mgAn \cdot L^{-1}$ (figure 4.11a). After the initial decrease, the aniline concentration increased over time. The difference between the results of the conditions amended with 10 and 20 $gVSS \cdot L^{-1}$ remained distinctive until the end of the experiment.

For the adsorption of aniline to mesophilic biomass, a reduction of the aniline concentration was not observed within 14 days of incubation (figure 4.11b). During incubation, the aniline concentration in the bottles amended with 10 and 20 $gVSS \cdot L^{-1}$ remained constant at 200 $mgAn \cdot L^{-1}$.

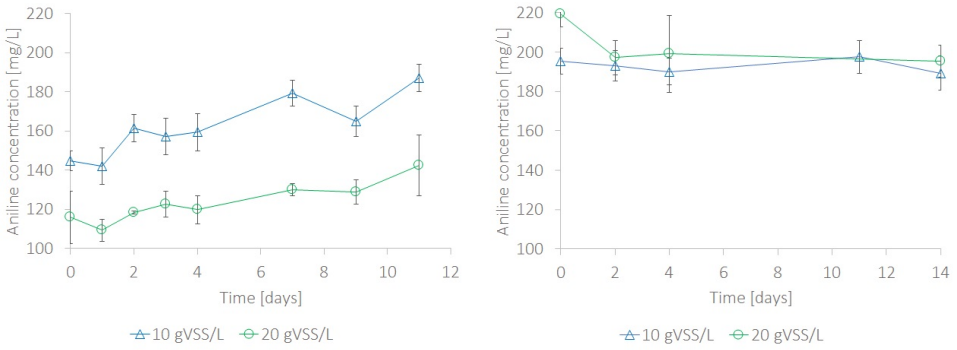


**(a)** Thermophilic biomass.

**(b)** Mesophilic biomass.

**Figure 4.11:** Average aniline concentrations during the adsorption test of aniline to biomass. The change in aniline concentration for the 10 $gVSS \cdot L^{-1}$ (△) condition is compared with the condition containing 20 $gVSS \cdot L^{-1}$ (◯), for thermophilic biomass **(a)** and mesophilic biomass **(b)**. The error bars indicate the SD, where $n$=3 for both conditions.

# 5 DISCUSSION

## 5.1 BATCH BIODEGRADABILITY ASSAYS

For the batch biodegradability assays amended with 100 $mgAn \cdot L^{-1}$ (=266 $mgCOD_{An} \cdot L^{-1}$) a biomass concentration of 0.5 $gVSS \cdot L^{-1}$ was applied to obtain an inoculum/substrate ratio of 2 $gVSS \cdot COD^{-1}$. The applied method was found reliable for assessing the methanogenic biodegradability of aniline, as the background (endogenous) cumulative methane production in the blanks was low, and a noticeable difference in cumulative methane production between the control group (16 $mL$ and 12$mL$) and the blank (6 $mL$ and 4 $mL$) was observed. However, in the case of the assays with a low concentration of aniline (26.6 and 53.2 $mgCOD_{An} \cdot L^{-1}$), a higher biomass concentration was applied (2.0 $gVSS \cdot L^{-1}$), which increased the background methane production. The lower theoretical methane yield in these assays (26.6 and 53.2 $mgCOD_{An} \cdot L^{-1}$) together with the higher background cumulative methane production (because of a higher VSS concentration) resulted in small differences between the cumulative methane production in the blank- and control group, and conditions with 20 $mgAn \cdot L^{-1}$, 10 $mgAn \cdot L^{-1}$, 10 $mgAn \cdot L^{-1}$ + 30 $mM$ $HCO_3^-$, 10 $mgAn \cdot L^{-1}$ + 15.9 $mg$ 4-aminobenzoic acid$\cdot L^{-1}$, and 31.7 $mg$ 4-aminobenzoic acid $\cdot L^{-1}$. Despite the small differences, the divergence in cumulative methane production made it possible to distinguish the control group from the groups amended with aniline, 4-aminobenzoic acid, and blanks.

In the batch assays with the UASB reactor- (petrochemical) or bitumen-degrading sludge, methanogenic aniline degradation was not observed after 140 days of incubation, nor after 50 days of incubation in the assays using aniline sludge, with and without 30 $mM$ sodium bicarbonate or 4-aminobenzoate. However, mineralisation of 4-aminobenzoate (53.2 $mgCOD_{4-Am} \cdot L^{-1}$) by methanogenic consortia in the aniline sludge was observed after 67 days of incubation. This is in agreement with the findings of Razo Flores et al. [1996], where a difference in cumulative methane production between the 4-aminobenzoate group and blank was observed after 50-70 days.

These results can be compared with only a few assays that have been reported. As described in chapter 2, neither Schink [1988] observed methanogenic aniline degradation in batch, nor did de Alexandra et al. [1994] when 23 $mg \cdot L^{-1}$ of aniline was inoculated in anaerobic sewage sludge with approximately 400 $mM$ bicarbonate at 25$^{\circ}C$ for more than 200 days.

Yumihara et al. [2002] claimed to have observed, after eight weeks of incubation at 37$^{\circ}C$, up to 15% aniline removal in batch experiment using acclimatised digested mesophilic sewage sludge inoculated with 130 $mgAn \cdot L^{-1}$. Besides, they reported up to 35% removal when glucose (non-reported concentration) was added as additional carbon and energy source. However, the occurrence of methanogenic biodegradation in this case could be related to the adsorption of aniline to particulate matter, as reported by Weber et al. [2001] and shown in this research. Additionally, the difference in the cumulative methane produced between the aniline amended (130 $mgAn \cdot L^{-1}$) group and blank, which was supposed to correspond to the aniline degradation, was observed just after 7 days of incubation, which would be an extremely fast process [Yumihara et al., 2002] .

Sun et al. [2015] reported aniline (10 $mgAn \cdot L^{-1}$) biodegradation in ten out of twelve replicates of batch biodegradability assays, using mesophilic (28$^{\circ}C$) anaero-

bic microcosms coming from an aniline contaminated industrial site. The degradation took place after a lag phase of 100 days. Correspondingly, after an incubation time of 60 days Carvalho and Gavazza observed methanogenic aniline biodegradation, when using the microbial community from azo dye-contaminated river sediments in batch tests, inoculated with 4 $mgAn \cdot L^{-1}$ [personal communication, December 2019]. In the batch studies performed by Sun et al. [2015] and Carvalho and Gavazza, analysis of aniline adsorption to the sediment was not reported. Nevertheless, from these reported observations, it can be concluded that methanogenic aniline degradation is most likely to be observed when the microbial communities have been exposed to aromatic amines for a long period.

## 5.2 INHIBITION & TOXICITY

With an $IC_{50}$ for the SMA of approximately 2.5 $g \cdot L^{-1}$, aniline was found to not significantly inhibit the methanogenesis of the granular mesophilic biomass. Comparing this result with the reported data by Donlon et al. [1995] (0.9 $g \cdot L^{-1}$) and [Kayembe et al., 2012] (1.4 $g \cdot L^{-1}$), it was found that the methanogenic activity of the UASB reactor granular sludge used in this experiment was less affected in the presence of aniline than the biomass used in those studies (figure 5.1). The experiments performed by Donlon et al. [1995] for assessing the inhibitive effect of N-substituted aromatic compounds on the SMA were performed with UASB granular sludge from the same source (Shell, Moerdijk) as in this project. However, knowing that these experiments were performed approximately 25 years ago, it is likely that the characteristics of the sludge have changed. Although, the maximum SMA of the sludge reported by Donlon et al. [1995] is equal to the SMA estimated in this study: 890 $mgCOD_{CH4} \cdot gVSS^{-1} \cdot day^{-1}$ [Donlon et al., 1995] vs. 891 $\pm$ 15 $mgCOD_{CH4} \cdot gVSS^{-1} \cdot day^{-1}$ (this study).

The $IC_{50}$ of phenol for the SMA (1.0 $g \cdot L^{-1}$) indicated that this compound had a more inhibitory effect on the methanogens compared to aniline. In comparison with reported $IC_{50}$ values of phenol for the [Donlon et al., 1995; Olguin-Lora et al., 2003; Kayembe et al., 2012; Poirier et al., 2016], the inhibitory effect of phenol on the methanogenic activity was found to be higher in this study, but in the same order of magnitude (figure 5.1).

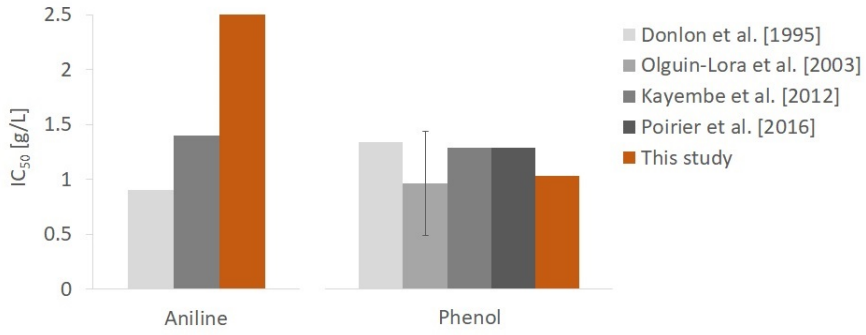


**Figure 5.1:** Comparison of the reported $IC_{50}$ values of aniline and phenol on the SMA with the $IC_{50}$ values determined in this study. For the $IC_{50}$ value reported by [Olguin-Lora et al., 2003], the 'error bar' refers to the actual reported values (0.47 and 1.4 $gPh \cdot L^{-1}$), and the solid bar indicates their average.

It must be stressed that the applied protocol for the SMA-inhibition test was different compared to the methodology of Donlon et al. [1995]. (1) The incubations were done in a temperature controlled shaker at 35 $\pm$ 1°C, compared to a temperature of 30 $\pm$ 2°C. (2) The AMPTS was applied for continuous monitoring of the methane production during the incubation period of 2 to 3 days, instead of measur-

ing the methane content in the headspace hourly during a 6 to 8 hour incubation period. (3) A final liquid volume of 200 $mL$ containing 2 $gCOD \cdot L^{-1}$ was applied for the actual SMA test, compared to <100 $mL$ containing 1 $gCOD \cdot L^{-1}$. (4) The effect of phenol and aniline on the SMA was assessed directly after injection of the substrate pulse (containing acetate and one of the inhibiting compounds) in the assay bottles, where Donlon et al. [1995] replenished the acetate to 1 $gCOD \cdot L^{-1}$ to start the SMA test after 3 days of exposure to the inhibitive compounds. (5) The composition of the basal media show differences regarding their constituents. $NaHCO_3$ (5 $g \cdot L^{-1}$) and $AlCl_3 \cdot H_2O$ (2 $mg \cdot L^{-1}$) that was included in the basal medium used by Donlon et al. [1995], was not included in the basal medium in this study, whereas $CoCl_2 \cdot 6H_2O$ (0.5 $mg \cdot L^{-1}$), $(NH_4)_6Mo_7O_2 \cdot 6H_2O$ (90 $mg \cdot L^{-1}$), $NiCl_2 \cdot 6H_2O$ (50 $mg \cdot L^{-1}$), and $Na_2WO_4$ (80 $mg \cdot L^{-1}$) were not included in the basal medium of Donlon et al. [1995]. (7) The SMA-inhibition tests were performed at a sodium concentration $< 3.5\ gNa^+ \cdot L^{-1}$, compared to 8 $gNa^+ \cdot L^{-1}$ in this study.

Astals et al. [2015] discussed that the addition of basal media can affect the microbial activity of the anaerobic biomass, due to a sudden change of conditions. Interactions between the compounds in the basal media, particularly cations, and the targeted inhibitors could influence the SMA, and consequently the determination of the $IC_{50}$ of the targeted inhibitor in the methanogenic activity [Chen et al., 2008].

Besides the contrasting applied methodology and the differences in basal media composition, the differences in microbial composition of the UASB reactor sludge used in the experiments can be one of the reasons that the $IC_{50}$ of aniline and phenol for the SMA reported by Donlon et al. [1995] (900 $mgAn \cdot L^{-1}$ and 1,300 $mgPh \cdot L^{-1}$, respectively) are different compared to the results in this study (2,500 $mgAn \cdot L^{-1}$ and 1,000 $mgPh \cdot L^{-1}$, respectively).

Regarding the effect of exposure to aniline and phenol on the CMI of the anaerobic biomass, it can be stated that the results indicate low toxicity of these compounds to anaerobic microorganisms. Neither aniline (0-4 $g \cdot L^{-1}$), nor phenol (0-2 $g \cdot L^{-1}$) appeared to drastically affect the CMI after exposing the anaerobic biomass to these compounds for ≈72 hours. In the applied concentration ranges for aniline and phenol, viable cells reduction up to 24 ± 4% and 20 ± 4% compared to the control group were observed, respectively. Nevertheless, a clear overall pattern was not identified.

Some studies have reported the toxic effect of aniline or phenol exposure on microbial metabolism (facultative anaerobic bacterium, crustaceans, and protozoan) [Sihtmäe et al., 2010], but to the best of the author's knowledge, no studies have quantified the effect of aniline or phenol on the cell viability of anaerobic biomass. Despite having no severe consequences for the CMI of anaerobic biomass after 72 $h$, the exposure to aniline can still be highly toxic for certain eukaryotic cells. For instance, Wang et al. [2016] reported 40% decrease of viable hepatocytes (cells of the main parenchymal tissue of the liver) after exposure to 10 $mg \cdot L^{-1}$ of aniline for 24 $h$.

## 5.3 ANMBR PERFORMANCE TREATING ANILINE CONTAINING WASTEWATER

### 5.3.1 Removal of aniline

Based on the lowest reported $IC_{50}$ value of aniline for the SMA (0.9 $g \cdot L^{-1}$), an initial aniline concentration of 100 $mg \cdot L^{-1}$ was applied in the feed to avoid inhibition of the aceticlastic methanogens, and to direct, by selective pressure, the microbial community towards anaerobic aniline degradation. After reaching a steady state regarding the degradation of phenol, benzoate, and VFAs at day 67, the aniline concentration in the feed was increased to 200 $mg \cdot L^{-1}$ to assess the effect of an aniline

peak load on the degradation of phenol, benzoate, and VFAs. After reaching steady state in these two stages of AnMBR operation, an aniline concentration decrease of 11% was observed. However, based on the volatilisation of aniline in batch experiments, it is likely that the observed decrease in the AnMBR was attributed to aniline volatilisation. A quantification of aniline volatilisation during the AnMBR operation was not performed.

Besides volatilisation, the increased aniline removal (13% at day 133 to 32% at day 172) at the end of stage V is presumably related to the observed darkening and decreasing aniline concentration of the AnMBR feed solution in this stage (appendix O). After a further decrease of the aniline concentration in the AnMBR feed to 20 $mg \cdot L^{-1}$ (a representative concentration for CGWW) in stage VI, the observed aniline loss was up to 19%. Again, it is likely that these losses were mainly the result of aniline volatilisation.

Only one study have reported methanogenic degradation of aniline in a continuous bioreactor. Yumihara et al. [2002] observed a 40% removal of aniline after 172 days of treatment in an UAFP reactor with a working volume of 0.78 $L$, when dosing synthetic wastewater with 500 $mg \cdot L^{-1}$ of aniline at approximately 0.75 $L \cdot day^{-1}$ (= 480 $mg \cdot L^{-1} \cdot day^{-1}$). Additionally, they reported an increase to 91% in the aniline biodegradation in the UAFP reactor, when glucose (4.9 mol glucose$\cdot$ $mol^{-1}$ aniline) was added, and 90% when acetic acid (35 mol acetic acid$\cdot$ $mol^{-1}$ aniline) was added. Compared to the continuous experiment in this research, the volumetric aniline loading rate applied Yumihara et al. [2002] was up to 100 times higher: 480 $mgAn \cdot L^{-1} \cdot day^{-1}$ compared to 5 $mgAn \cdot L^{-1} \cdot day^{-1}$ in the final stage of AnMBR operation. Adsorption of aniline to the solid fraction was reported to be negligible. In this continuous experiment, Yumihara et al. [2002] did not mention volatilisation as a possible explanation for the aniline loss in the UAFP bioreactor. After assessing alternative aniline removal mechanisms, it was found that volatilisation of aniline could be the cause of the observed removal. As the volatilisation rate was most likely depending on the aniline concentration in the solution, the area of the gas-liquid interface, and the degree of mixing of the solution, this number cannot be directly translated to the rate of volatilisation in the AnMBR. However, it does indicate that volatilisation of aniline can be an important contributing mechanism to the observed losses of aniline in the AnMBR.

In the study performed by de Alexandra et al. [1994], adsorption of aniline to the organic fraction of the biomass was not observed. However, in this study there were indications that adsorption of aniline to (organic) particulates did take place. In the adsorption experiment with thermophilic biomass, a clear difference can be observed between the conditions with a VSS concentration of 10 $gVSS \cdot L^{-1}$ and 20 $gVSS \cdot L^{-1}$, showing a significantly lower aniline concentration when exposed to higher VSS concentrations. As the test bottles were closed with a cap and flushed with nitrogen gas for 2 minutes (thereby ensuring anaerobic conditions), it is unlikely that these observed losses was the result of biodegradation, autoxidation, polymerisation or volatilisation. Most likely, during the batch test, adsorption of aniline to the sludge constituents is the responsible mechanism for the observed decrease in aniline concentration. These latter observations are supported by the reported results from Weber et al. [2001], where it was found that aniline adsorbs rapidly to sediments. In case of adsorption to sediments, it was reported that aniline cation-exchange and covalent binding are the main sorption mechanisms [Weber et al., 2001].

In addition, after increasing the aniline concentration in the AnMBR feed from 100 $mgAn \cdot L^{-1}$ to 200 $mgAn \cdot L^{-1}$ (stage III), it was found that the TSS and VSS concentration increased from 32 $gTSS \cdot L^{-1}$ to 45 $gTSS \cdot L^{-1}$ and from 12 $gVSS \cdot L^{-1}$ to 17 $gVSS \cdot L^{-1}$, respectively (appendix L). Where the increased VSS concentration can be attributed to biomass synthesis, the observed increase of TSS concentration can be attributed by the production of EPS by the biomass as a stress response to aniline exposure [Mohammed et al., 2020]. Presumably, the production of EPS by the biomass

after exposure to a higher aniline concentration caused the observed increase of TMP (appendix N) in stage III, which ultimately resulted in a completely clogged membrane. After performing chemical cleaning of the membrane to remove all organic- and inorganic matter, the AnMBR operation was resumed.

### 5.3.2 Removal of phenol and benzoate

During the AnMBR operation, a constant phenol loading rate of 115 $mgPh \cdot L^{-1} \cdot day^{-1}$ was applied. The removal of phenol and benzoate, its central degradation intermediate, from the system were divided in three intervals: (1) From day 0-20, the development of the phenol degrading microorganisms, (2) from day 20-50, the development of the benzoate degrading microorganisms, and (3) from day 50-end, >90% removal of phenol and benzoate. These first two intervals are regarded as the start-up period of the reactor, after which a steady state was reached. After this, the specific phenol conversion rate in the last interval had a value of 12 $mgPh \cdot gVSS^{-1} \cdot day^{-1}$. At the start of this last interval (stage III), when the aniline loading rate was doubled from 23 to 46 $mgAn \cdot L^{-1} \cdot day^{-1}$, a reduction of the phenol and benzoate removal was observed. The phenol conversion rate after this adjustment dropped from 12 to 6 $mgPh \cdot gVSS^{-1} \cdot day^{-1}$. This was attributed to the changing VSS concentration in the broth.

### 5.3.3 Removal of VFAs and total COD

The degradation of VFAs after 30 days of treatment in the AnMBR was nearly constant with removal percentages of >95% (acetate), 100% (butyrate), and >90% (propionate). However, simultaneous with the increased aniline removal at the end of stage V (darkening and decreasing aniline concentration of the AnMBR feed solution, appendix O), the removal of butyrate decreased from 100% to 95%. Correspondingly, a decreased total COD removal (99% to 96%) was observed at the end of stage V. It is hypothesised that this could have been the result of the formation of inhibitory components after autoxidation of aniline in the AnMBR feeding solution. The biogas production (i.e. the converted COD) and its composition during the AnMBR operation can be found in appendix J. The biogas composition over the whole operational period remained relatively constant with a methane content of 80%, which corresponds to a pH of 7.5 as measured during the AnMBR operation (appendix K). However, as is visualised in figure J.1, the effect of benzoate degradation in stage II (days 16-46) on the biogas composition is noticeable, as the methane content (84%) was slightly higher. The COD balance as depicted in figure I.1 (appendix I) shows that the residual COD is 15% (influent COD - effluent COD - methane COD $\neq$ 0), indicating that besides the volatilised aniline 15% of the influent COD is not converted to methane or detected the permeate. This COD-gap could be attributed to inconsistent functioning of the gas meter and/or the influent pump, or to unidentified volatilisation of other organic components such as phenol or VFAs.

# 6 CONCLUSION

## 6.1 CONCLUSION

The main objectives of this research were (1) to assess the biodegradation of aniline under methanogenic and saline conditions in an AnMBR and batch reactors, (2) to assess the inhibitory effect of aniline and phenol on the aceticlastic methanogenesis, (3) to assess the effect of aniline and phenol on the CMI of anaerobic biomass, and (4) to get insight into the microbial community dynamics in the AnMBR during treatment of aniline- and phenol containing wastewater. The following conclusions can be derived.

- **After 200 days of AnMBR operation, the methanogenic enrichment culture was not able to biodegrade aniline.** The treatment of synthetic aniline-containing wastewater (with phenol, acetate, propionate, and butyrate as additional carbon and energy sources) in an AnMBR for 200 days under methanogenic conditions at 8 $gNa^{+} \cdot L^{-1}$, using granular biomass from an UASB reactor treating petrochemical wastewater as seed sludge, resulted in a decrease in the aniline concentration up to 32%. However, this removal was mainly attributed to volatilisation of aniline.

- **The presence of aniline seems to affect the complete degradation of phenol in the AnMBR.** After increasing the aniline concentration in the feed from 100 $mgAn \cdot L^{-1}$ to 200 $mgAn \cdot L^{-1}$, the phenol conversion rate dropped from 12 to 6 $mgPh \cdot gVSS^{-1} \cdot day^{-1}$. However, this was attributed to the changing VSS concentration in the broth. Nevertheless, it was observed that when the aniline loading rate was doubled from 23 to 46 $mgAn \cdot L^{-1} \cdot day^{-1}$, elevated concentrations of phenol (20 $mgCOD \cdot L^{-1}$) and benzoate (100 $mgCOD \cdot L^{-1}$) were detected in the effluent.

- **Biodegradation of aniline under methanogenic conditions did not take place in batch assays after 177 days using non-adapted sludge, or after 85 days using sludge exposed to aniline for >100 days.** From the biodegradability batch assays, it was found that aniline degradation under methanogenic conditions did not take place in the assays inoculated with (1) granular sludge coming from an UASB reactor treating petrochemical wastewater (Shell, Moerdijk, NL), (2) bitumen condensate-degrading sludge (BioXtreme), and (3) AnMBR sludge exposed to aniline for >100 days. The observed methane formation was attributed to endogenous biogas production. Therefore, it can be concluded that the anaerobic biodegradability of aniline under saline (8 $gNa^{+} \cdot L^{-1}$) conditions after 177 days (non-adapted sludge) or 85 days (sludge exposed to aniline for >100 days) is 0 $gCOD_{CH_4} \cdot gCOD^{-1}_{aniline}$.

- **The inhibitory effect of aniline on the SMA of UASB reactor sludge was smaller compared to reported $IC_{50}$ values.** Results from the SMA-inhibition test with the use of UASB reactor sludge amended with aniline (0-4,000 $mg \cdot L^{-1}$), indicated that the $IC_{50}$ of aniline for the aceticlastic methanogenesis is 2.5 $gAn \cdot L^{-1}$. This is higher than reported $IC_{50}$ values (0.9 and 1.4 $gAn \cdot L^{-1}$).

- **The inhibitory effect of phenol on the SMA of UASB reactor sludge was comparable to reported $IC_{50}$ values.** Results from the SMA-inhibition test with the

use of UASB reactor sludge amended with phenol (0-2,000 $mg \cdot L^{-1}$), indicated that the $IC_{50}$ of phenol for the aceticlastic methanogenesis is 1.0 $gPh \cdot L^{-1}$. This is comparable to reported $IC_{50}$ values (0.47 to 1.4 $gPh \cdot L^{-1}$).

- **Exposure of the UASB reactor sludge to 4 $gAn \cdot L^{-1}$ and 2 $gPh \cdot L^{-1}$ for 72 hours did not drastically affect the CMI of the anaerobic biomass.** With the use of FC to assess the effect of exposure to aniline and phenol on the CMI of the anaerobic biomass, it was found that after exposure of 72 $h$ (approx.) to the maximum applied concentrations of aniline and phenol, the cell viability decreased with 24 $\pm$ 4% and 20 $\pm$ 4% with respect to the control group, respectively. Based on the observed cell viability reductions after 72 $h$ exposure to aniline and phenol, the $LC_{50}$ for these compounds on the anaerobic biomass could not be determined, as the used concentrations of aniline and phenol did not result in a reduction of cell viability of $>$50%.

This research constituted the first report demonstrating the application of an AnMBR with the aim to biodegrade aniline-containing synthetic wastewater under methanogenic saline conditions. The results of this research demonstrated that, after 200 days of AnMBR operation, the methanogenic enrichment culture was not able to biodegrade aniline. Based on the limited demonstrations of methanogenic aniline biodegradation in literature (including this research), the feasibility of this methanogenic degradation pathway is still questionable.

## 6.2 RECOMMENDATIONS

Until methanogenic aniline biodegradation has been proven achievable, a sequenced anaerobic-aerobic treatment would be appropriate to mineralise the aniline in CGWW. A single aerobic biological treatment would suffice in case of wastewater where aniline is the main constituent, such as those produced in the pharmaceutical- or chemical industry. To overcome inhibition of the nitrifiers due to high aniline concentrations ($>$100 $mg \cdot L^{-1}$) when treating concentrated aniline wastewaters under aerobic conditions, as reported by Gheewala and Annachhatre [1997] and J.W. Mulder [email communication, December 2019], it can be considered to apply a higher effluent recycling ratio, so that the raw wastewater is diluted at the entrance points of the reactors. Consequently, more completely mixed flow patterns can be achieved in the reactor which minimizes potential inhibition [van Lier et al., 2015]. Hypothesising that methanogenic aniline biodegradation can occur, staged reactor configurations can be considered for the treatment of textile wastewaters. Through treatment of these textile wastewaters in reactors operated in (pseudo-) plug flow mode, the nitroaromatics are reduced to aromatic amines in the first stage. In the second stage, the solution will be free of nitroaromatics, so that the nitroaromatics with their inhibitive- and toxic characteristics cannot affect the methanogenic degradation of the aromatic amines.

For continuation of the pursuit to achieve methanogenic biodegradation of aniline, conditions can be optimised, and alternative mechanisms can be utilised:

- **Apply a substrate medium in the absence of dissolved oxygen.** During the preparation of the substrate medium, dissolved oxygen is inevitably introduced to the solution. To minimise the occurrence of autoxidation of constituents in the substrate medium, it is recommended to remove all dissolved oxygen before dosing the substrate medium to the inoculum when performing batch experiments, or before applying it in continuous experiments. This can be achieved by vacuum degassing, and/or flushing with nitrogen gas. Additionally, the stock solutions can be prepared with a reducing agent such as ascorbic acid (vitamin C), which prevents oxidative coupling of aniline [Donlon et al., 1995]. However, it should be considered that the addition of ascorbic

acid will modify the pH, which can lead to polymerisation of aniline. Therefore, a phosphate buffer solution (this research) or bicarbonate buffer solution should be applied to ensure neutral pH.

- **Assess the aniline degrading potential of sludge from AD systems that treat textile wastewater.** In the studies that have reported methanogenic aniline degradation, microbial communities were obtained from waterbody sediments (i.e. canal/river or aquifer) at industrial sites contaminated with a mixture of chemicals including aniline, monochlorobenzene, dichlorobenze, polycyclic aromatic hydrocarbons and azo dyes [Sun et al., 2015; Carvalho and Gavazza, personal communication, December 2019]. Therefore, it is recommended to assess the potential of sludge from AD systems that treat textile wastewater, which could provide follow-up research with the most suitable inoculum to achieve methanogenic degradation of aniline. Due to time limitations, the aniline degrading ability of the IC reactor sludge treating azo dye containing textile wastewater (Ten Cate, Nijverdal), which would be suitable for this purpose, was not comprehensively assessed.
- **Continue research with AnMBRs for assessing the biodegradability of recalcitrant compounds, such as aniline.** The AnMBR would still be a suitable system to achieve methanogenic aniline degradation using e.g. IC reactor sludge treating textile wastewater. The species mass balance with respect to organic substrates should be monitored conscientiously. Analysis of the permeate can be performed with the use of GC for detection of aniline, benzoate and VFAs, and with the use of high-performance liquid chromatography (HPLC) for detection of 4-aminobenzoate, the expected intermediate after carboxylation of aniline. Additionally, gas analysis based on mass spectrometry could be applied to detect the presence of volatilised aniline in the gas from the headspace of the bioreactor. In addition, BAs with this inoculum under conditions with elevated $CO_2$ partial pressure or bicarbonate concentrations can be performed.
- **Assess the methanogenic aniline-degrading ability of phototrophic bacteria in a membrane photobioreactor.** Facultative photosynthetic bacteria are able to use energy from a light source, instead of through oxidation of organic material under anaerobic conditions. Already in 1960 it was found by Scher and Proctor that photosynthetic bacteria can utilise benzoate for growth under anaerobic conditions in the presence of a light source. Similar findings were reported by Dutton and Evans [1969], Harwood and Gibson [1988] and Koch et al. [1993], who observed growth of the rod-shaped purple bacterium Rhodopseudomonas palustris on benzoate, 3-hydroxybenzoate, and 4-hydroxybenzoate. Additionally, several proteobacteria of the family Rhodospirillaceae have been recognised as photosynthetic purple bacteria with the ability of photoorganotrophic growth on aromatic compounds [Pfennig, 1978; Heider and Fuchs, 1997].
- **Consider supplementation of iron-based conductive materials.** Iron-based conductive materials such as zerovalent iron (ZVI) and iron (II/III) oxides, could be considered to support a variety of mechanisms in the AD process of complex organics. Where ZVI supplementation could promote the growth of hydrogenotrophic methanogens, iron oxides such as magnetite could enhance the degradation of complex organics through direct interspecies electron transfer between methanogens and organic-oxidising microorganisms. It has already been shown that the supplementation of these conductive materials improves the anaerobic degradation of phenol [He et al., 2019].
- **Introduce micro-aerobic conditions in the anaerobic system.** Micro-aeration could be introduced in the anaerobic reactor to achieve micro-aerobic removal of aniline. Carvalho et al. [2020] has applied this technique successfully for the treatment of azo dye containing textile wastewater.

# BIBLIOGRAPHY


Abou-Elela, S. I., Kamel, M. M., and Fawzy, M. E. (2010). Biological treatment of saline wastewater using a salt-tolerant microorganism. *Desalination*, 250:1–5.

Afzal, M., Iqbal, S., Rauf, S., and Khalid, Z. M. (2007). Characteristics of phenol biodegradation in saline solutions by monocultures of pseudomonas aeruginosa and pseudomonas pseudomallei. *Journal of Hazardous Materials*, 149:60–66.

Al-Kahlid, T. and El-Naas, M. H. (2012). Aerobic biodegradation of phenols: A comprehensive review. *Critical Reviews in Environmental Science and Technology*, 42:1631–1690.

An, F., Feng, X., and Gao, B. (2009). Adsorption of aniline from aqueous solution using novel adsorbent pam/sio_2. *Chemical Engineering Journal*, 151:183–187.

An, H., Qian, Y., Gu, X., and Tang, W. Z. (1996). Biological treatment of dye wastewaters using an anaerobic-oxic system. *Chemosphere*, 330:2533–2542.

Angelidaki, I., Alves, M., Bolzonella, D., Borzacconi, L., Campos, J. L., Guwy, A. J., Kalyuzhnyi, S., Jenicek, P., and van Lier, J. B. (2009). Defining the biomethane potential (bmp) of solid organic wastes and energy crops: a proposed protocol for batch assays. *Water Science & Technology*, 59:927–934.

Arora, P. K. (2015). Bacterial degradation of monocyclic aromatic amines. *Frontiers in Microbiology*, 6.

Astals, S., Batstone, D. J., Tait, S., and Jensen, P. D. (2015). Development and validation of a rapid test for anaerobic inhibition and toxicity. *Water Research*, 819:208–215.

Barbesti, S., Citterio, S., Labra, M., Baroni, M. D., Neri, M. G., and Sgorbati, S. (2000). Two and three-color fluorescence flow cytometric analysis of immunoidentified viable bacteria. *Cytometry*, 40:214–218.

Battersby, N. S. and Wilson, V. (1989). Survey of the anaerobic biodegradation potential of organic chemicals in digesting sludge. *Applied and Environmental Microbiology*, 55:433–439.

Berg, J. M., Tymoczko, J. L., Stryer, L., and Gatto Jr., G. J. (2012). *Biochemistry*. W. H. Freeman and Company, New York, seventh edition.

Boll, M. and Fuchs, G. (1995). Benzoyl-coenzyme a reductase (dearomatizing), a key enzyme of anaerobic aromatic metabolism. *European Journal of Biochemistry*, 233:921–933.

Boyd, S. A., Shelton, D. R., Berry, D., and Tiedje, J. M. (1983). Anaerobic biodegradation of phenolic compounds in digested sludge. *Applied and Environmental Microbiology*, 46:50–54.

Brillas, E. and Casado, J. (2002). Aniline degradation by electro-fenton®and peroxi-coagulation processes using a flow reactor for wastewater treatment. *Chemosphere*, 47:241–248.

Brown, D. and Hamburger, B. (1987). The degradation of dyestuffs: Part iii, investigations of their ultimate degradability. *Chemosphere*, 16:1539–1553.

Burnett, W. E. (1974). The effect of salinity variations on the activated sludge process. *Water & Sewage Works*, 121:37–38.

Cardillo, G. (2012). Four parameters logistic regression - there and back again. [https://it.mathworks.com/matlabcentral/fileexchange/38122]. Accessed: 18 December 2019.

Carliell, C. M., Barclay, S. J., Naidoo, N., Buckley, C. A., Mulholland, D. A., and Senior, E. (1995). Microbial decolourisation of a reactive azo dye under anaerobic conditions. *Water SA*, 21:61–69.

Carvalho, J. R. S., Amaral, F. M., Florencio, I., Kato, M. T., Delforno, T. P., and Gavazza, S. (2020). Microaerated uasb reactor treating textile wastewater: The core microbiome and removal of azo dye direct black 22. *Chemosphere*, 242.

Castillo-Carvajal, L. C., Sanz-Martín, J. L., and Barragán-Huerta, B. E. (2014). Biodegradation of organic pollutants in saline wastewater by halophilic microorganisms: a review. *Environmental Science and Pollution Research*, 21:9578–9588.

Chen, Y., Cheng, J. J., and Creamer, K. S. (2008). Inhibition of anaerobic digestion process: a review. *Bioresource technology*, 99:4044–4064.

Coe, R. H. (1952). Bench-scale biological oxidation of refinery wastes with activated sludge. *Sewage and Industrial Wastes*, 24:731–749.

de Alexandra, M., O'Connor, O. A., and Kosson, D. S. (1994). Metabolism of aniline under different anaerobic electron-accepting and nutritional conditions. *Environmental Toxicology and Chemistry*, 13:233–239.

Dean, J. A., editor (1999). *Lange's Handbook of Chemistry*. McGraw-Hill, Inc., New York, fifteenth edition.

DeLaune, R. D. and Reddy, K. R. (2005). *Redox Potential.*, pages 366–371. Elsevier, Oxford. In: *Hillel D (ed) Encyclopedia of Soils in the Environment.*

Dereli, R. K., Ersahin, M. E., Ozgun, H., Ozturk, I., Jeison, D., van der Zee, F., and van Lier, J. B. (2012). Potentials of anaerobic membrane bioreactors to overcome treatment limitations induced by industrial wastewaters. *Bioresource Technology*, 122:160–170.

Dickel, O., Haug, W., and Knackmuss, H. J. (1993). Biodegradation of nitrobenzene by a sequential anaerobic-aerobic process. *Biodegradation*, 4:187–194.

Donlon, B. A., Razo-Flores, E., Field, J. A., and Lettinga, G. (1995). Toxicity of n-substituted aromatics to acetoclastic methanogenic activity in granular sludge. *Applied and Environmental Microbiology*, 61:3889–3893.

Dutton, P. L. and Evans, W. C. (1969). The metabolism of aromatic compounds by *Rhodopseudomonas palustris*: A new, reductive, method of aromatic ring metabolism. *Biochemical Journal*, 113:525–536.

Dvořák, L., Gómez, M., Dolina, J., and Černín, A. (2015). Anaerobic membrane bioreactors—a mini review with emphasis on industrial wastewater treatment: applications, limitations and perspectives. *Desalination and Water Treatment*, 57:1–15.

Dvořák, L., Lederer, T., Jirků, V., J, M., and L, N. (2014). Removal of aniline, cyanides and diphenylguanidine from industrial wastewater using a full-scale moving bed biofilm reactor. *Process Biochemistry*, 49:102–109.

EPA (2000). Aniline. [https://www.epa.gov/sites/production/files/2016-08/documents/aniline.pdf]. U.S. Environmental Protection Agency. Accessed: 18 July 2020.

Escher, B. I., Snozzi, M., and Schwarzenbach, R. P. (1996). Uptake, speciation, and uncoupling activity of substituted phenols in energy transducing membranes. *Environmental Science & Technology*, 30:3071–3079.

Falcioni, T., Manti, A., Boi, P., Canonico, B., Balsamo, M., and Papa, S. (2006). Comparison of disruption procedures for enumeration of activated sludge floc bacteria by flow cytometry. *Cytometry Part B: Clinical Cytometry*, 70:149–153.

Fedorak, P. M., Kindzierski, W. B., and Hrudey, S. E. (1990). Effects of anilines and hydantoins on the methanogenic degradation of selected phenols. *Water Research*, 24:241–262.

Feijoo, G., Soto, M., Méndez, R., and Lema, J. M. (1995). Sodium inhibition in the anaerobic digestion process: Antagonism and adaptation phenomena. *Enzyme and Microbial Technology*, 17:180–188.

Field, J. A. (2002). Limits of anaerobic biodegradation. *Water Science and Technology*, 45:9–18.

Field, J. A., Stams, A. J. M., Kato, M., and Schraa, G. (1995). Enhanced biodegradation of aromatic pollutants in cocultures of anaerobic and aerobic bacterial consortia. *Antoine van Leeuwenhoek*, 67:47–77.

Fitzgerald, S. W. and Bishop, P. L. (1995). Two stage anaerobic/aerobic treatment of sulfonated azo dyes. *Journal of Environmental Science and Health*, A30:1251–1276.

Fu, H. Y., Zhang, Z. B., Chai, T., Huang, G. H., Yu, S. J., and Liu, Z. (2017). Bacterial growth on aniline: Implications for the biotreatment of industrial wastewater. *Water*, 9:365.

Fuchs, G., Boll, M., and Heider, J. (2011). Microbial degradation of aromatic compounds — from one strategy to four. *Nature Reviews Microbiology*, 9:803–816.

Gagliano, M. C., Ismail, S. B., Stams, A. J. M., Plugge, C. M., Temmink, H., and van Lier, J. B. (2017). Biofilm formation and granule properties in anaerobic digestion at high salinity. *Water Research*, 121:61–71.

Galinha, C. F., Sanches, S., and Crespo, J. G. (2018). *Membrane bioreactors*, chapter 6. Elsevier Ltd, Amsterdam. In: *Fundamental Modeling of Membrane Systems: Membrane and Process Performance*. Edited by Luis, P.

Gao, C. (2019). Impact of increased phenol loading rate on the phenol removal of an anaerobic membrane bioreactor operated at high sodium concentration. Master's thesis, Delft University of Technology.

Gheewala, S. H. and Annachhatre, A. P. (1997). Biodegradation of aniline. *Water Science and Technology*, 10:53–63.

Gómez, J. L., León, G., Hidalgo, A. M., Gómez, M., Murcia, M. D., and Griñán, G. (2009). Application of reverse osmosis to remove aniline from wastewater. *Desalination*, 245:687–693.

Goberna, M., Gadermaier, M., García, C., Wett, B., and Insam, H. (2010). Adaptation of methanogenic communities to the cofermentation of cattle excreta and olive mill wastes at $37^{\circ}c$ and $55^{\circ}c$. *Applied and Environmental Microbiology*, 76:6564–6571.

Gray, N. D., Sherry, A., Hubert, C., Dolfing, J., and Head, I. M. (2010). Methanogenic degradation of petroleum hydrocarbons in subsurface environments: Remediation, heavy oil formation, and energy recovery. *Advances in Applied Microbiology*, 72:137–161.

Grégori, G., Citterio, S., Ghiani, A., Labra, M., Sgorbati, S., Brown, S., and Denis, M. (2001). Resolution of viable and membrane-compromised bacteria in freshwater and marine waters based on analytical flow cytometry and nucleic acid double staining. *Applied and Environmental Microbiology*, 67:4662–4670.

Hanselmann, K. W. (1991). Microbial energetics applied to waste repositories. *Experientia*, 47:645–687.

Harwood, C. S. and Gibson, J. (1988). Anaerobic and aerobic metabolism of diverse aromatic compounds by the photosynthetic bacterium *Rhodopseudomonas palustris*. *Applied and Environmental Microbiology*, 54:712–717.

Haug, W., Schmidt, A., Nortermann, B., Hempel, D. C., Stolz, A., and Knackmuss, H. J. (1991). Mineralization of the sulfonated azo dye mordant-yellow 3 by a 6-aminonaphthalene-2-sulfonate degrading bacterial consortium. *Applied and Environmental Microbiology*, 57:144–149.

He, C., Lin, W., Zheng, X., Wang, C., Hu, Z., and Wang, W. (2019). Synergistic effect of magnetite and zero-valent iron on anaerobic degradation and methanogenesis of phenol. *Bioresource Technology*, 291.

Healy Jr., J. B. and Young, L. Y. (1978). Catechol and phenol degradation by a methanogenic population of bacteria. *Applied and Environmental Microbiology*, 35:216–218.

Heider, J. and Fuchs, G. (1997). Microbial anaerobic aromatic metabolism. *Anaerobe*, 3:1–22.

Heijnen, J. J. and Kleerebezem, R. (2010). *Bioenergetics of Microbial Growth*. John Wiley % Sons, Inc., New Jersey, US. In: *Encyclopedia of Industrial Biotechnology: Bioprocess, Bioseparation, and Cell Technology*. Edited by Flickinger, M. C.

Heijnen, J. J., van Loosdrecht, M. C. M., and Tijhuis, L. (1992). A black box mathematical model to calculate auto- and heterotrophic biomass yields based on gibbs energy dissipation. *Biotechnology and Bioengineering*, 40:1139–1154.

Heipieper, H.-J., Keweloh, H., and Rehm, H.-J. (1991). Influence of phenols on growth and membrane permeability of free and immobilized *Escherichia coli*. *Applied and Environmental Microbiology*, 57:1213–1217.

Huang, Y., Li, H., Rensing, C., Zhao, K., Johnstone, L., and Wang, G. (2012). Genome sequence of the facultative anaerobic arsenite-oxidizing and nitrate-reducing bacterium *Acidovorax* sp. strain no1. *Journal of Bacteriology*, 194.

Hulshoff Pol, L. W., Lens, P. N. L., Stams, A. J. M., and Lettinga, G. (1998). Anaerobic treatment of sulphate-rich wastewaters. *Biodegradation*, 9:213–224.

Hwu, C.-S., van Lier, J. B., and Lettinga, G. (1998). Physicochemical and biological performance of expanded granular sludge bed reactors treating long-chain fatty acids. *Process Biochemistry*, 33:75–81.

Ismail, S. B., Gonzalez, P., Jeison, D., and van Lier, J. B. (2008). Effects of high salinity wastewater on methanogenic sludge bed systems. *Water Science & Technology*, 58:1963–1970.

IWA (2005). *Anaerobic Digestion Model No.1 (ADM1)*. IWA Publishing, London, UK. IWA task group for mathematical modelling of anaerobic digestion processes.

Jeison, D. and van Lier, J. B. (2008). Anaerobic wastewater treatment and membrane filtration: a one night stand or a sustainable relationship? *Water Science & Technology*, 57:527–532.

Ji, Q., Tabassum, S., Hena, S., Silva, C. G., Yu, G., and Zhang, Z. (2016). A review on the coal gasification wastewater treatment technologies: past, present and future outlook. *Journal of Cleaner Production*, 126:38–55.

Jin, Q., Hu, Z., Jin, Z., Qiu, L., Zhong, W., and Pan, Z. (2012). Biodegradation of aniline in an alkaline environment by a novel strain of the halophilic bacterium, *Dietzia natronolimnaea* jq-an. *Bioresource Technology*, 117:148–154.

Judd, S. and Judd, C., editors (2011). *The MBR Book: Principles and Applications of Membrane Bioreactors for Water and Wastewater Treatment*. Elsevier Ltd, Oxford, second edition.

Kahl, T., Schröder, K. W., Lawrence, F. R., Marshall, W. J., Höke, H., and Jäckh, R. (2012). *'Aniline' in Ullmann's Encyclopedia of Industrial Chemistry.* Wiley-VCH Verlag GmbH & Co. KGaA, Weinheim.

Karickhoff, S. W., Brown, D. S., and Scott, T. A. (1979). Sorption of hydrophobic pollutants on natural sediments. *Water Research*, 13:241–248.

Kayembe, K., Basosila, L., Mpiana, P. T., Makambo, L., Sikulisimwa, P. C., Tshibangu, D. S. T., Tshilanda, D. D., and Tati, R. K. (2012). The effect of the monosubstituted benzenes functional groups on the inhibition of methane gas biosynthesis. *Journal of Sustainable Bioenergy Systems*, 2:92–96.

Keweloh, H., Weyrauch, G., and Rehm, H.-J. (1990). Phenol-induced membrane changes in free and immobilized *Escherichia coli*. *Applied Microbiology and Biotechnology*, 33:66–71.

Kinncannon, D. F. and Gaudy, A. F. (1966). Some effects of high salt concentrations on activated sludge. *Journal Water Pollution Control Federation*, 38:1148–1156.

Kirk, D. W., Sharifian, H., and Foulkes, F. R. (1985). Anodic oxidation of aniline for waste water treatment. *Journal of Applied Electrochemistry*, 15:285–292.

Kleerebezem, R. (1999). *Anaerobic Treatment of Phthalates, Microbiological and Technological Aspects.* PhD thesis, Wageningen University.

Kleerebezem, R. and van Loosdrecht, M. C. M. (2010). A generalized method for thermodynamic state analysis of environmental systems. *Critical Reviews in Environmental Science & Technology*, 40:1–54.

Knackmuss, H. J. (1996). Basic knowledge and perspectives of bioelimination of xenobiotic compounds. *Journal of Biotechnology*, 51:287–295.

Koch, J., Eisenreich, W., Bacher, A., and Fuchs, G. (1993). Products of enzymatic reduction of benzoyl-coa, a key reaction in anaerobic aromatic metabolism. *European Journal of Biochemistry*, 211:649–661.

Koch, J. and Fuchs, G. (1992). Enzymatic reduction of benzoyl-coa to alicyclic compounds, a key reaction in anaerobic aromatic metabolism. *European Journal of Biochemistry*, 205:195–202.

Kudlich, M., Bishop, P. L., Knackmuss, H. J., and Stolz, A. (1996). Simultaneous anaerobic and aerobic degradation of the sulfonated azo dye mordant yellow 3 by immobilized cells from a naphthalenesulfonate-degrading mixed culture. *Applied and Environmental Microbiology*, 46:597–603.

Ladino-Orjuela, G., Gomes, E., da Silva, R., Salt, C., and Parsons, J. R. (2016). Metabolic pathways for degradation of aromatic hydrocarbons by bacteria. *Reviews of Environmental Contamination and Toxicology*, 237:105–117.

Laempe, D., Jahn, M., and Fuchs, G. (1999). 6-hydroxycyclohex-1-ene-1-carbonyl-coa dehydrogenase and 6-oxocyclohex-1-ene-1-carbonyl-coa hydrolase, enzymes of the benzoyl-coa pathway of anaerobic aromatic metabolism in the denitrifying bacterium thauera aromatica. *European Journal of Biochemistry*, 263:420–429.

Le Borgne, S., Paniagua, D., and Vazquez-Duhalt, R. (2008). Biodegradation of organic pollutants by halophilic bacteria and archaea. *Journal of Molecular Microbiology and Biotechnology*, 15:74–92.

Le Clech, P., Jefferson, B., Chang, I. S., and Judd, S. J. (2003). Critical flux determination by the flux-step method in a submerged membrane bioreactor. *Journal of Membrane Science*, 227:81–93.

Lefebvre, O., Quentin, S., Torrijos, M., Godon, J. J., Delgenès, J. P., and Moletta, R. (2007). Impact of increasing nacl concentrations on the performance and community composition of two anaerobic reactors. *Applied Microbiology and Biotechnology*, 75:61–69.

Li, J. and Jin, Z. (2009). Effect of hypersaline aniline-containing pharmaceutical wastewater on the structure of activated sludge-derived bacterial community. *Journal of Hazardous Materials*, 172:432–438.

Li, X., Jin, X., Zhao, N., Angelidaki, I., and Zhang, Y. (2017). Efficient treatment of aniline containing wastewater in bipolar membrane microbial electrolysis cell-fenton system. *Water Research*, 119:67–72.

Li, Y. (2014). *Biotransformation of aniline, para-chloroaniline and pentachloronitrobenzene and environmental implications.* PhD thesis, Rutgers, The State University of New Jersey.

Liao, B. Q., Kraemer, J. T., and Bagley, D. M. (2006). Anaerobic membrane bioreactors: applications and research directions. *Critical Reviews in Environmental Science & Technology*, 36:489–530.

Lin, H. J., Xie, K., Mahendran, B., Bagley, D. M., Leung, K. T., Liss, S. N., and Liao, B. Q. (2009). Sludge properties and their effects on membrane fouling in submerged anaerobic membrane bioreactors (sanmbrs). *Water Research*, 43:3827–3837.

Liu, Q. Y., Liu, Y. X., and Lu, X. J. (2012). Combined photo-fenton and biological oxidation for the treatment of aniline wastewater. *Procedia Environmental Sciences*, 12:341–348.

Liu, Y.-B., Qu, D., Wen, Y.-J., and Ren, H.-J. (2015). Low-temperature biodegradation of aniline by freely suspended and magnetic modified *Pseudomonas migulae* an-1. *Applied Microbiology and Biotechnology*, 99:5317–5326.

Lyons, C. D., Katz, S., and Bartha, R. (1984). Mechanisms and pathways of aniline elimination from aquatic environments. *Applied and Environmental Microbiology*, 48:491–496.

Margesin, R. and Schinner, F. (2001). Potential of halotolerant and halophilic microorganisms for biotechnology. *Extremophiles*, 5:73–83.

McKinney, R. E., D, T. H., and Wilcox, R. L. (1956). Metabolism of aromatic compounds by activated sludge. *Sewage and Industrial Wastes*, 28:547–557.

McMurry, J., editor (2011). *Organic Chemistry.* Brooks/Cole, Belmont.

Meabe, E., Déléris, S., Soroa, S., and Sancho, L. (2013). Performance of anaerobic membrane bioreactor for sewage sludge treatment: Mesophilic and thermophilic processes. *Journal of Membrane Science*, 446:26–33.

Mecozzi, S., West Jr., A. P., and Dougherty, D. A. (1996). Cation-$\pi$ interactions in aromatics of biological and medicinal interest: Electrostatic potential surfaces as a useful qualitative guide. *Proceedings of the National Academy of Sciences of the United States of America*, 93:10566–10571.

Merkel, S. M., Eberhard, A. E., Gibson, J., and Harwood, C. S. (1989). Involvement of coenzyme a thioesters in anaerobic metabolism of 4-hydroxybenzoate by rhodopseudomonas palustris. *Journal of Bacteriology*, 171:1–7.

Mohammed, M., Mekala, L. P., Chintalapati, S., and Chintalapati, V. R. (2020). New insights into aniline toxicity: Aniline exposure triggers envelope stress and extracellular polymeric substance formation in *Rubrivivax benzoatilyticus* ja2. *Journal of Hazardous Materials*, 385.

Muñoz Sierra, J. D., Lafita, C., Gabaldon, C., Spanjers, H., and van Lier, J. B. (2017). Trace metals supplementation in anaerobic membrane bioreactors treating highly saline phenolic wastewater. *Bioresource Technology*, 234:106–114.

Muñoz Sierra, J. D., Oosterkamp, M. J., Wang, W., Spanjers, H., and van Lier, J. B. (2018a). Impact of long-term salinity exposure in anaerobic membrane bioreactors treating phenolic wastewater: Performance robustness and endured microbial community. *Water Research*, 141:172–184.

Muñoz Sierra, J. D., Wang, W., Cerqueda-Garcia, D., Oosterkamp, M. J., Spanjers, H., and van Lier, J. B. (2018b). Temperature susceptibility of a mesophilic anaerobic membrane bioreactor treating saline phenol-containing wastewater. *Chemosphere*, 213:92–102.

Mujahid, M., Prasuna, M. L., Sasikala, C., and Ramana, C. V. (2015). Integrated metabolomic and proteomic analysis reveals systemic responses of *Rubrivivax benzoatilyticus* ja2 to aniline stress. *Journal of Proteome Research*, 14:711–727.

Neufeld, R. F. and Spinola, A. A. (1978). Ozonation of coal gasification plant wastewater. *Environmental Science & Technology*, 12:470–472.

Olguin-Lora, P., Puig-Grajales, L., and Razo-Flores, E. (2003). Inhibition of the acetoclastic methanogenic activity by phenol and alkyl phenols. *Environmental Technology*, 24:999–1006.

O'Neill, F. J., Bromley-Challenor, K. C. A., Greenwood, R. J., and Knapp, J. S. (2000). Bacterial growth on aniline: Implications for the biotreatment of industrial wastewater. *Water Resources*, 34:4397–4409.

Orshansky, F. and Narkis, N. (1997). Characteristics of organics removal by pact simultaneous adsorption and biodegradation. *Water Resources*, 3:391–398.

Ozgun, H., Dereli, R. K., Ersahin, M. E., Kinaci, C., Spanjers, H., and van Lier, J. B. (2013). A review of anaerobic membrane bioreactors for municipal wastewater treatment: Integration options, limitations and expectations. *Separation and Purification Technology*, 118:89–104.

Parks, G. S. and Huffman, H. M., editors (1932). *The Free Energies of Some Organic Compounds.* The Chemical Catalog Company, Inc., New York. American chemical society. Monograph series. No. 60.

Patil, S. S. and Shinde, V. M. (1988). Biodegradation studies of aniline and nitrobenzene in aniline plant waste water by gas chromatography. *Environmental Science & Technology*, 22:1160–1165.

Pentair (2015). X-flow compact 33: Ultrafiltration membrane. Membrane Element Datasheet.

Pereira, R., Pereira, L., van der Zee, F. P., and Alves, M. M. (2011). Fate of aniline and sulfanilic acid in uasb bioreactors under denitrifying conditions. *Water Research*, 45:191–200.

Pfennig, N. (1978). *Rhodocyclus purpureus* gen. nov. and sp. nov., a ring-shaped, vitamin $b_{12}$-requiring member of the family *Rhodospirillaceae*. *International Journal of Systematic Bacteriology*, 28:283–288.

Philipp, B. and Schink, B. (2012). Different strategies in anaerobic biodegradation of aromatic compounds: nitrate reducers versus strict anaerobes. *Environmental Microbiology Reports*, 4:469–478.

Poirier, S., Bize, A., Bureau, C., Bouchez, T., and Chapleur, O. (2016). Community shifts within anaerobic digestion microbiota facing phenol inhibition: Towards early warning microbial indicators? *Water Research*, 100:296–305.

Prest, E. I., Hammes, F., Kötzch, S., van Loosdrecht, M. C. M., and Vrouwenvelder, J. S. (2013). Monitoring microbiological changes in drinking water systems using a fast and reproducible flow cytometric method. *Water Research*, 47:7131–7142.

Qi, X. H., Zhuang, Y. Y., Yuan, Y. C., and Gu, W. X. (2002). Decomposition of aniline in supercritical water. *Journal of Hazardous Materials*, B90:51–62.

Rava, E., Chirwa, E., P, A., van Niekerk, M., and Augustyn, M. P. (2016). The use of exogenous microbial species to enhance the performance of a hybrid fixed-film bioreactor treating coal gasification wastewater to meet discharge requirements. *Water SA*, 42:483–489.

Rawlings, G. D. and Samfield, M. (1979). Textile plant wastewater toxicity. *Environmental Science & Technology*, 13:160–164.

Razo Flores, E. (1997). *Biotransformation and Biodegradation of N-substituted Aromatics in Methanogenic Granular Sludge.* PhD thesis, Wageningen University.

Razo Flores, E., Donlon, B. A., Field, J. A., and Lettinga, G. (1996). Biodegradability of n-substituted aromatics and alkylphenols under methanogenic conditions using granular sludge. *Water Science and Technology*, 33:47–57.

Ren, Z., Zhu, X., Sun, W., Zhang, W., and Liu, J. (2014). Removal of aniline from wastewater using hollow fiber renewal liquid membrane. *Chinese Journal of Chemical Engineering*, 22:1187–1192.

Rice, E. W., Baird, R. B., Eaton, A. D., and Clesceri, L. S., editors (2012). *Standard Methods for the Examination of Water and Wastewater,* $22^{nd}$ *Edition.* American Public Health Association (APHA), American Water Works Association (AWWA), and Water Environment Federation (WEF), New York.

Rosenkranz, F., Cabrol, L., Carballa, M., Donoso-Bravo, A., Cruz, L., Ruiz-Filippi, G., Chamy, R., and Lema, J. M. (2013). Relationship between phenol degradation efficiency and microbial community structure in an anaerobic sbr. *Water Research*, 47:6739–6749.

Sarasa, J., Roche, M. P., Ormad, M. P., Gimeno, E., Puig, A., and Ovelleiro, J. L. (1998). Treatment of a wastewater resulting from dyes manufacturing with ozone and chemical coagulation. *Water Resources*, 32:2721–2727.

Scher, S. and Proctor, M. H. (1960). *Studies with photsynthetic bacteria: Anaerobic oxidation of aromatic compounds.* Academic Press, New York, third edition. In: *Comparative Biochemistry of Photoreactive Pigments*.

Schink, B. (1988). Fermentative degradation of nitrogenous aliphatic and aromatic compounds. *Hall ER & Hobson PN (Eds) Anaerobic Digestion 1988, Proceedings of the 5th International Symposium on Anaerobic Digestion held in Bologna, Italy, 22-26 May, 1988*, pages 459–464. Pergamon Press, Oxford.

Schink, B., Philipp, B., and Muller, J. (2000). Anaerobic degradation of phenolic compounds. *Naturwissenschaften*, 87:12–23.

Schnell, S. and Schink, B. (1991). Anaerobic aniline degradation via reductive deamination of 4-aminobenzoyl-coa in desulfobacterium anilini. *Archives of Microbiology*, 155:183–190.

Schülhe, K. and Fuchs, G. (2004). Phenylphosphate carboxylase: a new c-c lyase involved in anaerobic phenol metabolism in *Thauera aromatica*. *Journal of Bacteriology*, 186:4556–4567.

Sherry, A., Gray, N. D., Ditchfield, A. K., Aitken, C. M., Jones, D. M., Röling, W. F. M., Hallmann, C., Larter, S. R., Bowler, B. F. J., and Head, I. M. (2013). Anaerobic biodegradation of crude oil under sulphate-reducing conditions leads to only modest enrichment of recognized sulphate-reducing taxa. *International Biodeterioration & Biodegradation*, 81:105–113.

Sierra-Alvarez, R. and Lettinga, G. (1991). The effect of aromatic structure on the inhibition of acetoclastic methanogenesis in granular sludge. *Applied Microbiology and Biotechnology*, 34:544–550.

Sihtmäe, M., Mortimer, M., Kahru, A., and Blinova, I. (2010). Toxicity of five anilines to crustaceans, protozoa and bacteria. *Journal of the Serbian Chemical Society*, 9:1291–1302.

Sikkema, J., de Bont, J. A. M., and Poolman, B. (1995). Mechanisms of membrane toxicity of hydrocarbons. *Microbiological Reviews*, 59:201–222.

Singer, P. C., Pfaender, F. K., Chinchilli, J., Maciorowski, A. F., Lamb lll, J. C., and Goodman, R., editors (1978). *Assessment of Coal Conversion Wastewaters: Characterization and Preliminary Biotreatability*. United States Environmental Protection Agency, Washington DC.

Spanjers, H. and Vanrolleghem, P. A. (2016). *Respirometry*, chapter 3, pages 133–176. IWA Publishing, London, UK. In: *Experimental Methods In Wastewater Treatment*. Edited by van Loosdrecht, M.C.M., Nielsen, P.H., Lopez-Vazquez, C.M. and Brdjanovic, D.

Speece, R. E. (1983). Anaerobic biotechnology for industrial wastewater treatment. *Environmental Science & Technology*, 17:416–427.

Speece, R. E., editor (1996). *Anaerobic Biotechnology*. Archae Press, Nashville, Tennessee.

Sun, W., Li, Y., McGuinness, L. R., Luo, S., Huang, W., Kerkhof, L. J., Mack, E. E., Häggblom, M. M., and Fennell, D. E. (2015). Identification of anaerobic aniline-degrading bacteria at a contaminated industrial site. *Environmental Science & Technology*, 49:11079–11088.

Takeo, M., Ohara, A., Sakae, S., Okamoto, Y., Kitamura, C., Kato, D.-I., and Negoro, S. (2013). Function of a glutamine synthetase-like protein in bacterial aniline oxidation via $\gamma$-glutamylanilide . *Journal of Bacteriology*, 195:4406–4414.

Tan, N. C. G. (2001). *Integrated and sequential anaerobic/aerobic biodegradation of azo dyes.* PhD thesis, Wageningen University.

Tan, N. C. G., Prenafeta-Boldú, F. X., Opsteeg, J. L., Lettinga, G., and Field, J. A. (1999). Biodegradation of azo dyes in cocultures of anaerobic granular sludge with aerobic aromatic amine degrading enrichment cultures. *Applied Microbiology and Biotechnology*, 51:865–871.

Travis, A. S. (1997). Poisoned groundwater and contaminated soil: The tribulations and trial of the first major manufacturer of aniline dyes in basel. *Environmental History*, 2:343–365.

Tschech, A. and Fuchs, G. (1987). Anaerobic degradation of phenol by pure cultures of newly isolated denitrifying pseudomonads. *Archives of Microbiology*, 148:213–217.

Tschech, A. and Fuchs, G. (1989). Anaerobic degradation of phenol via carboxylation to 4-hydroxybenzoate: in vitro study of isotope exchange between $^{14}$co2 and 4-hydroxybenzoate. *Archives of Microbiology*, 152:594–599.

van Lier, J. B. (2008). High-rate anaerobic wastewater treatment: diversifying from end-of-the-pipe treatment to resource-oriented conversion techniques. *Water Science & Technology*, 57:1137–1148.

van Lier, J. B., Mahmoud, N., and Zeeman, G. (2008). *Anaerobic Wastewater Treatment*, chapter 16, pages 401–442. IWA Publishing, London, UK. In: *Biological Wastewater Treatment: Principles, Modelling and Design*. Edited by Hense, M., van Loosdrecht, M.C.M., Ekama, G.A. and Brdjanovic, D.

van Lier, J. B., Rebac, S., and Lettinga, G. (1997). High-rate anaerobic wastewater treatment under psychrophilic and thermophilic conditions. *Water Science and Technology*, 35:199–206.

van Lier, J. B., Tilche, A., Ahring, B. K., Macarie, H., Moletta, R., Dohanyos, M., Hulshoff Pol, L. W., Lens, P., and Verstraete, W. (2001). New perspectives in anaerobic digestion. *Water Science and Technology*, 43:1–18.

van Lier, J. B., van der Zee, F. P., Frijters, C. T. M. J., and Ersahin, M. E. (2015). Celebrating 40 years anaerobic sludge bed reactors for industrial wastewater treatment. *Reviews in Environmental Sciences & Biotechnology*, 14:681–702.

van Schie, P. M. and Young, L. Y. (2000). Biodegradation of phenol: Mechanisms and applications. *Bioremediation Journal*, 4:1–18.

Vyrides, I. and Stuckey, D. C. (2009). Effect of fluctuations in salinity on anaerobic biomass and production of soluble microbial products (smps). *Biodegradation*, 20:165–175.

Vyrides, I. and Stuckey, D. C. (2011). Fouling cake layer in a submerged anaerobic membrane bioreactor treating saline wastewaters: curse or a blessing? *Water Science & Technology*, 63:2902–2908.

Wada, S., Ichikawa, H., and Tatsumi, K. (1995). Removal of phenols and aromatic amines from wastewater by a combination treatment with tyrosinase and a coagulant. *Biotechnology and Bioengineering*, 46:304–309.

Wang, L., Barrington, S., and Kim, J. W. (2007). Biodegradation of pentyl amine and aniline from petrochemical wastewater. *Journal of Environmental Management*, 83:191–197.

Wang, S., Hou, X., and Su, H. (2017a). Exploration of the relationship between biogas production and microbial community under high salinity conditions. *Scientific Reports*, 7:1–10.

Wang, W., Wu, B., Pan, S., Yang, K., Hu, Z., and Yuan, S. (2017b). Performance robustness of the uasb reactors treating saline phenolic wastewater and analysis of microbial community structure. *Journal of Hazardous Materials*, 331:21–27.

Wang, Y., Gao, H., Na, X.-L., Dong, S.-Y., Dong, H.-W., Yu, L., Jia, L., and Wu, Y.-H. (2016). Aniline induces oxidative stress and apoptosis of primary cultured hepatocytes. *Internation Journal of Environmental Research and Public Health*, 13.

Weber, E. J., Colón, D., and Baughman, G. L. (2001). Sediment-associated reactions of aromatic amines. 1. elucidation of sorption mechanisms. *Environmental Science & Technology*, 35:2470–2475.

Wilczyńska-Piliszek, A. J., Piliszek, S., and Falandysz, J. (2012). Qspr models for prediction of the soil sorption coeffi cient (log koc) values of 209 polychlorinated trans-azobenzenes (pct-abs). *Journal of Environmental Science and Health*, pages 441–449.

Wittmann, C., Zeng, A. P., and Deckwer, W. D. (1995). Growth inhibition by ammonia and use of a ph-controlled feeding strategy for the effective cultivation of mycobacterium chlorophenolicum. *Applied Microbiology & Biotechnology*, 44:519–525.

Wood, J. M. (2015). Bacterial responses to osmotic challenges. *The Journal of General Physiology*, 5:381–388.

Yamada, T., Sekiguchi, Y., Hanada, S., Imachi, H., Ohashi, A., Harada, H., and Kamagata, Y. (2006). *Anaerolinea thermolimosa* sp. nov., *Levilinea saccharolytica* gen. nov., sp. nov. and *Leptolinea tardivitalis* gen. nov., sp. nov., novel filamentous anaerobes, and description of the new classes *Anaerolineae* classis nov. and *Caldilineae* classis nov. in the bacterial phylum *Chloroflexi*. *International Journal of Systematic and Evolutionary Microbiology*, 56:1331–1340.

Yang, K., Wu, W., Jing, Q., and Zhu, L. (2008). Aqueous adsorption of aniline, phenol, and their substitutes by multi-walled carbon nanotubes. *Environmental Science & Technology*, 42:7931–7936.

Yogalakshmi, K. N. and Joseph, K. (2010). Effect of transient sodium chloride shock loads on the performance of submerged membrane bioreactor. *Bioresource Technology*, 101:7054–7061.

Yuan, Y. L., Wen, Y. Z., Li, X. Y., and Luo, S. Z. (2006). Treatment of wastewater from dye manufacturing industry by coagulation. *Journal of Zhejiang University SCIENCE A*, 7:340–344.

Yumihara, K., Shigematsu, T., Hamada, K., Morimura, S., and Kida, K. (2002). Anaerobic degradation of terephtalic acid and aniline by methanogenic consortia. *Japanese Journal of Water Treatment Biology*, 38:1–9.

Zhang, S., Zhao, X., Niu, H., Shi, Y., Cai, Y., and Jiang, G. (2009). Superparamagnetic fe304 nanoparticles as catalysts for the catalytic oxidation of phenolic and aniline compounds. *Journal of Hazardous Materials*, 167:560–566.

Zhang, X. and Wiegel, J. (1994). Reversible conversion of 4-hydroxybenzoate and phenol by *Clostridium hydroxybenzoicum*. *Applied and Environmental Microbiology*, 60:4182–4185.

Zhao, Q. and Liu, Y. (2016). State of the art of biological processes for coal gasification wastewater treatment. *Biotechnology Advances*, 34:1064–1072.

Ziels, R. M., Nobu, M. K., and Sousa, D. Z. (2019). Elucidating syntrophic butyrate-degrading populations in anaerobic digesters using stable-isotope-informed genome-resolved metagenomics. *mSystems (American Society for Microbiology)*, 4:1–16.

Zwietering, M. H., Jongenburger, I., Rombouts, F. M., and van 't Riet, K. (1990). Modeling of the bacterial growth curve. *Applied and Environmental Microbiology*, 56:1875–1881.

# A CHEMICAL OXYGEN DEMAND

**Table A.1:** COD-content of the compounds relevant in this project. The values were obtained from Kleerebezem and van Loosdrecht [2010] or calculated based on equation A.10 (as proposed by Kleerebezem and van Loosdrecht [2010]).

| **Compound** | **Structure** | **Molar mass** | **COD** |
|---|---|---|---|
| | | $(g \cdot mol^{-1})$ | $(gO_2 \cdot g^{-1})$ |
| Phenol | $C_6H_5OH$ | 94.11 | 2.380 |
| Aniline | $C_6H_5NH_2$ | 93.13 | 2.405 |
| 4-aminobenzoic acid | $HOOCC_6H_5NH_2$ | 138.14 | 1.679 |
| Benzoate | $C_6H_5COO^-$ | 121.11 | 1.982 |
| Benzoic acid | $C_6H_5COOH$ | 122.12 | 1.965 |
| Propionate | $C_2H_5COO^-$ | 73.07 | 1.533 |
| Propionic acid | $C_2H_5COOH$ | 74.08 | 1.512 |
| Butyrate | $C_3H_7COO^-$ | 87.08 | 1.837 |
| n-Butyric acid | $C_3H_7COOH$ | 88.10 | 1.816 |
| Acetate | $CH_3COO^-$ | 59.04 | 1.084 |
| Acetic acid | $CH_3COOH$ | 60.05 | 1.066 |
| Biomass | $CH_{1.8}O_{0.5}N_{0.2}$ | 24.63 | 1.364 |
| Water | $H_2O$ | 18.01 | |
| Carbon dioxide | $CO_2$ | 44.01 | 0.00 |
| Bicarbonate | $HCO_3^-$ | 61.02 | 0.00 |
| Methane | $CH_4$ | 16.04 | 3.989 |
| Ammonia | $NH_3$ | 17.03 | |
| Ammonium | $NH_4^+$ | 18.04 | |
| Proton | $H^+$ | 1.01 | |
| Electron | $e^-$ | 0.00 | |

**From Kleerebezem and van Loosdrecht [2010]:**

For an arbitrary organic compound $C_cH_bO_oN_n^z$, the donor reaction can be written in generalised terms as:

$$-1 \cdot C_cH_bO_oN_n^z + Y^D_{NH_4^+} \cdot NH_4^+ + Y^D_{CO_2} \cdot CO_2 + Y^D_{H_2O} \cdot H_2O + Y^D_{H^+} \cdot H^+ + Y^D_{e^-} \cdot e^- \quad \text{(A.1)}$$

From this, balances for the four elements and for the electro-neutrality can be derived:

$$C - balance : -c + Y^D_{CO_2} = 0 \quad \text{(A.2)}$$

$$H - balance : -b + Y^D_{H^+} + 4 \cdot Y^D_{NH_4^+} + 2 \cdot Y^D_{H_2O} = 0 \quad \text{(A.3)}$$

$$O - balance : -o + 2 \cdot Y^D_{CO_2} + Y^D_{H_2O} = 0 \quad \text{(A.4)}$$

$$N - balance : -n + Y^D_{NH_4^+} = 0 \quad \text{(A.5)}$$

$$EN - balance : -z + Y^D_{H^+} - Y^D_{e^-} + Y^D_{NH_4^+} = 0 \tag{A.6}$$

This set of equations can be solved for $Y^D_e$

$$Y^D_{e^-}[mol - e^-/mol] = 4 \cdot c + b - 2 \cdot o - 3 \cdot n - z \tag{A.7}$$

From the electron acceptor reaction, $Y^A_{e^-}$ can be obtained:

$$-1 \cdot O_2 - 4 \cdot H^+ - 4 \cdot e^- + 2 \cdot H_2O = 0 \tag{A.8}$$

$$Y^A_{e^-} = 4mol - e^-/mol - O_2 \tag{A.9}$$

Combined, this gives the equation for calculating the COD-equivalent concentration:

$$Y^{Cat}_{O_2/S}[mol - O2/mol - S] = \frac{Y^D_e}{Y^A_e} = \frac{4 \cdot c + b - 2 \cdot o - 3 \cdot n - z}{4} \tag{A.10}$$

# B THERMODYNAMIC DATA

**Table B.1:** Thermodynamic data: standard Gibbs free energy of formation ($G_f^0$) and the standard enthalpy of formation ($H_f^0$) of the compounds used in this project. The thermodynamic values are obtained from Hanselmann [1991], Kleerebezem and van Loosdrecht [2010] and Dean [1999]. The negative $G_f^0$ value for aniline of Hanselmann [1991] was copied from Parks and Huffman [1932] incorrectly: it should be +148.1 $kJ \cdot mol^{-1}$. This corresponds with the value reported by Dean [1999] (+149.2 $kJ \cdot mol^{-1}$).

| **Compound** | **Structure** | **Phase** | $G_f^0$ **(**$kJ \cdot mol^{-1}$**)** | | | $H_f^0$ **(**$kJ \cdot mol^{-1}$**)** | | |
|---|---|---|---|---|---|---|---|---|
| | | | Ref. 1[a] | Ref. 2[b] | Ref. 3[c] | Ref. 1[a] | Ref. 2[b] | Ref. 3[c] |
| Phenol | $C_6H_5OH$ | g | -29.7 | | -32.9 | -93.3 | | -96.4 |
| Aniline | $C_6H_5NH_2$ | l | -148.1 | | +149.2 | | | +31.3 |
| | | | (+148.1)[d] | | | (+30.7)[d] | | |
| | | g | | | -7.0 | | | +87.5 |
| 4-aminobenzoic acid | $HOOCC_6H_5NH_2$ | s | | | | | | -412.9 |
| Benzoate | $C_6H_5COO^-$ | aq | | -218.6 | | | | |
| Benzoic acid | $C_6H_5COOH$ | g | -133.5 | | | -211.7 | | |
| | | s | | | -245.3 | | | -385.2 |
| Propionate | $C_2H_5COO^-$ | aq | | -361.1 | | | -510.4 | |
| Propionic acid | $C_2H_5COOH$ | g | -367.3 | | | -453.9 | | |
| Butyrate | $C_3H_7COO^-$ | aq | | -352.6 | | | -535.0 | |
| n-Butyric acid | $C_3H_7COOH$ | g | -358.7 | | | -474.5 | | |
| Acetate | $CH_3COO^-$ | aq | -369.4 | -369.4 | -369.65 | -486.0 | -485.8 | -486.34 |
| Acetic acid | $CH_3COOH$ | l | -389.9 | | -390.2 | -484.5 | | -484.4 |
| | | g | -374.0 | | -374.2 | -432.2 | | -432.2 |
| - unionised | | aq | -372.4 | | | -425.4 | | |
| Biomass | $CH_{1.8}O_{0.5}N_{0.2}$ | s | | -67.0 | | | -91.0 | |
| Water | $H_2O$ | l | -237.2 | -237.2 | | -285.8 | -285.8 | |
| Carbon dioxide | $CO_2$ | g | -394.4 | -394.4 | | -393.5 | -393.5 | |
| | | aq | -386.0 | | | -413.8 | | |
| Bicarbonate | $HCO_3^-$ | aq | -586.9 | -586.9 | | -692.0 | -692.0 | |
| Methane | $CH_4$ | g | -50.8 | -50.7 | -50.5 | -74.8 | -74.8 | -74.6 |
| | | aq | -34.4 | | | -89.0 | | |
| Ammonia | $NH_3$ | g | -16.5 | | -16.4 | -46.1 | | -45.94 |
| | | aq | -26.6 | | | -80.3 | | |
| Ammonium | $NH_4^+$ | aq | -79.4 | -79.4 | -79.37 | -133.3 | -133.3 | -133.26 |
| Hydrogen | $H_2$ | g | 0.0 | 0.0 | | 0.0 | 0.0 | |
| Proton | $H^+$ | aq | 0.0 | 0.0 | | 0.0 | 0.0 | |
| Electron | $e^-$ | g/aq | 0.0 | 0.0 | | 0.0 | 0.0 | |

**References:** [a]Hanselmann [1991]; [b]Kleerebezem and van Loosdrecht [2010]; [c]Dean [1999] [d]Parks and Huffman [1932]

# C MATLAB SCRIPT GOMPERTZ MODEL

MATLAB script for the Gompertz model, modified from Cardillo [2012]. Original script for the four parameters logistic regression can be found on https://it.mathworks.com/matlabcentral/fileexchange/38122.

```
function [cf,G]=Gompertz(x,y,varargin)

p = inputParser;
addRequired(p,'x',@(x) validateattributes(x,–'numeric'″,–'column','real','finite','nonnan','nonempty'″));
addRequired(p,'y',@(x) validateattributes(x,–'numeric'″,–'2d','real','finite','nonnan','nonempty'″));
addOptional(p,'st',[],@(x) validateattributes(x,–'numeric'″,–'row','real','finite','nonnan','ncols',4″));
addOptional(p,'L',[],@(x) validateattributes(x,–'numeric'″,–'row','real','nonnan','ncols',4″));
addOptional(p,'U',[],@(x) validateattributes(x,–'numeric'″,–'row','real','nonnan','ncols',4″));
parse(p,x,y,varargin–:″);
st=p.Results.st; L=p.Results.L; U=p.Results.U;
clear p
assert(size(x,1)==size(y,1),'X and Y must have the same rows number')
assert(size(x,1)¿=4,'Not enough Data points')

if ˜isvector(y)
we=std(y,0,2);
y=mean(y,2);
else
we=zeros(size(x));
end

slope=(y(end)-y(1))/(x(end)-x(1));
if isempty(st)
[˜,Idx]=min(abs((y-max(y)/2)));
st=[sign(slope) x(Idx) max(y)];
end

if isempty(L)
L=zeros(1,3);
if slope¡0
L(2)=-Inf;
end
end

if isempty(U)
U=Inf(1,3);
if slope¡0
U(2)=0;
end
end

%----------------------------Fit the data--------------------------------
fo = fitoptions('method','NonlinearLeastSquares','Lower',L,'Upper',U);
set(fo,'Startpoint',st);
```

```
if all(we) % if y was a matrix use std as weights for fitting
set(fo,'Weights',we);
end
ft = fittype('a*exp(-exp((lambda*(mu/a*exp(1))+1)-(mu/a*exp(1))*x))',...
'dependent',–'y'″,'independent',–'x'″,...
'coefficients',–'a', 'lambda', 'mu'″);
[cf,G] = fit(x,y,ft,fo);
```

# D ANMBR FEED

**Table D.1:** Feed for the continuous AnMBR operation during this project. The composition of the macro- & micronutrient solutions and phosphate buffer solutions A & B can be found in appendix E. In week 16 (9 December 2019 – 15 December 2019) the AnMBR was not fed due to a malfunctioning.

| **Compound** | | **Week nr.** (Week 1 started at 26 August 2019) | | | | | | | | | | | | | | | | | | | | | | | | | | | | | (Week 29 ended at 15 March 2020) |
|---|---|---|---|---|---|---|---|---|---|---|---|---|---|---|---|---|---|---|---|---|---|---|---|---|---|---|---|---|---|---|---|
| | Unit | 1 | 2 | 3 | 4 | 5 | 6 | 7 | 8 | 9 | 10 | 11 | 12 | 13 | 14 | 15 | 16 | 17 | 18 | 19 | 20 | 21 | 22 | 23 | 24 | 25 | 26 | 27 | 28 | 29 |
| Macronutrient sol. | $ml/L$ | 45.84 | 45.84 | 15.28 | 15.28 | 15.28 | 15.28 | 15.28 | 15.28 | 15.28 | 16.04 | 15.28 | 15.28 | 15.28 | 15.28 | 15.28 | - | 15.28 | 15.28 | 15.28 | 15.28 | 15.28 | 15.28 | 15.28 | 15.28 | 15.28 | 15.28 | 15.28 | 15.28 | 15.28 |
| Micronutrient sol. | $ml/L$ | 22.92 | 22.92 | 7.64 | 7.64 | 7.64 | 7.64 | 7.64 | 7.64 | 7.64 | 8.02 | 7.64 | 7.64 | 7.64 | 7.64 | 7.64 | - | 7.64 | 7.64 | 7.64 | 7.64 | 7.64 | 7.64 | 7.64 | 7.64 | 7.64 | 7.64 | 7.64 | 7.64 | 7.64 |
| Buffer sol. A | $ml/L$ | 30.50 | 30.50 | 30.50 | 30.50 | 30.50 | 30.50 | 30.50 | 30.50 | 30.50 | 32.03 | 30.50 | 30.50 | 30.50 | 30.50 | 30.50 | - | 30.50 | 30.50 | 30.50 | 30.50 | 30.50 | 30.50 | 30.50 | 30.50 | 30.50 | 30.50 | 30.50 | 30.50 | 30.50 |
| Buffer sol. B | $ml/L$ | 19.50 | 19.50 | 19.50 | 19.50 | 19.50 | 19.50 | 19.50 | 19.50 | 19.50 | 20.48 | 19.50 | 19.50 | 19.50 | 19.50 | 19.50 | - | 19.50 | 19.50 | 19.50 | 19.50 | 19.50 | 19.50 | 19.50 | 19.50 | 19.50 | 19.50 | 19.50 | 19.50 | 19.50 |
| Yeast extract | $mg/L$ | 0.5 | 0.5 | 0.5 | 0.5 | 0.5 | 0.5 | 0.5 | 0.5 | 0.5 | 0.53 | 0.5 | 0.5 | 0.5 | 0.5 | 0.5 | - | 0.5 | 0.5 | 0.5 | 0.5 | 0.5 | 0.5 | 0.5 | 0.5 | 0.5 | 0.5 | 0.5 | 0.5 | 0.5 |
| Aniline | $g/L$ | 0.1 | 0.1 | 0.1 | 0.1 | 0.1 | 0.1 | 0.1 | 0.1 | 0.1 | 0.11 | 0.2 | 0.2 | 0.2 | 0.2 | 0.05 | | 0.05 | 0.02 | 0.02 | 0.02 | 0.02 | 0.02 | 0.02 | 0.02 | 0.02 | 0.02 | 0.02 | 0.02 | 0.02 |
| Phenol | $g/L$ | 0.5 | 0.5 | 0.5 | 0.5 | 0.5 | 0.5 | 0.5 | 0.5 | 0.5 | 0.53 | 0.5 | 0.5 | 0.5 | 0.5 | 0.5 | - | 0.5 | 0.5 | 0.5 | 0.5 | 0.5 | 0.5 | 0.5 | 0.5 | 0.5 | 0.5 | 0.5 | 0.5 | 0.5 |
| $NaCH_3COO \cdot 3H_2O$ | $g/L$ | 30.39 | 30.39 | 9.12 | 9.12 | 9.12 | 9.12 | 9.12 | 9.12 | 9.12 | 9.57 | 8.86 | 8.86 | 8.86 | 8.86 | 9.24 | - | 9.24 | 9.32 | 9.32 | 9.32 | 9.32 | 9.32 | 9.32 | 9.32 | 9.32 | 9.32 | 9.32 | 9.32 | 9.32 |
| $NaC_2H_5COO$ | $g/L$ | 5.02 | 5.02 | 1.50 | 1.50 | 1.50 | 1.50 | 1.50 | 1.50 | 1.50 | 1.58 | 1.46 | 1.46 | 1.46 | 1.46 | 1.53 | - | 1.53 | 1.54 | 1.54 | 1.54 | 1.54 | 1.54 | 1.54 | 1.54 | 1.54 | 1.54 | 1.54 | 1.54 | 1.54 |
| $NaC_3H_7COO$ | $g/L$ | 6.13 | 6.13 | 1.84 | 1.84 | 1.84 | 1.84 | 1.84 | 1.84 | 1.84 | 1.93 | 1.79 | 1.79 | 1.79 | 1.79 | 1.86 | - | 1.86 | 1.88 | 1.88 | 1.88 | 1.88 | 1.88 | 1.88 | 1.88 | 1.88 | 1.88 | 1.88 | 1.88 | 1.88 |
| $NaCl$ | $g/L$ | 0.75 | 0.75 | 14.30 | 14.30 | 14.30 | 14.30 | 14.30 | 14.30 | 14.30 | 15.02 | 14.46 | 14.46 | 14.46 | 14.46 | 14.22 | - | 14.22 | 14.17 | 14.17 | 14.17 | 14.17 | 14.17 | 14.17 | 14.17 | 14.17 | 14.17 | 14.17 | 14.17 | 14.17 |
| $Na^+$ | $Na^+ \cdot L^{-1}$ | 8 | 8 | 8 | 8 | 8 | 8 | 8 | 8 | 8 | 8 | 8 | 8 | 8 | 8 | 8 | - | 8 | 8 | 8 | 8 | 8 | 8 | 8 | 8 | 8 | 8 | 8 | 8 | 8 |
| Phosphates | $mM$ | 10 | 10 | 10 | 10 | 10 | 10 | 10 | 10 | 10 | 10 | 10 | 10 | 10 | 10 | 10 | - | 10 | 10 | 10 | 10 | 10 | 10 | 10 | 10 | 10 | 10 | 10 | 10 | 10 |
| $K^+$:$Na^+$ | $gK^+/gNa^+$ | 0.059 | 0.059 | 0.059 | 0.059 | 0.059 | 0.059 | 0.059 | 0.059 | 0.059 | 0.059 | 0.059 | 0.059 | 0.059 | 0.059 | 0.059 | - | 0.059 | 0.059 | 0.059 | 0.059 | 0.059 | 0.059 | 0.059 | 0.059 | 0.059 | 0.059 | 0.059 | 0.059 | 0.059 |

# E MACRO- & MICRONUTRIENT SOLUTIONS AND PHOSPHATE BUFFER

**Table E.1:** Micronutrient solution used in the biodegradability studies.

| Compound | Chemical formula | Concentration |
|---|---|---|
| Iron(III) Chloride Hexahydrate | $FeCl_3 \cdot 6H_2O$ | 2 $g \cdot L^{-1}$ |
| Cobalt(II) Chloride Hexahydrate | $CoCl_2 \cdot 6H_2O$ | 2 $g \cdot L^{-1}$ |
| Manganese(II) Chloride Tetrahydrate | $MnCl_2 \cdot 4H_2O$ | 0.5 $g \cdot L^{-1}$ |
| Copper(II) Chloride Dihydrate | $CuCl_2 \cdot 2H_2O$ | 30 $mg \cdot L^{-1}$ |
| Zinc Chloride | $ZnCl_2$ | 50 $mg \cdot L^{-1}$ |
| Boric Acid | $H_3BO_3$ | 50 $mg \cdot L^{-1}$ |
| Ammonium Molybdate Tetrahydrate | $(NH_4)_6Mo_7O_2 \cdot 4H_2O$ | 90 $mg \cdot L^{-1}$ |
| Sodium Selenite | $Na_2SeO_3$ | 100 $mg \cdot L^{-1}$ |
| Nickel(II) Chloride Hexahydrate | $NiCl_2 \cdot 6H_2O$ | 50 $mg \cdot L^{-1}$ |
| Disodium EDTA | $C_{10}H_{16}N_2Na_2O_8$ | 1 $g \cdot L^{-1}$ |
| Sodium Tungstate | $Na_2WO_4$ | 80 $mg \cdot L^{-1}$ |

**Table E.2:** Macronutrient solution used in the biodegradability studies, as suggested by Spanjers and Vanrolleghem [2016]

| Compound | Chemical formula | Concentration |
|---|---|---|
| Ammonium Chloride | $NH_4Cl$ | 170 $g \cdot L^{-1}$ |
| Calcium Chloride Dihydrate | $CaCl_2 \cdot 2H_2O$ | 8 $g \cdot L^{-1}$ |
| Magnesium Sulfate Heptahydrate | $MgSO_4 \cdot 7H_2O$ | 9 $g \cdot L^{-1}$ |

**Table E.3:** Phosphate buffer solutions used in the biodegradability studies.

| Compound | Chemical formula | Concentration |
|---|---|---|
| "A": Dipotassium Phosphate (0.2M) | $K_2HPO_4$ | 34.85 $g \cdot L^{-1}$ |
| "B": Monosodium Phosphate (0.2M) | $NaH_2PO_4$ | 24.00 $g \cdot L^{-1}$ |

# F PREPARATION OF STAIN SOLUTIONS

**Required consumables:**

- Trizma Base, MW = 121.14
- SG nucleic acid gel stain, Invitrogen/Molecular Probes S7563
- PI powder, Invitrogen/Molecular Probes P1304MP
- dimethyl sulfoxide (DMSO)

## F.1 10 $mM$ TRIS BUFFER PH 8 (1 $L$)

1. Dissolve 1.21 $g$ Trizma Base in 800 $mL$ ultra pure water.
2. Check pH (if necessary adjust by adding $HCl$ conc.)
3. Adjust volume to 1 $L$ with ultrapure water.
4. Divide into aliquots (e.g. 4x 250 $mL$).
5. Sterilise by autoclaving and store at 4°$C$.

## F.2 SG WORKING SOLUTION

1. Dilute 10 $\mu L$ of SG stock solution (10,000x conc.) in 990 $\mu L$ of DMSO.
2. Divide into aliquots (e.g. 500 $\mu L$) in amber glass vials.
3. Store at -20°$C$.
4. Use 1:100 diluted in your samples.

## F.3 SGPI WORKING SOLUTION

1. Add 5 $mL$ of DMSO (0.1 $\mu L$ filtered) to PI powder to make a 30 $mM$ stock solution of PI.
2. Mix 10 $\mu L$ of SG stock solution (10,000x conc.) with 20 $\mu L$ PI stock solution in 0.97 $mL$ of 10 $mM$ Tris pH 8.
3. Divide into aliquots (e.g. 50 $\mu L$) in amber glass vials.
4. Store at -20°$C$.
5. Use 1:2 diluted in your samples.

# G DATA PROCESSING SMA-INHIBITION TEST

## G.1 EFFECT OF ANILINE ON THE SMA

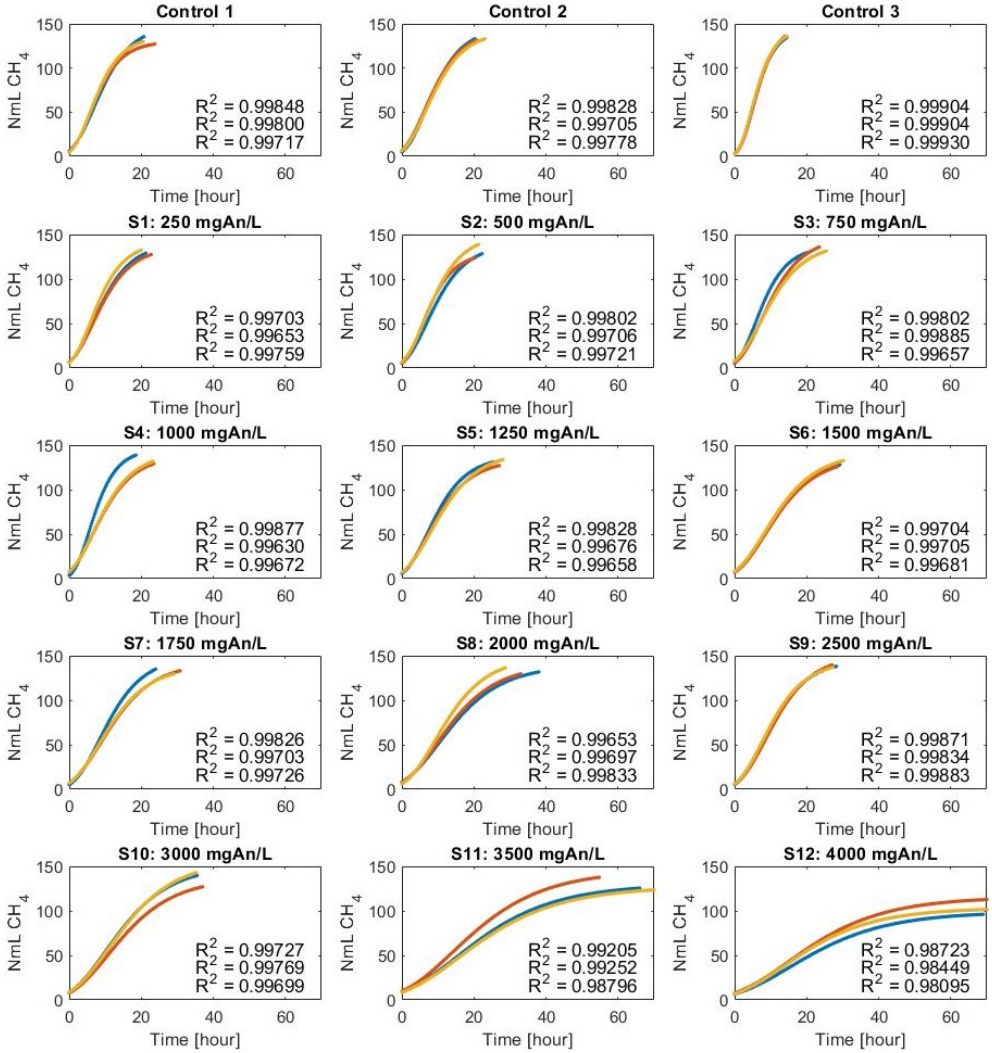


**Figure G.1:** Gompertz model fit (equation 3.3) based on data obtained from the AMPTS by performing an SMA inhibition test with aniline concentrations varying from 0 - 4000 $mg \cdot L^{-1}$ (in triplicates).

### G.1.1 Effect of phenol on the SMA

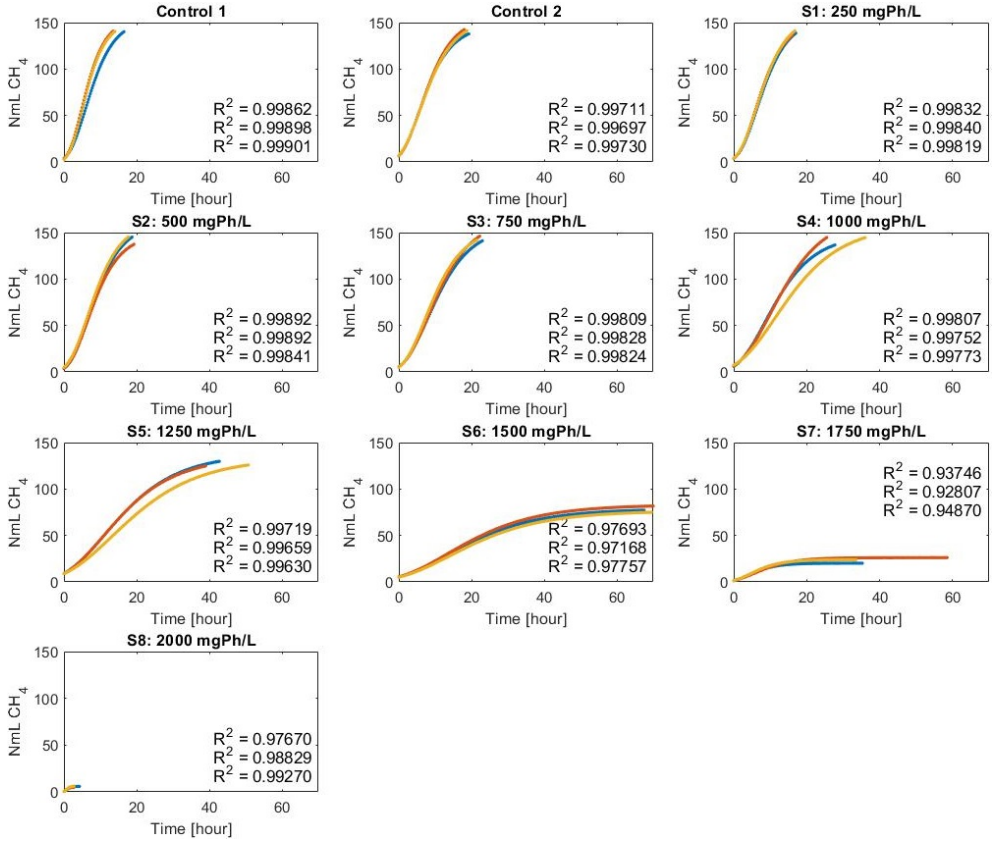


**Figure G.2:** Gompertz model fit (equation 3.3) based on data obtained from the AMPTS by performing an SMA inhibition test with phenol concentrations varying from 0 - 2000 $mg \cdot L^{-1}$ (in triplicates).

# H MEMBRANE CRITICAL FLUX

The flux-step method was carried out to assess the critical flux of the PVDF UF membrane of an AnMBR seeded with granular mesophilic sludge ($34.9 \pm 0.5\ gVSS \cdot L^{-1}$) from an UASB reactor. By increasing the flux 3.82 *LMH* every 15 minutes, the critical flux was determined based on the point where a discontinuity in the trend was observed. In other words, at the flux at which a significant difference between $TMP_f^n$ and $TMP_i^n$ was observed. From figure H.1 the critical flux was determined to be 29.3 *LMH*.

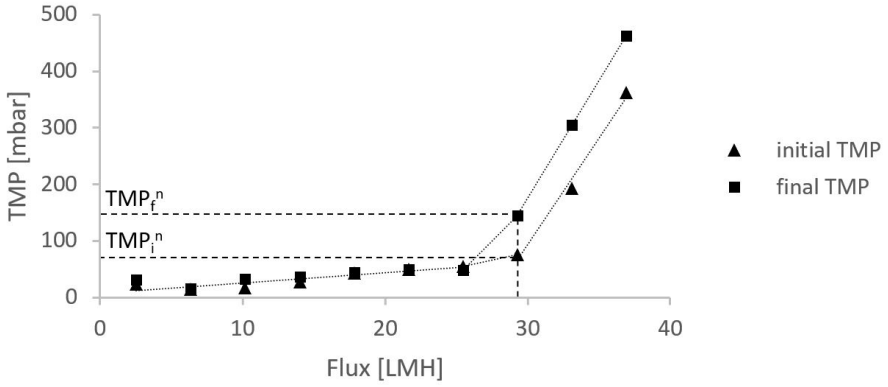


**Figure H.1:** Determination of the critical flux, based on the flux-step method as demonstrated by Le Clech et al. [2003]. The first significant difference between $TMP_f^n$ (■) and $TMP_i^n$ (▲) indicates the critical flux.

# I COD BALANCE

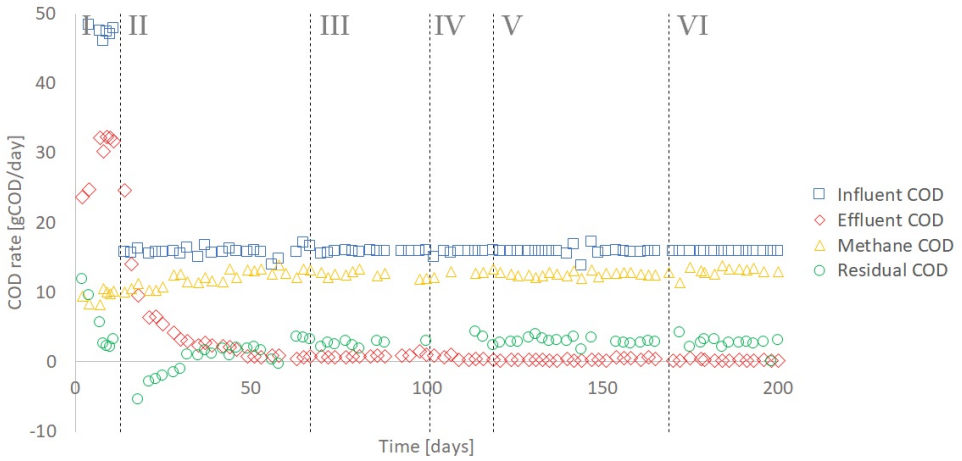


**Figure I.1:** The COD balance in the AnMBR over time. From the vertical axis the COD rates with respect to the influent (□), effluent (◊), methane (△), and residual (◯) can be read. The numerals indicate stages as defined in table 3.5.

# J | BIOGAS PRODUCTION IN THE ANMBR

The biogas production in the AnMBR and its composition were continuously monitored. Figure J.1 shows the methane production rate ($R_{CH_4}$) in $gCOD \cdot L^{-1} \cdot day^{-1}$, and the percentage of methane and carbon dioxide in the biogas. $R_{CH_4}$ is 1.6 $gCOD \cdot L^{-1} \cdot day^{-1}$ at the start-up of the reactor (stage I). In stage II, $R_{CH_4}$ gradually increases to 2.0 $gCOD \cdot L^{-1} \cdot day^{-1}$. When the aniline concentration in the feed is increased to 200 $mgAn \cdot L^{-1}$ in stage III, $R_{CH_4}$ decreases to 1.8 $gCOD \cdot L^{-1} \cdot day^{-1}$. After decreasing the aniline concentration in stage IV and V, $R_{CH_4}$ increases slowly to a plateau 2.0 $gCOD \cdot L^{-1} \cdot day^{-1}$. The biogas composition over the whole operational period remained relatively constant with a methane content of 80%. Only in stage II, specifically from day 16-46, the methane content was slightly higher with 84%.

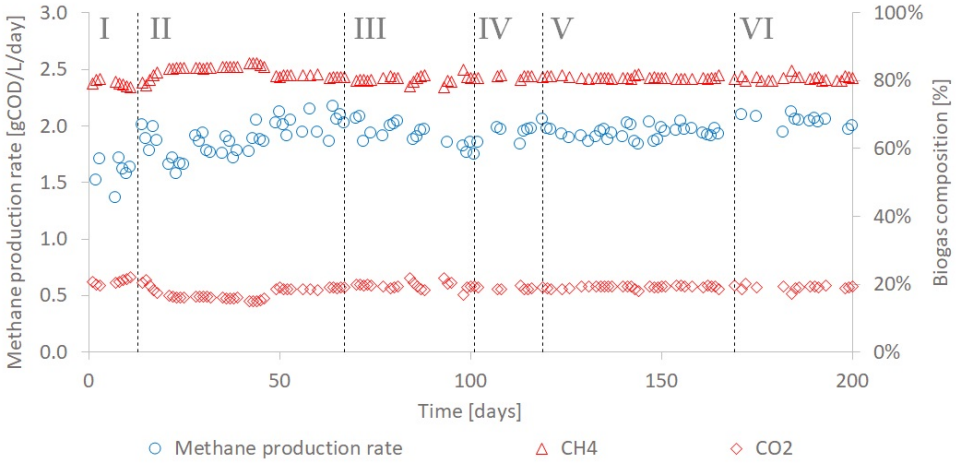


**Figure J.1:** The methane production rate and composition of the biogas in the AnMBR over time. From the primary vertical axis the methane production rate (◯) can be read, and from the secondary vertical axis the biogas composition can be read (△: methane, and ◊: $CO_2$). The numerals indicate stages as defined in table 3.5.

# K TEMPERATURE AND PH IN THE ANMBR

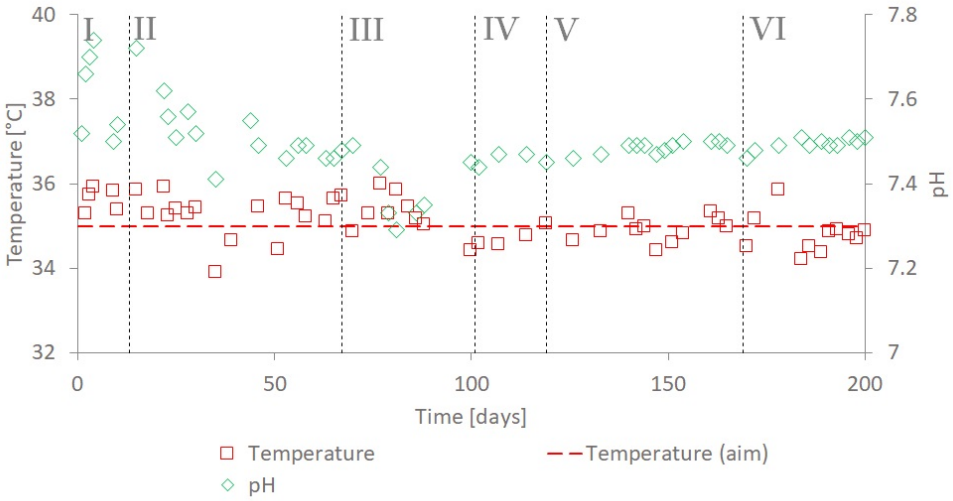


**Figure K.1:** Temperature (□) and pH (◊) in the AnMBR over time. The temperature in the AnMBR was maintained at $35 \pm 1°C$ using a thermostatic water bath, and the pH was buffered with a phosphate buffer solution. The numerals indicate stages as defined in table 3.5

# L | SUSPENDED SOLIDS IN THE ANMBR

The TSS and VSS concentration in the AnMBR were measured once a week to obtain an approximation of the biomass concentration in the system. As depicted in figure L.1, in stage I and II the TSS concentration dropped from 50 to 25 $gTSS \cdot L^{-1}$ and the VSS concentration from 35 to 10 $gVSS \cdot L^{-1}$. This was most likely caused by a combination of stresses caused by the exposure to toxic compounds, and the changing conditions compared to the UASB reactor and storage. Additionally, the VSS/TSS ratio decreases from 0.7 to 0.37 $gVSS \cdot gTSS^{-1}$. In stage III and IV, an increase of the solids concentrations to 45 $gTSS \cdot L^{-1}$ and 17 $gVSS \cdot L^{-1}$ can be observed. The increase of the VSS concentration was most likely the result of microbial community development (i.e. biomass synthesis), regarding the complete degradation of the VFA mixture, phenol, and benzoate. In stage V, both the TSS and VSS concentrations dropped again to a value of 20 $gTSS \cdot L^{-1}$ and 10 $gVSS \cdot L^{-1}$. In this last stage, the VSS/TSS ratio increases to 0.5 $gVSS \cdot gTSS^{-1}$.

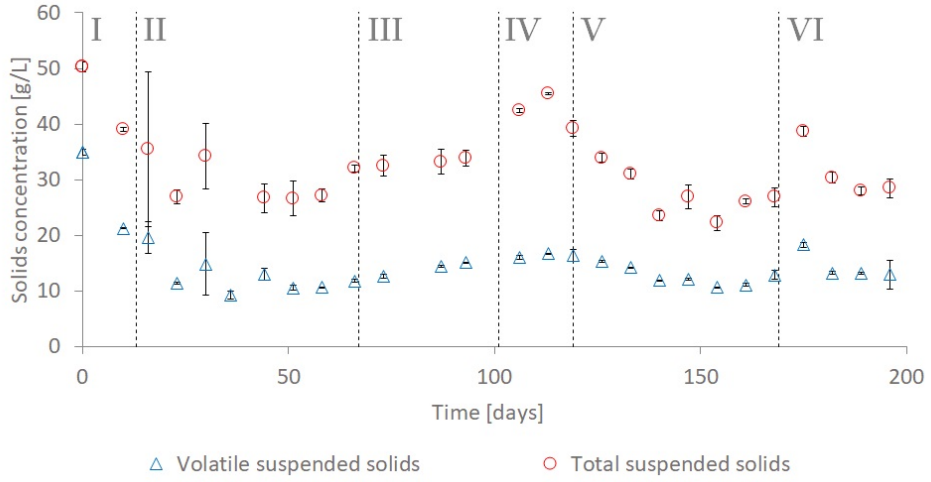


**Figure L.1:** Concentration of the TSS (◯) and VSS (△) in the AnMBR over time. The error bars indicate the SD, where $n$=3 for both conditions. The numerals indicate stages as defined in table 3.5.

# M PARTICLE SIZE DISTRIBUTION

The evolution of the PSD of the particulates in the broth can be seen in figure M.1. From the PSD analysis, it was found that the median particle size decreased from 773 $\mu m$ (seed sludge) to 212 $\mu m$ (day 5), further to 70-81 $\mu m$ (day 49-138), and finally to 38 $\mu m$ (day 194). This particle size reduction was within the expectations, due to the described stresses from the applied conditions. However, after this rather constant PSD during this interval, a decrease of the median particle size to 44 $\mu m$ on day 168 was observed after reducing the aniline concentration in the feed to 20 $mgAn \cdot L^{-1}$.

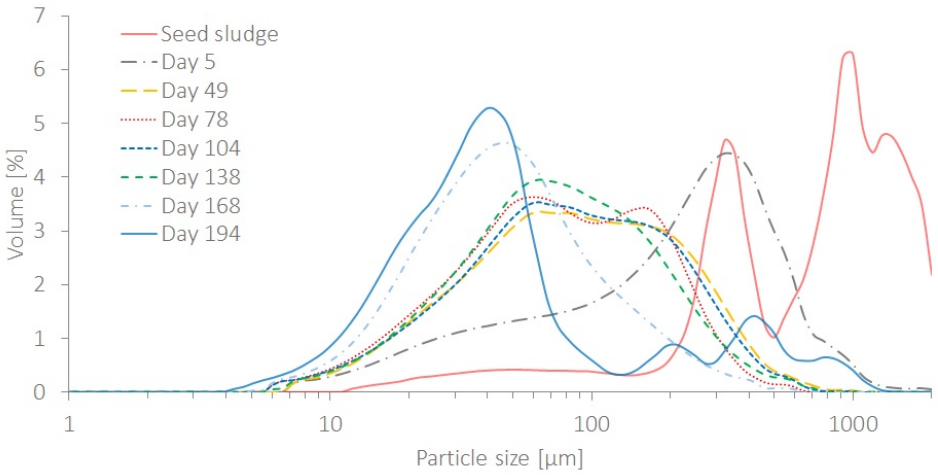


**Figure M.1:** Evolution of the PSD of the AnMBR broth.

# N | TRANSMEMBRANE PRESSURE

From figure L.1, it seems that the increasing TSS and VSS concentration in stage III and IV was related to an increased TMP (figure N.1). A possible explanation for the increase in TMP (which ultimately lead to complete clogging of the membrane) after increasing the aniline concentration in the AnMBR feed to 200 mgAn L in stage III was the production of EPS by the biomass as a stress response to aniline exposure [Mohammed et al., 2020]. Correspondingly, the production of EPS could explain the observed increase in TSS concentration (figure L.1).

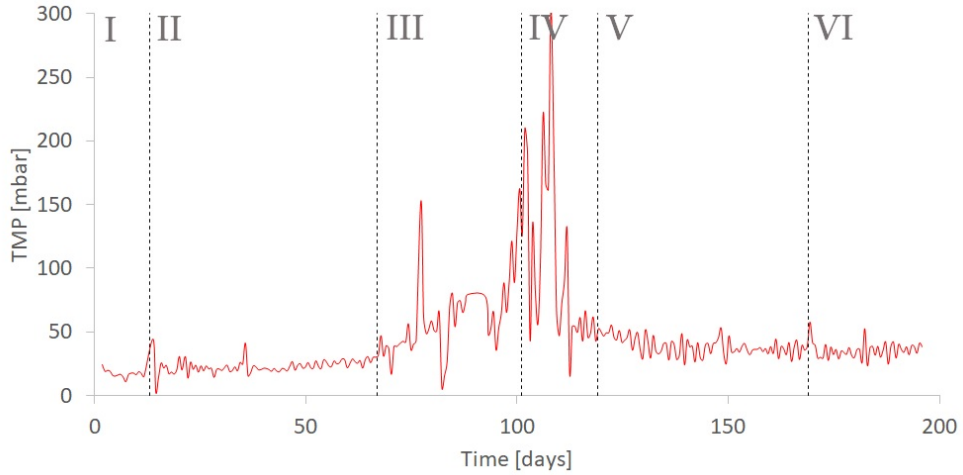


**Figure N.1:** Evolution of the TMP during the AnMBR operation. The numerals indicate stages as defined in table 3.5.

# O ADDITIONAL OBSERVATIONS

Within the timespan of one week, it was observed that the colour of the AnMBR feed solution turned darker over time when the feed solution was not degassed (figure O.1). The colouring was initiated by the formation of light-coloured precipitates, which together with the solution turn to a dark red/brown colour over time. This colour change of the feed solution did not occur in the absence of aniline (figure O.2). However, formation of precipitates was also observed in the feed without aniline.
Additionally, it was found that the aniline concentration in the feed gradually decreased from 20 $mgAn \cdot L^{-1}$ to 13 $mgAn \cdot L^{-1}$ after one week (figure O.3). This was specifically notable in stage V of the AnMBR operation, when the aniline concentration in the feed was 20 $mgAn \cdot L^{-1}$ and degassing of the AnMBR feed solution was not applied. When degassing (by vacuum) was applied, the colour of the AnMBR feed solution did not change in this timeframe, nor was a decrease in aniline concentration observed. As the feed was stored in a fridge at $4^{\circ}C$ and closed with a cap, it is not likely that aniline volatilisation is the responsible mechanism for the observed decrease.

**Figure O.1:** Colour change of the AnMBR feed solution over after one week.

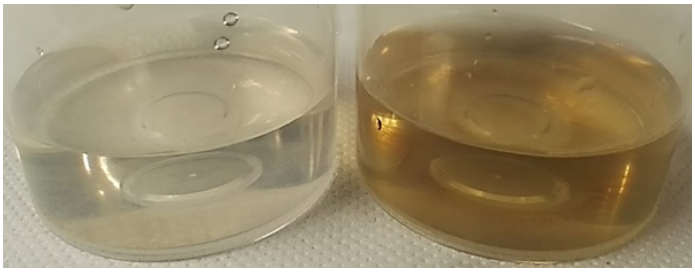

**Figure O.2:** The colour of the AnMBR feed does not change when aniline is not present in the feed (left bottle).

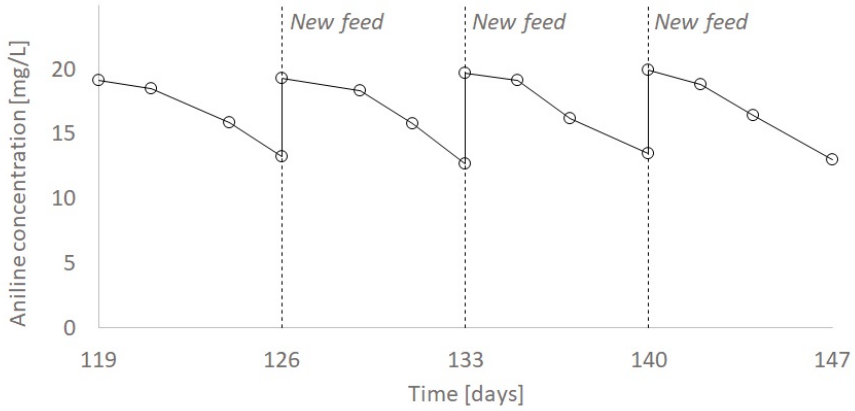


**Figure O.3:** Concentration of aniline in the AnMBR feed feed over time. The vertical dashed lines indicate the supplementation of the freshly prepared feed.

Batch experiments were performed to assess whether these observations do also occur in an aniline solution (demineralised water + aniline). 250 $mL$ Schott Duran glasses ($n$=3) were filled with 150 $mL$ of a 20 $mgAn \cdot L^{-1}$ aniline solution. The bottles were stored with a sealed cap under the same conditions as the feed, in a fridge at 4°$C$. Three times a week, the bottles were opened and mixed manually to allow oxygen to enter into the solution. Samples were extracted regularly over a period of 7 days, and analysed with GC to determine the aniline concentration. A decrease of the aniline concentration could indicate autoxidation and/or polymerisation of aniline.

Furthermore, the AnMBR feed solution was exposed to different conditions to examine its constancy under these conditions. (1) AnMBR feed incl. 20 $mgAn \cdot L^{-1}$, (2) AnMBR feed excl. 20 $mgAn \cdot L^{-1}$, and (3) degassed AnMBR feed incl. 20 $mgAn \cdot L^{-1}$, stored under anaerobic conditions.

The experiment to assess autoxidation and/or polymerisation of aniline in the 20 $mgAn \cdot L^{-1}$ aniline solution under the same conditions as the AnMBR feed (in a fridge at 4°$C$), did not show a decrease in aniline concentration after seven days, nor was a colour change observed.

## COLOPHON

This document was typeset using LaTeX. The document layout was generated using the arsclassica package by Lorenzo Pantieri, which is an adaption of the original classicthesis package from André Miede.